

7-12-2014

Modeling of Kinetically Limited Growth Rate for Solution-Synthesized Germanium Nanocrystals

Nicholas Shoop

Follow this and additional works at: https://digitalrepository.unm.edu/cbe_etds

Recommended Citation

Shoop, Nicholas. "Modeling of Kinetically Limited Growth Rate for Solution-Synthesized Germanium Nanocrystals." (2014).
https://digitalrepository.unm.edu/cbe_etds/45

This Thesis is brought to you for free and open access by the Engineering ETDs at UNM Digital Repository. It has been accepted for inclusion in Chemical and Biological Engineering ETDs by an authorized administrator of UNM Digital Repository. For more information, please contact disc@unm.edu.

Nicholas Shoop

Candidate

Chemical Engineering

Department

This thesis is approved, and it is acceptable in quality and form for publication:

Approved by the Thesis Committee:

Sang M Han, Chairperson

Dimiter N Petsev

Timothy J Boyle

**Modeling of Kinetically Limited Growth Rate for Solution-Synthesized
Germanium Nanocrystals**

By

**Nicholas Shoop
Bachelors of Science
Chemical Engineering**

**THESIS
Submitted in Partial Fulfillment of the Requirements for the Degree of
Masters of Science
Chemical Engineering**

**The University of New Mexico
Albuquerque, New Mexico**

May, 2014

Modeling of Kinetically Limited Growth Rate for Solution-Synthesized Germanium Nanocrystals

By

Nicholas Shoop

B.S., Chemical Engineering, Iowa State University, 2000

M.S. Chemical Engineering, University of New Mexico, 2014

Abstract

Solution synthesis is a common method of generating semiconductor nanocrystals. For solution synthesis, many studies have assumed that the growth rate is diffusion-limited with an unphysically low diffusion constant. In this thesis, a model is developed that considers both diffusion and surface kinetics. The diffusion coefficient of Ge monomers through the solvent, octadecene, at elevated synthesis temperatures is estimated to be on the order of 10^{-5} to 10^{-4} cm^2/sec , while the mass transfer boundary layer thickness is estimated to be on the order of a few nanometers, similar to the nanocrystal size. These two realistic conditions strongly suggest that the common assumption on diffusion limitation may not be warranted and that surface adsorption and desorption of growth precursors and ligands must govern the nanocrystal growth rate. The modeling incorporates the surface rate coefficients as fitting parameters, where the rate coefficients of organic ligands experimentally measured on Ge (111) surface are used as initial values. It is assumed that Ge monomers adsorb on the nanocrystal surface

irreversibly. The modeling results on nanocrystal size as a function of time agree well with the experimental outcome, strongly supporting that the Ge nanocrystal growth rate is governed by the surface kinetics and not by the boundary layer diffusion.

Table of Contents

| | |
|--|------|
| List of Figures | vi |
| List of Tables | viii |
| Chapter 1 Introduction | 1 |
| Goals | 2 |
| Motivation..... | 3 |
| Chapter 2 Model Development Methodology | 4 |
| Chapter 3 Synthesis of Germanium Nanocrystals | 6 |
| Synthesis | 6 |
| Results..... | 8 |
| Chapter 4 Modeling of Nanocrystal Growth | 11 |
| Boundary Layer | 13 |
| Diffusion | 20 |
| Surface Kinetics | 28 |
| Growth Model..... | 42 |
| Optimization | 46 |
| Optimization Process | 46 |
| Results of Optimization | 49 |
| Chapter 5 Discussion of Modeling Results..... | 55 |
| Model vs. Experimental Data | 55 |
| Limitations of Model | 58 |
| Possibilities for future study | 60 |
| Conclusion | 61 |
| Appendix A Calculations..... | 64 |
| Appendix B Mathematica™ Code: Numerical solutions of $\theta(t)$ for Ge and Ligands | 79 |
| Appendix C Mathematica™ Code: Model Optimization | 89 |
| References..... | 102 |

List of Figures

| | |
|--|----|
| Figure 1: TEM image of Ge nanocrystal | 7 |
| Figure 2: Plot of Ge nanocrystal radius growth over time..... | 9 |
| Figure 3: Plot of Ge nanocrystal radius growth with empirical growth model | 10 |
| Figure 4: Stable Ge nucleus at $R_0 = 0.75$ nm | 12 |
| Figure 5: Ge nanocrystal and boundary layer | 13 |
| Figure 6: Diffusion coefficient for Ge monomer in octadecene vs. temperature | 17 |
| Figure 7: Boundary layer thickness as a function of velocity and nanocrystal diameter | 19 |
| Figure 8: Zones of Ge concentration surrounding the nanocrystal..... | 21 |
| Figure 9: Estimate of C_{G3} | 25 |
| Figure 10: Plot of $\gamma(t)$ which is equivalent to $\int C_E(t)dt$ over the nanocrystal growth time | 26 |
| Figure 11: Plot of $d\gamma(t)/dt$ over time overlaid with $C_E(t)$ | 27 |
| Figure 12: Numerical solution to the integral in Equation (38)..... | 32 |
| Figure 13: Numerical solution for $\theta_{Ge}(t)$ results from Equation (34) | 34 |
| Figure 14: $d\theta_{Ge}/dt$ over growth timeframe as calculated from numerical solution..... | 36 |
| Figure 15: Fractional coverage, $\theta(t)$, of the growing Ge nanocrystal as a function of time..... | 38 |
| Figure 16: Fractional coverage, $\theta(t)$, of the growing Ge nanocrystal as a function of time with numerical solution and analytical estimate | 41 |
| Figure 17: $d\theta_I/dt$ over growth timeframe as calculated from numerical solution | 42 |
| Figure 18: Flow diagram of the method used to find the values for adsorption and desorption coefficients for Ge monomer and organic ligands | 48 |

| | |
|---|----|
| Figure 19: Model for $R(t)$ overlaid with experimental data | 50 |
| Figure 20: Optimized numerical solution for $\theta_{Ge}(t)$ with single exponential fit..... | 51 |
| Figure 21: Optimized numerical solution for $\theta_{Ge}(t)$ with double exponential fit | 52 |
| Figure 22: $\theta_L(t)$ and $\theta_{Ge}(t)$ plotted with optimized adsorption and desorption coefficients | 53 |
| Figure 23: Residual values plotted against run order and standard deviation | 56 |
| Figure 24: Model for $R(t)$ with different initial Ge monomer concentration..... | 61 |
| Figure A1. Empirical fit of single exponential to the experimental data..... | 72 |
| Figure A2. Fit to estimates of C_{G3} used to calculate characteristic time constant τ_G | 73 |
| Figure A3. Empirical fit to the numerical solution to $\gamma(t)$ | 74 |
| Figure A4. Empirical fit to numerical solution for $\theta_{Ge}(t)$ with double exponential..... | 75 |
| Figure A5. Empirical fit to numerical solution for $\theta_{Ge}(t)$ with single exponential | 76 |
| Figure A6. Empirical fit to numerical solution for $\theta_{Ge}(t)$ with single double exponential to optimized values for k_{ad} , k'_{ad} and k'_{des} | 77 |
| Figure A7. R^2 determination for the $R(t)$ model fit to experimental data | 78 |

List of Tables

| | |
|--|----|
| Table 1: Mean radius of Ge Nanocrystal at different time intervals..... | 8 |
| Table 2: Model input parameters for plotting of Ge monomer and organic ligand nanocrystal surface coverage over time..... | 40 |
| Table 3: Initial values for model input parameters | 45 |
| Table 4: Initial and optimized values for model parameters..... | 49 |
| Table A1: Input variables for calculating D_{AB} | 66 |
| Table A2: Values for $\gamma(t)$, C_{G3} and ΔC | 67 |
| Table A3: Values for numerical solution of Equation (38) | 67 |
| Table B1: Table relating Mathematica script variable to the Thesis text variable | 79 |
| Table C1: Table relating Mathematica™ script variable to the Thesis text variable | 89 |

Chapter 1

Introduction

Introduction

Numerous researchers have studied nanocrystal (NC) growth kinetics during solution synthesis[1-3]. Understanding the key factors that limit NC growth is paramount for the scaling of synthesis for larger batch sizes or commercial production, however, the majority of these previous investigations largely focus on the synthesis and the resulting particle size distribution, aiming towards monodispersity[4, 5]. Monodispersity is important for systematic characterization of NCs for their electronic/optical properties and their ultimate end use. However, the surface kinetics of the NC growth has not been characterized thoroughly as they relate to growth rate for NCs. The growth of nanocrystals is often described to be limited by diffusion, such as LaMer *et al.*[6], who described his work only in terms of being limited by diffusion. More recent articles[2, 3] discount the kinetically limited case by making assumptions that slow diffusion across very large boundary layers limit the growth.

Departing from the diffusion limited growth assumption, a number of authors[7-9] have presented general theoretical models of combined kinetic and diffusion limited crystal growth. While these models do differentiate between diffusion and kinetically controlled growth, specific surface kinetics are not discussed. In this work, the growth rate of germanium (Ge) NCs was analyzed in consideration of both boundary layer (BL) diffusion and surface kinetics. This work proves that the diffusion through the boundary layer did not limit the growth. Rather, it is the surface kinetics that limits the adsorption of Ge monomer to the surface of the NC. The surface kinetics limited case was

developed into a model to describe the growth of Ge NCs in this experiment. To simplify the modeling analysis, only the NC growth immediately following the NC nucleation that occurred in the solution after injection of the Ge amide precursor (Ge amide) is considered. The change in the radius of the NC, with respect to time, was predicted with a construction of model. The model incorporated a coordinating ligand surface coverage model combined with a kinetic model designed around the adsorption and desorption of the Ge monomer and ligands in the synthesis.

Goals

This thesis was undertaken to distinguish the kinetically limited NC growth versus the diffusion limited NC growth processes. This was accomplished by modeling the convective transport as well as the kinetic process for adsorption to the Ge NC. This study of the mass transport and kinetic limitations on the NC synthesis has revealed the nature of the growth rate determining factors. While a diffusion model is disproved, a kinetically limited model has been created and fitted to the experimental data to provide proof that Ge NCs are not diffusion limited. The study of the convective diffusion conditions has been explored thoroughly to prove that boundary layer thickness for NC in stirred solution is on the same order of magnitude as the NC and not a key driver of the growth rate. Additionally, the modeling of the surface kinetics adsorption rate should have shown that kinetically limited growth is possible and probable.

By proving that the NC growth is kinetically limited, further understanding of the growth mechanisms has been presented. The synthesis of the Ge NC through the reduction of Ge(2) to Ge(0) monomer in solution has been published previously[10],

therefore, additional discussion of the synthesis method is not needed and a singular focus on understanding the growth rate factors was initiated. Rather, a more profound understanding of the mechanisms in which the NC is grown was desired. Proving, convincingly, that the Ge NC synthesis used in this work was kinetically limited would be a change in conventional wisdom about NC growth mechanisms commonly witnessed by investigators in semiconductor NCs.

Motivation

The motivation for this thesis was driven by a need to better characterize the surface kinetics of the NC, specifically the Ge NCs grown for study[10] in this work. Understanding the surface kinetics and successful incorporation into a growth model allows one to make predictions about the outcome of synthesis conditions a priori. Additionally, a surface kinetics based model would allow the study undertaken to discover if the synthesis was diffusion limited or kinetically limited. Many articles found in a literature search did not fully explore the possibility of having kinetically limited growth, and often eliminate it as a possibility with assumed, unusually low diffusion coefficients or assumed very large diffusion boundary layers. This work aimed to prove that this NC synthesis is kinetically limited and that a model could be created to predict the growth rate of the NC.

Chapter 2

Methodology

The aim of this thesis was to develop a mathematical model incorporating the limiting factors for the growth of Ge NCs when synthesized in solution. This has been done in three distinct steps; 1) calculating the boundary layer (BL) thickness around the NC during growth; 2) determine whether the solution synthesis method is a diffusion limited or a surface kinetics limited system; 3) and after the limiting mechanism is determined, a model for the growth rate was created that incorporated the limiting mechanisms and the experimental conditions.

In order to realize this goal, a description of the flow characteristics and boundary layer thickness around the NC must be developed first. This included calculating the size of the boundary layer and the conditions for convective transport through that boundary layer. Once those have been defined, a schematic of the convective transport of Ge monomer to the surface of the NC will need to be drawn and used to describe the system throughout this work. The different concentration regimes will be defined, and assumptions about the solution parameters are detailed in order to set up further testing of the diffusion and kinetically limited scenarios.

Second, the limiters in the NC growth must be fully elucidated. Both diffusion and surface kinetics need to be considered in a useful model. The rate of diffusion will be calculated by using the diffusion coefficient and by calculating the driving force in the system. The surface kinetics of Ge monomer adsorption will be calculated using a

Langmuir type adsorption site balance based upon surface coverage of Ge monomers and coordinating ligands. The surface coverage will be derived as a function of time.

Next, an expression for the growth of an NC as a function of time is derived from the surface coverage expressions as well as the experimental conditions to develop a model for the NC radial growth rate as a function of time. Lastly, the model will then be fitted to the experimental data to reveal the empirical adsorption and desorption coefficients, as well as an effective mass transfer coefficient allowing the limiting factor of the Ge NC synthesis to be determined.

Chapter 3

Synthesis

Synthesis

{ The complete details of the precursor synthesis and the subsequent Ge(0) NC synthesis have been discussed in previous publications [10-12]. In brief, Ge NCs were synthesized from decomposition of Ge(II) amide in a solution of hexadecylamine (HDA), oleylamine (OA) and 1-octadecene (OD). The synthesis of the Ge amide was synthesized from the reaction of lithium bis(trimethylsilyl)amide and germanium(II) chloride dioxane. All chemicals and solvents were used as received; (Sigma Aldrich) HDA, OA, OD, Ge(II) chloride dioxane, lithium bis(trimethylsilyl)amide, diethyl ether, and hexane and (Burdick and Jackson Laboratories) Methanol, chloroform, and acetone.

A 100 cm³ three-neck round bottom flask was fitted with a rubber septa which has a temperature probe that reaches into the solution and two rubber stoppers. The flask is mounted on top of a heating mantle and stir-plate. The heating mantle was plugged into a Variac power supply that is controlled by an Omega CN9000 temperature controller with input from the flask's temperature probe. The starting solution in the flask contained: a stir bar, 10 mmol OD (2.525 g), 3 mmol HDA (0.725 g), and 3 mmol OA (0.802 g). The solution was degassed for 5 minutes under rough vacuum at 125 °C while stirring with the magnetic stir bar. Then, the container's atmosphere was back filled with argon gas and the heating continues to 300 °C at atmospheric pressure. The flask atmosphere was filled with Ar to prevent autoignition of OD in solution. Once the temperature was stable at 300 °C, a syringe was loaded with 1 mmol of the Ge amide

(0.393 g). The Ge amide was then rapidly injected into the hot solution through a rubber stopper. After the required reaction time, the heating mantle was removed to quench the reaction. The temperature, on average, decreases from 300 °C to below 200 °C within 20 s. The threshold in which slow nucleation begins for the Ge amide has been experimentally observed at ~200 °C, at or below this temperature, the growth and nucleation is much slower and it was assumed that the 20 s needed to cool it to 200 °C would not produce substantial growth of the NCs further.

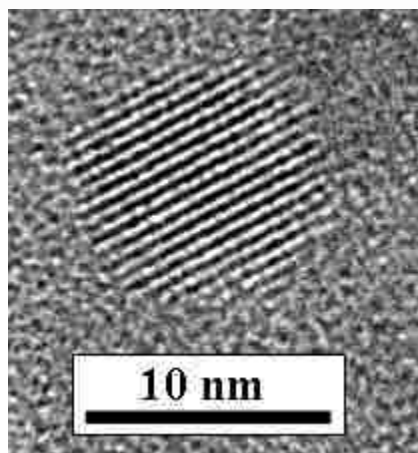


Figure 1. A TEM image[13] of a Ge(0) NC that was observed after 60 min reaction time.

Once the solution cooled to room temperature, the NCs were extracted from the extra surfactants and precursor by-products by repeatedly (3-times) centrifuging and rinsing the nanocrystal suspension with chloroform. Four cm³ of chloroform is used to dissolve the surfactants and suspend the nanocrystals in a centrifuge tube. A 3:1 volumetric mixture of methanol and acetone is added to the chloroform suspension until the mixture flocculates. The solution was then centrifuged for 5 min at 5000 rpm, which separated the NCs from the solvated surfactants.

After the cleaning process, the NCs are suspended in hexanes and drop cast onto a carbon TEM grid. A JEOL 2010 TEM was used to image the NCs seen in Figure 1 to measure their size (Table 1).}[13]

The experiment was performed with 5 iterations of the conditions described. Each experimental run is set up identically and allowed to progress to the prescribed times shown in Table 1 and graphically in Figure 2.

Results

Table 1: Mean radius of Ge NC at different time intervals. Standard deviation is denoted by σ [13] and related to the measurements of multiple NCs within a single synthesis run. The radius measurements were done from TEM images from prepared NC samples.

| Time (min) | Radius (nm) | σ (nm) | σ (%) |
|---------------|----------------|------------------|-----------------|
| 1 | 1.53 | 0.65 | 21.3 |
| 3 | 1.6 | 0.64 | 20 |
| 5 | 3.7 | 2.3 | 31.1 |
| 30 | 7.5 | 3.3 | 22 |
| 60 | 6.55 | 3.7 | 28.2 |

The standard deviation within the measurement group, σ , varied between 20 % and 32 % of the diameter mean in the 5 reaction runs. The σ does not have a strong trend as the reaction time increases. This indicates that there was no significant increase in the NC size distribution as the reaction progresses, meaning there was no appreciable nucleation after the initial nucleation step at time zero. Therefore, ignoring any nucleation effects on the reaction is reasonable if the trend in σ % is random or flat. Additionally, minimal Ostwald ripening is assumed due to a flat trend of σ as a percentage of the radius.

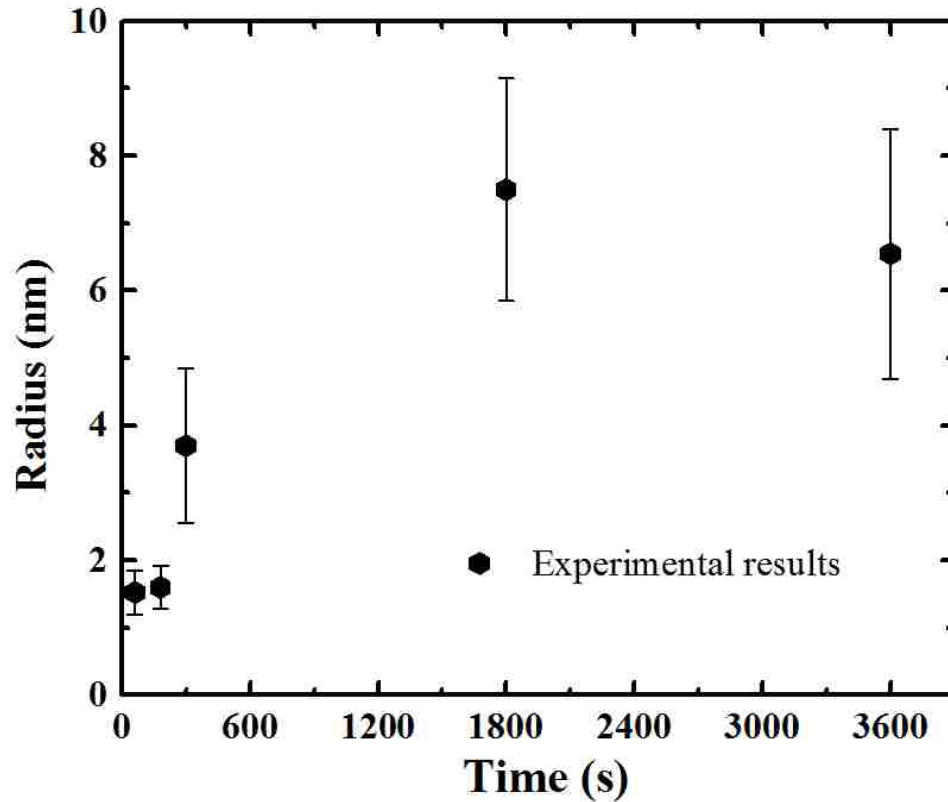


Figure 2. Plot of Ge NC radius growth over time (s). Bars indicate σ for each batch of the experiment.

The experimental data shows a steady increase in radius for the first 30 min of the reaction, then decrease to a slower growth rate for the last 30 min. A fitting equation with an asymptotic form best fits the growth rate of the radius over the 1 hour reaction timeframe. The NC radial growth over time is described with an equation of the form

$$R = R_t [1 - \exp(-t/\tau_R)] \quad (1)$$

where R is the NC radius, R_t (7.06 nm) is the terminal radius and τ_R (446 s) is the characteristic time constant when empirically fitted to the experimental data. The resulting R^2 value is 0.93 using the Levenberg-Marquardt algorithm in Origin™ to fit the experimental data. This does not help with the determination of diffusion or kinetic

processes directly but this does give an approximate growth rate fit line, Equation (1), for this experimental run is used in the diffusion characterization. Figure 3 shows the experimental data and Equation (1) fitted to that data.

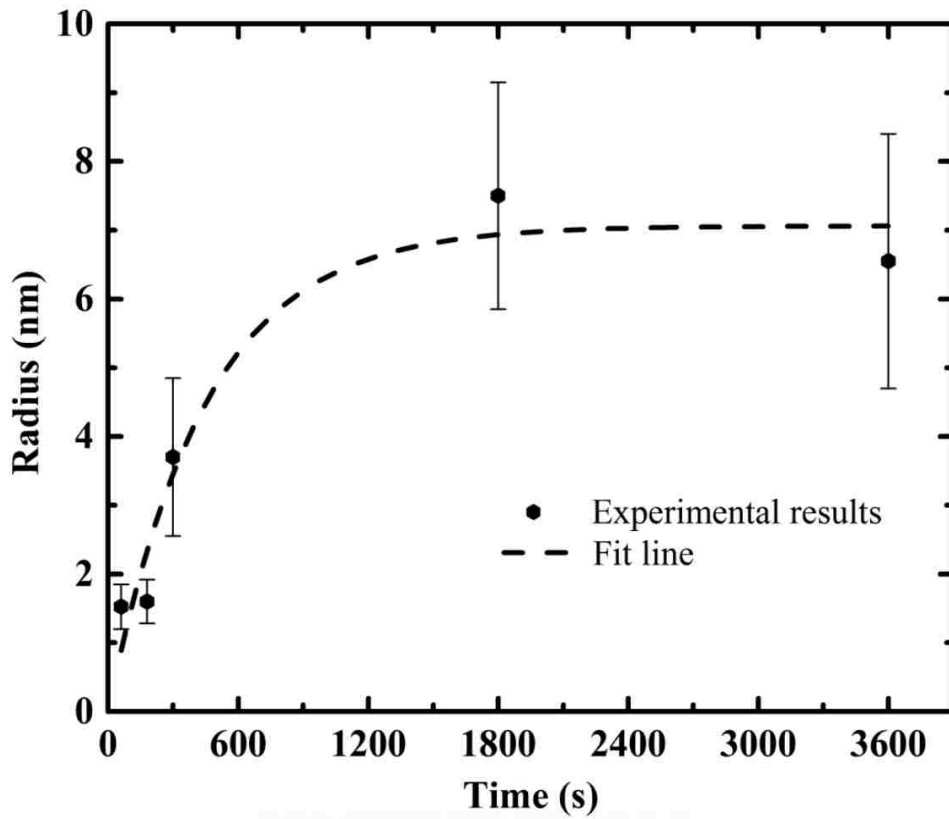


Figure 3. Experimental data fitted with empirical growth rate expression from Equation (1).

Chapter 4

Modeling

According to LaMer *et al.*[6], the growth of colloidal NCs begins with the nucleation phase initiated by supersaturation of the crystal monomer material in solution. The solution increases to a super-saturated condition with respect to Ge(0) concentration after the Ge amide is injected at time zero. To simplify the calculation of the Ge amide concentration as a function of time, the decomposition from a Ge(II) state to the Ge(0) state as Ge monomer in the synthesis solution is assumed to occur rapidly enough as to not significantly influence the growth rate in this model. The decomposition temperature of Ge Amide is well below the reaction temperature, and the synthesis solution rapidly changes color upon injection of the Ge Amide[10], indicating that a rapid reduction from Ge(II) Amide to Ge(0) monomer (Ge monomer) in solution is expected. A more detailed analysis of the decomposition rate of the Ge Amide would be necessary to provide a more accurate decomposition rate, and therefore a more precise Ge monomer concentration profile with respect to time. The presence of Ge monomer in the supersaturated state initiates the homogeneous nucleation in solution. An assumption is made that the decomposition process happens sufficiently fast, that the nucleation and growth also are not limited by the availability of Ge monomer. The nucleation and reduction is not initiated by a catalyst, therefore, the formation of the Ge NCs happens homogeneously due to a supersaturation of the Ge monomer. These conditions are consistent with a high initial concentration of Ge monomer in the solution just after Ge Amide injection. To simplify the calculations for the growth model generated, the

nucleation phase of the synthesis are not incorporated into the model. The nucleation will be treated as a separate process the initial conditions are the same; therefore the nucleation occurs identically in this work will ignore the nucleation phase.

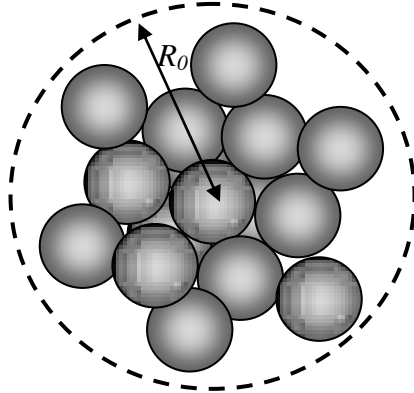


Figure 4. Stable Ge nucleus at $R_0 = 0.75$ nm. Each gray sphere represents a Ge atom.

If the nucleation phase is not being considered as part of the growth model, the radius after nucleation will be the initial radius in the growth model. Using the calculations of Jiang, *et al.* [14], the minimum stable nucleus radius has been calculated to be 3 times the atomic diameter of the species in the NC. The radius of this NC such that half of the atoms are exposed and available for binding on the surface. The initial radius R_0 (0.75 nm) would be stable enough to continue growth once it reached this size. Once a stable NC nucleus of radius R_0 has formed (Figure 4), the NC can transition to the growth phase. This growth is primarily controlled by two factors; (i) diffusion of Ge monomers through the BL and (ii) kinetic adsorption rate of Ge monomers to the surface. For sustained growth, the Ge monomers must first diffuse from the bulk solution of Ge monomer (C_{G3}) across the BL and adsorb to the surface of the nucleus of the NC at concentration C_E (Figure 3). The model will describe the growth of a single NC in the

system rather than a collection of all Ge NCs growing in the synthesis solution. The model was tested for validity by comparing the results of the predicted radius with the experimental data.

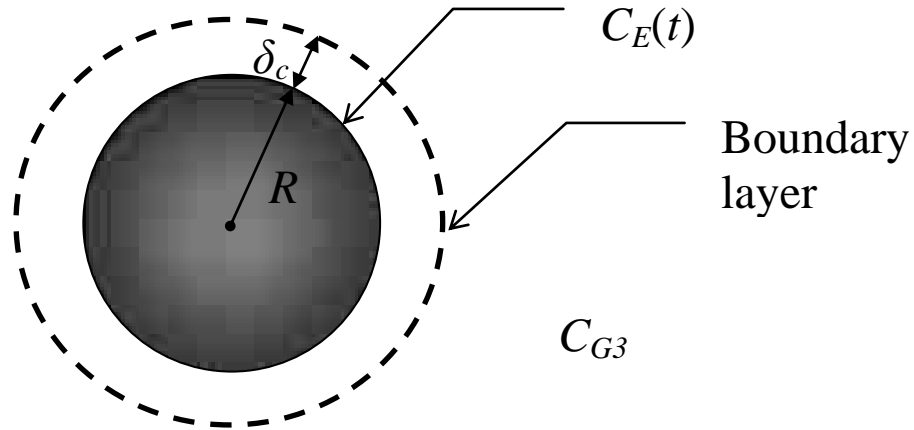


Figure 5: The sphere represents a NC in a stirred solution. $C_E(t)$ represents the concentration of Ge monomer in equilibrium with the surface of the NC. C_{G3} represents the bulk concentration of the Ge monomer in the solution. δ_c represents the mass transfer boundary layer thickness.

Boundary Layer

The mass transfer BL thickness (δ_c) represents the section of solvent through which the Ge monomer diffuses to get from an area of bulk Ge monomer concentration (C_{G3}) to an area of lower concentration at equilibrium with the surface (C_E). This is illustrated in Figure 5. Each NC is entrained in the growth solution, the conditions of which, determine the BL thickness. An expression for δ_c is

$$\delta_c = \frac{D}{2 + .6\text{Re}^{1/2} \text{Sc}^{1/3}}, \quad (2)$$

where D is the diameter of the NC, Re is Reynolds number as defined by Equation (3) and Sc is Schmidt number as defined by Equation (4). Re generally gives a ratio of the inertia to the viscous forces in a fluid flow relative to an object. The starting point of calculating the BL is determining Re of the solution with respect to the NC. Re is calculated with

$$Re = \frac{D\rho v}{\mu}, \quad (3)$$

where D (7 nm) is the NC diameter, ρ is the solvent density, v (0 to 37.7 cm/s) is the characteristic velocity of the solution with respect to the NC and μ (0.3206 cP) is the solvent viscosity. Sc is a representation of the ratio diffusivity determined by fluid viscosity over the diffusivity determined by mass. Sc is calculated with

$$Sc = \frac{\mu}{\rho D_{AB}}, \quad (4)$$

where D_{AB} is the diffusion coefficient of the solute Ge monomer through the solvent OD. The calculation of v in the solvent stirred by the magnetic stir bar with respect to the NC is complex[15] if all mixing effects are taken into consideration. However, a simplified method of determining Re can be realized by using the extreme case that assumes the NC are stationary in the vessel, and not well entrained in the fluid. If this is so, the maximum characteristic velocity of the liquid would represent a maximum Re and consequently a minimum δ_c .

The maximum velocity of solvent, v_{max} , is assumed to be the tangential speed of the tip of the stir bar. The solution, contained in a 100 mL, round bottom, three neck flask, is mixed with a magnetic stir bar with dimensions of 12 x 2 x 2 mm rotating at 600 rpm for the duration of the reaction. Assuming a no slip condition at the stir bar/liquid interface, the solution will travel at approximately the same speed as the stir bar. The

tangential speed of the stir bar tip and the assumed maximum solvent speed (v_{max}) are 37.7 cm/s.

The NCs forming are entrained in the solution and will not experience a true velocity as high as v_{max} . A range of v (0 to 37.7 cm/s) is used to determine the possible range of BL thickness. The nominal size of the NC during the growth phase ($D_N = 7$ nm) will be used to calculate the lower bound for boundary layer thickness.

OD viscosity at the experimental conditions of $T = 573$ K is estimated with the Walther equation as modified by Mehrotra *et al.*[16],

$$\log(\mu + 0.8) = 10^{b_1 T^{b_2}}, \quad (5)$$

where b_1 (9.806) and b_2 (-4.032) are the coefficients for OD from the literature.

Substituting the coefficients into the Walther equation and solving for μ yields a viscosity of 0.3206 cP.

OD density (ρ) at experimental conditions is estimated at 0.5732 g/cm³ with the method created by Yaws[17],

$$\rho = AB^{-(1-T/C)^n} \quad (6)$$

where A (0.24050), B (0.24731), C (748) and n (0.32724) are coefficients specific to OD in this function.

Now that all the variables for the Re are determined the calculation for Re (4.7×10^{-3}) is performed. This Re is much below 1 which is a laminar flow regime. The fluid flow is within the creeping flow regime once Re is $\ll 1$ [18]. Lowering v , lowers Re as well, pushing it further into the creeping flow domain and resulting in a larger BL

thickness. This will not affect the outcome of the BL thickness by a significant amount as demonstrated in Figure 7.

The next component of Equation (2) is Sc , which is calculated with Equation (4). Unknown at this point is the diffusion coefficient. The main component of the solvent is OD, therefore OD is used as the solvent to simplify the calculation of D_{AB} . The diffusion coefficient for Ge monomer in OD is estimated with a method by Sitaraman, Ibrahim and Kuloor[19] with the form

$$D_{AB} = 5.4 \times 10^{-8} \left(\frac{M_s^{1/2} L_s^{1/3} T}{\mu_s V_m^{0.5} L^{0.3}} \right)^{0.93}, \quad (7)$$

where M_s is the molecular weight of solvent (252.54 g/mol), L_s is the solvent latent heat of vaporization (53.34 kJ/mol), L is the solute latent heat of vaporization (334.3 kJ/mol), V_m is the molecular volume of the solute (16.7 cm³/mol) which is calculated using amorphous Ge[20, 21] for solute density, μ_s is the viscosity of the solvent (0.321 cP) and T (573 K) is the temperature of the solution. After inserting in values for the experimental conditions, D_{AB} is estimated at 5.3×10^{-5} cm²/s at 298 K and 9.6×10^{-5} cm²/s for experimental conditions ($T = 573$ K). The diffusion coefficient increases roughly 2 fold from room temperature to reaction temperature and is shown in Figure 6. The relatively high temperature drives a proportional increase in the diffusion coefficient. Using the new estimate for diffusion coefficient, Sc is calculated to be 58.

Some investigations estimate the BL as orders of magnitude greater than the NC diameter[2, 5, 9] and therefore δ_c would limit the growth via diffusion. Equation (2) and inputs D , Re and Sc are used to calculate δ_c (3.3 nm), which is the same order of

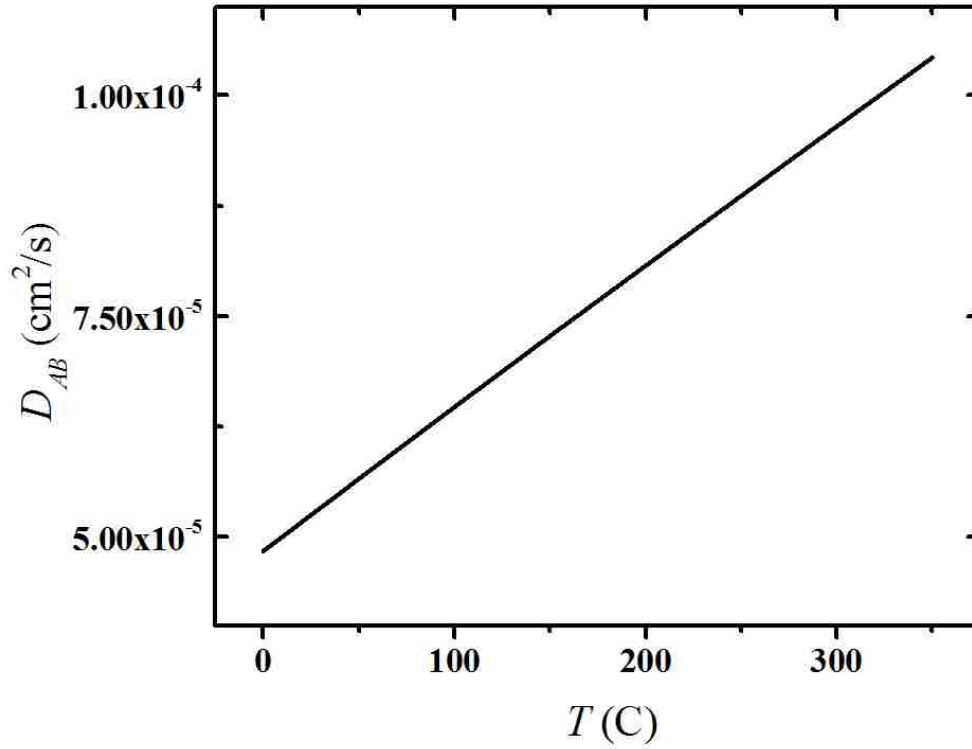


Figure 6. D_{AB} for Ge monomer in OD from ambient temperature to experimental conditions.

magnitude of the nanocrystal radius. The results for the δ_c in this thesis do not support the hypothesis for a diffusion limited growth, simply due to an assumed very thick BL, so further examination is required to determine if the BL thickness and subsequently diffusion of Ge monomer is a limiter in the NC growth.

To simplify this model, an assumption is made that there is no reaction over the boundary layer. Therefore, Sc can relate the kinematic BL, δ_k and the mass transfer BL thickness, δ_c [22] with

$$\frac{\delta_k}{\delta_c} = Sc^{1/3} \quad , \quad (8)$$

which can be rearranged to

$$\delta_k = Sc^{1/3} \delta_c \quad (9)$$

Using the existing values for Sc and δ_c , δ_k is calculated to be 13 nm, which is only 2 times larger than the NC radius in this calculation.

The δ_c thickness represents the thinnest BL to be expected from a system where the characteristic velocity is the same of that of the stir bar edge velocity. In actual experimental conditions the characteristic velocity is certain to be lower than v_{max} . As demonstrated in Figure 7a, the change in δ_c over the range of v is approximately 0.2 nm. This change is small compared to the total BL thickness at v_{max} . As v approaches a zero velocity condition, δ_c approaches 3.5 nm. The characteristic velocity of the solution passing by the NC is bounded by 0 and 38 cm/s results in a range of δ_c between 3.3 and 3.5 nm, with the upper bound more accurately describing the actual solution conditions.

Increasing the NC radius input to the calculation for δ_c results in an increase in the BL thickness as well. Figure 7b shows the BL thickness during different stages of the NC growth process. The BL starts at 1 nm shortly after the NC nucleation process is complete and is roughly 7 nm in thickness by the time the NC has reached its critical size of ~ 14 nm in diameter.

Determining the mass transfer coefficient (k_c) is necessary to gauge the rate of diffusion mass transfer through the BL. The Ranz-Marshall correlation[23] which describes heat transfer conditions at $Re < 200$ is written as

$$Nu = 2 + .6Re^{1/2} Pr^{1/3} \quad (10)$$

where Nu is the Nusselt number and Pr is the Prandlt number. Nu is the dimensionless

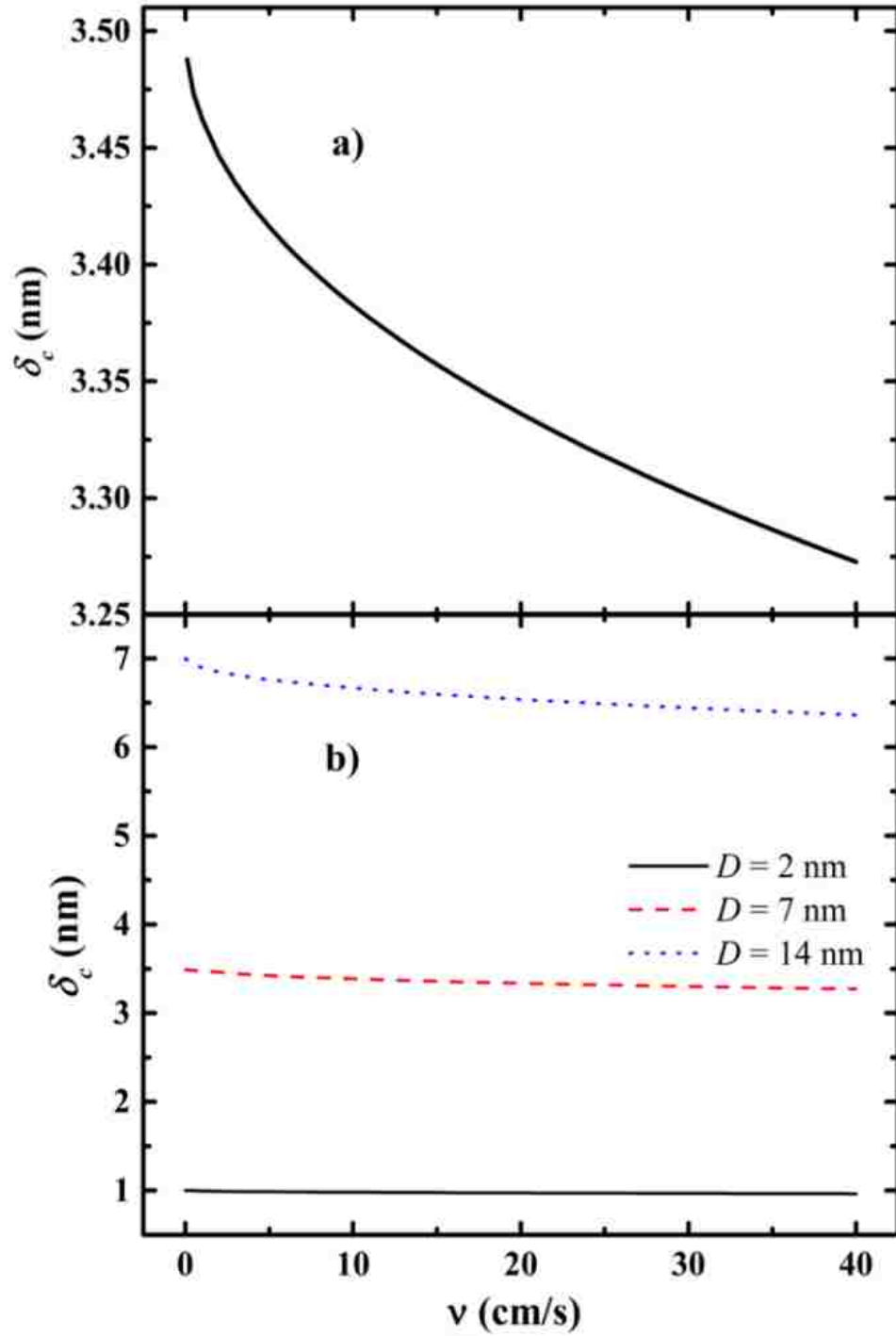


Figure 7. Boundary layer thickness, δ_c , with respect to v of solution impinging on NCs for a) 7 nm diameter NC and b) δ_c for NCs with 2 to 14 nm diameter.

ratio of conductive to convective heat transfer and Pr is the dimensionless ratio of viscous to thermal diffusion rate. The expression has an analogous relationship for mass transfer if the Pr number is exchanged for Sc and Nu exchanged for the Sherwood number (Sh). Sh , which is the dimensionless ratio of convective and diffusive mass transfer coefficients is shown below in the form of the Ranz-Marshall correlation converted for mass transfer.

$$Sh = \frac{k_c D}{D_{AB}} = 2 + .6Re^{1/2} Sc^{1/3} \quad (11)$$

Sh is also equivalent to $k_c D/D_{AB}$ [22]. Rearranging the Ranz-Marshall correlation an expression is created for k_c ;

$$k_c = \left[2 + .6Re^{1/2} Sc^{1/3} \right] \cdot \frac{D_{AB}}{D} \quad (12)$$

For this system the mass transfer coefficient, k_c , is calculated to be 305 cm/s. The mass transfer coefficient, k_c can also be expressed with the following expression[18]. This

$$k_c \sim \frac{D_{AB}}{\delta_c} \quad (13)$$

relationship if substituted into Equation (10) and simplified, creates the expression for δ_c in Equation (2).

Diffusion

With the given synthesis parameters, δ_c will approach 3.5 nm as the velocity approaches zero. Thus, δ_c is dominated by the influence of the Re which itself is influenced by particle diameter and solvent to NC characteristic velocity. Ge monomer has to diffuse through the BL surrounding the NC shown in Figure 8 prior to adsorbing to

the surface. The following chapter will determine if δ_c is large enough to create a diffusion limiting rate step in the model.

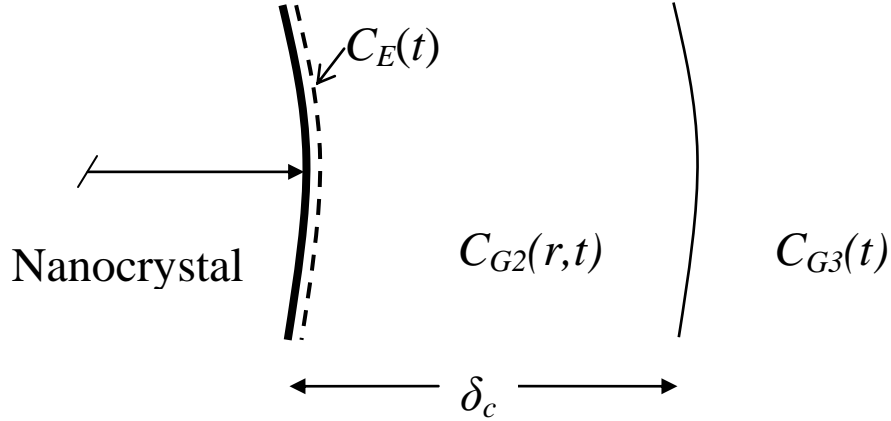


Figure 8. Zones of Ge concentration surrounding the NC. C_{G3} represents the bulk concentration outside the NC boundary layer. The second zone, contained by the boundary layer is represented by C_{G2} is a function of the distance from the NC (r) and time, t . C_E represents the concentration of Ge monomer just above and in equilibrium with the Ge NC surface.

The rate of Ge monomer diffusing to the surface of the NC is calculated using an adaptation of Fick's 1st law of diffusion to experimental parameters. With Fick's 1st law equation, consideration for the surface area of the NC and the relevant variables an expression for diffusion flow rate (J_{BL}) into the boundary layer around the nanocrystal is written as

$$J_{BL} = 4\pi r^2 D_{AB} \left(\frac{dC_{Ge}}{dr} \right) \Big|_{R < r < R + \delta_c}, \quad (14)$$

where r is bounded by a region equal to or larger than that of R and less than the $R + \delta_c$ and C_{Ge} represents Ge monomer concentration around the NC. Using a method from Sugimoto and Talapin[8, 9], the variables r and t are separated and assuming a constant

diffusion coefficient, the left side of the expression is integrated from R to $R+\delta$, where R is the radius of the nanocrystal. The right side is integrated from C_E to C_{G3} resulting in

$$J_{BL} \int_R^{R+\delta} \frac{1}{r^2} dr = 4\pi D_{AB} \int_{C_E}^{C_{G3}} dC_{Ge} \quad . \quad (15)$$

Equation (15) where C_E represents the concentration of Ge monomer just above the crystal surface and C_{G3} represents the concentration of Ge monomer in the bulk solution just outside the boundary layer. Integrating both sides results in Equation (16).

$$J_{BL} \left[-\frac{1}{r} \right]_R^{R+\delta} = 4\pi D_{AB} [C_{G3}(t) - C_E(t)] \quad (16)$$

Evaluating the left hand side of the equation and simplifying results in Equation (17) for diffusive molar flow rate.

$$J_{BL} = \frac{4\pi R(R+\delta_c)D_{AB}}{\delta_c} [C_{G3}(t) - C_E(t)] \quad (17)$$

The molar flow rate just above the surface of the NC, J_E , through the radius of concentration C_E in units of mol/s can be described as the product of molar density of Ge and the rate of change of the NC volume. Adapted from an expression used by Sugimoto[8] , the molar flow rate in terms of the rate of change of the radius is

$$J_E = \frac{\rho_{Ge}}{MW_{Ge}} 4\pi R^2 \frac{dR}{dt} \quad , \quad (18)$$

where R is the radius of the NC. Two expressions for flow into the boundary layer have been created. One, relating growth in size of the nanocrystal to the flow and the other relating diffusion, and it's driving force, to the flow at the radius where C_E is present. For simplification, J_{BL} and J_E will be considered equivalent due to the incredibly small difference between the radius of the NC and the radius where C_E is present. There won't be measureable change of Ge monomer concentration between the surface of the NC and

the radius where C_E is present. Setting both of these equations equal to each other gives the ordinary differential equation (ODE)

$$\frac{\rho_{Ge}}{MW} 4\pi R^2 \frac{dR}{dt} = \frac{R(R+\delta_c)}{\delta_c} 4\pi D_{AB} [C_{G3}(t) - C_E(t)], \quad (19)$$

where R represents the radius of the growing crystal. R and t are separable in this ODE.

Terms containing R and t are consolidated on their respective sides resulting in the following expression.

$$\frac{\rho_{Ge}}{MW} 4\pi R^2 \left(\frac{\delta_c}{R(R+\delta_c)} \right) dR = 4\pi D_{AB} [C_{G3}(t) - C_E(t)] dt \quad (20)$$

The left side is integrated from R_0 to $R_0+\Delta R$ which represents the change in radius from R_0 at time t_0 to the new radius, $R_0+\Delta R$ at time t . The right side is then integrated from t_0 to t revealing the expression

$$\int_{R_0}^{R_0+\Delta R} \frac{\rho_{Ge}}{MW} \left(\frac{\delta_c R}{(R+\delta_c)} \right) dR = D_{AB} \int_{t_0}^t [C_{G3}(t) - C_E(t)] dt, \quad (21)$$

where the equation for $C_{G3}(t)$ and the change in R over time has yet to be determined.

The driving force will diminish as the concentration C_{G3} decays with time. In order to determine the change in C_E over time, an expression for $C_{G3}(t)$ and values of $R(t)$ must be established. Equation (1) is used to provide values of R with respect to time. Some assumptions must be made of the decay of bulk concentration C_{G3} . First, the initial Ge monomer concentration, C_{Gi} (1.59×10^{-4} mol/cm³) will be assumed to be the same as the initial concentration of Ge amide in solution to simplify the estimation of change of C_{G3} . The conversion of Ge amide to Ge monomer will happen rapidly. In reality, C_{G3} may increase rapidly directly after injection of Ge amide and during nucleation and then decrease throughout the growth as the Ge monomer is consumed into NCs. Second, the decrease of C_{G3} will be 1st order exponential because the production of Ge monomer is

from the decomposition of a single species, Ge amide. C_{G3} decay will be represented with the expression

$$C_{G3}(t) = C_{Gi} \exp\left[-t/\tau_G\right], \quad (22)$$

where C_{Gi} (1.59×10^{-4} mol/cm³) is the initial concentration of Ge amide and τ_G (estimated 960 s) is the characteristic time constant describing the decay of C_{G3} .

The characteristic time constant (τ_G) is estimated by fitting an exponential decay equation to estimated $C_{G3}(t)$ values. C_{G3} can be estimated with

$$C_{G3}(t) = \frac{N_{Ge} - N_{NC} \left(\frac{4}{3} \pi R_t^3 \frac{\rho_{Ge}}{MW_{Ge}} \right)}{V_{sol}}, \quad (23)$$

where N_{Ge} (0.001 mol) is the number of moles of Ge monomer present in solution, N_{NC} is the number of Ge NCs, R_t is the NC radius at time t calculated with Equation (1) and V_{sol} (6.318 cm³) is the volume of solution. N_{NC} is calculated with the assumption that there is 90% conversion of Ge monomer to Ge NC and that the total number of moles converted is present in NC of the average size of the final NC radius measurement R_∞ ($t = 3600$ s).

N_{NC} is calculated with the expression;

$$N_{NC} = \frac{N_{Ge} MW_{Ge} \varepsilon}{\frac{4}{3} \pi R_\infty^3 \rho_{Ge}}, \quad (24)$$

where ε (0.9) is the yield of Ge monomer converted to NCs. The C_{G3} estimate is calculated and plotted in Figure 9. The C_{G3} estimate is fitted with an exponential decay expression;

$$C_{G3} = C_{est} \exp\left[-t/\tau_G\right] + A_{est}, \quad (25)$$

where C_{est} (1.7×10^{-4} mol/cm³) and A_{est} (6.2×10^{-6} mol/cm³) are fitting constants and τ_G (960 s) is the characteristic time constant. As this is an estimate based upon an

assumption of no change in N_{NC} over time, the C_{est} and A_{est} in this expression are not used, but rather Equation (22) is created with the characteristic time constant from Equation (25). C_{Gi} is calculated from the experimental conditions and is assumed to be the most accurate value for the initial concentration of Ge monomer.

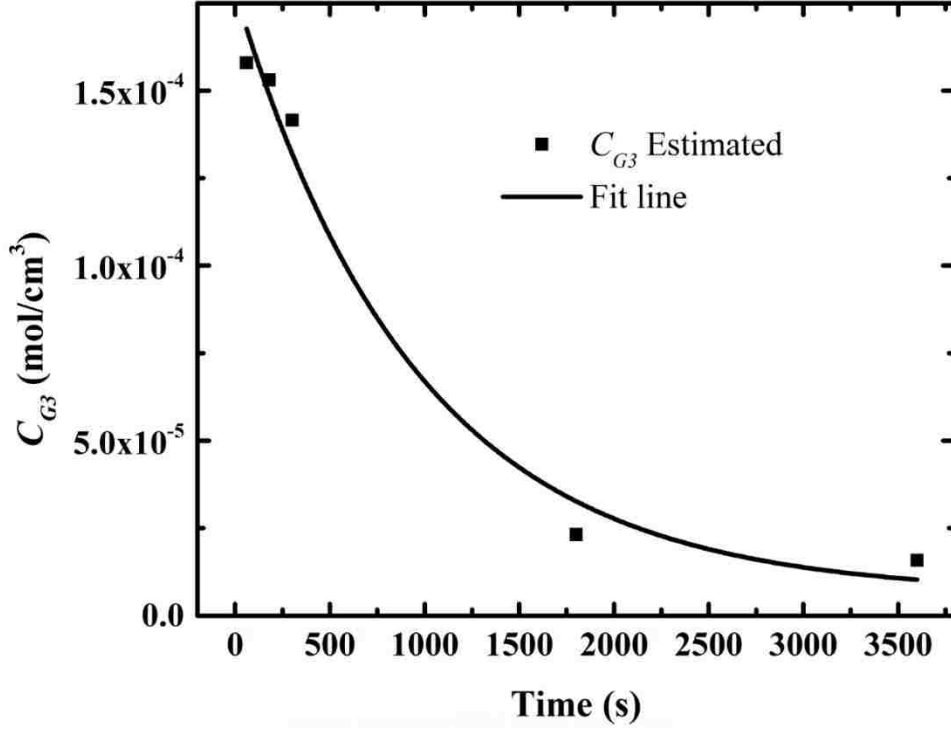


Figure 9. Estimate of C_{G3} for time interval in the synthesis. Line is fitted estimated $R(t)$ from Equation (1).

The expression for $C_{G3}(t)$ is inserted into Equation (26) to calculate flow of Ge monomer through the BL. The RHS is now integrated from t_0 to t , with $t_0 = 0s$ as the initial condition. The left side is integrated from R_0 to $R_0 + \Delta R$ resulting in

$$\frac{\rho_{Ge}\delta_c}{MW} (R - \delta_c \ln(R + \delta_c)) \Big|_{R_0}^{R_0 + \Delta R} = D_{AB} \left[\left[-C_{Gi} e^{[-t/\tau_G]} \right]_{t_0}^t - \int_{t_0}^t C_E(t) dt \right], \quad (26)$$

where $\int C_E dt$ is the only unknown quantity. The equation is simplified further to

$$\frac{\rho_{Ge}\delta_c}{MW} (R - \delta_c \ln(R + \delta_c)) \Big|_{R_0}^{R_0 + \Delta R} = D_{AB} \left[C_{Gi} \tau_G \left(1 - e^{[-t/\tau_G]} \right) - \int_{t_0}^t C_E(t) dt \right], \quad (27)$$

then rearranged with $\int C_E(t)dt$ on the LHS makes $\int C_E(t)dt$ become the dependent variable in the following expression.

$$\int_{t_0}^t C_E(t)dt = - \left(\frac{\rho_G e \delta_c}{D_{AB} M W} (R - \delta_c \ln(R + \delta_c)) \Big|_{R_0}^{R_0 + \Delta R} - C_{Gi} (1 - e^{[-t/\tau_G]}) \right) \quad (28)$$

For simplification, $\int C_E(t)dt$ is represented by $\gamma(t)$. Plotting the RHS of Equation (28) returns the numerical values of $\gamma(t)$. Incremental values of t are input to $R(t)$ generated by the fit line in Equation (1) to approximate the experimental data provided by Tribby *et al.*[13]. Once values for $\gamma(t)$ are calculated, they are plotted in increments of 500 s from 0 to 4000 s in Figure 10.

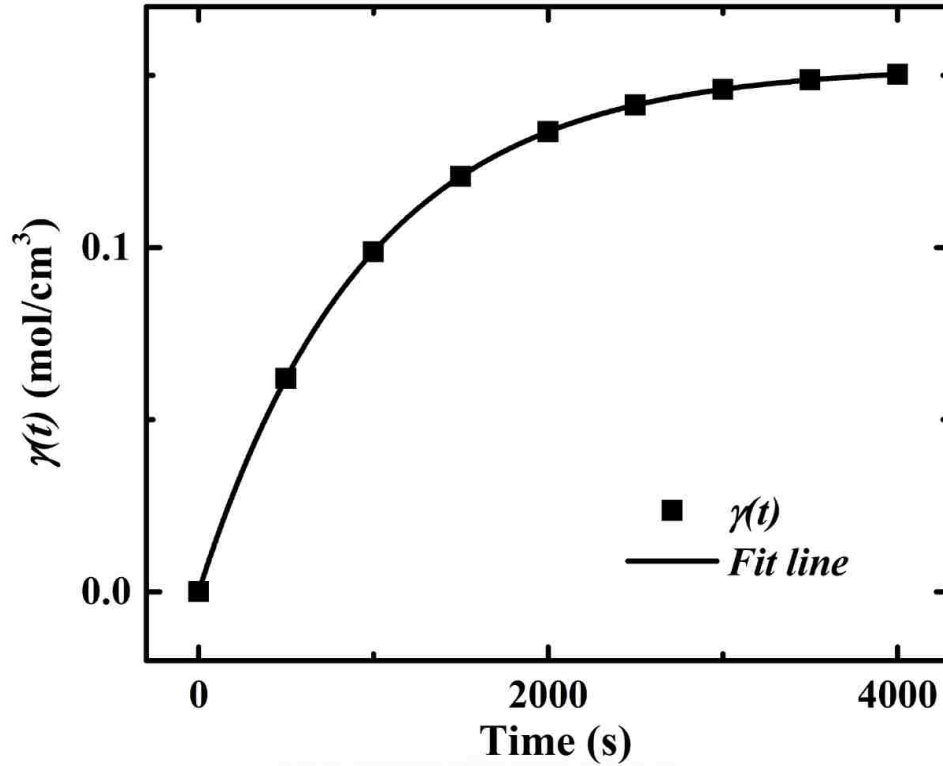


Figure 10: Plot of $\gamma(t)$ which is equivalent to $\int C_E(t)dt$ over the reaction time in the experiment.

Casual observation would suggest that the general form of $\gamma(t)$ is similar to $R(t)$.

Fitting a curve empirically to numerical values of $\gamma(t)$ yields an equation with the form

$$\gamma_{fit}(t) = C_{Ei}\tau_c \left[1 - \exp\left[-t/\tau_c\right] \right] , \quad (29)$$

where C_{Ei} ($1.587E^{-6}$ mol/cm³) is the saturation concentration of Ge monomer and τ_c (960 s) represents a characteristic timescale for the decay in concentration of Ge monomer just above the surface of the crystal. The $\gamma(t)$ fitted to the numerical solution has an R^2 value of 1. Now that there is an analytical expression for $\gamma(t)$, both sides of the expression are differentiated to produce the expression

$$\frac{d\gamma(t)}{dt} = C_E(t) = C_{Ei}\exp\left[-t/\tau_c\right] , \quad (30)$$

which is an expression for the change in C_E with respect to time.

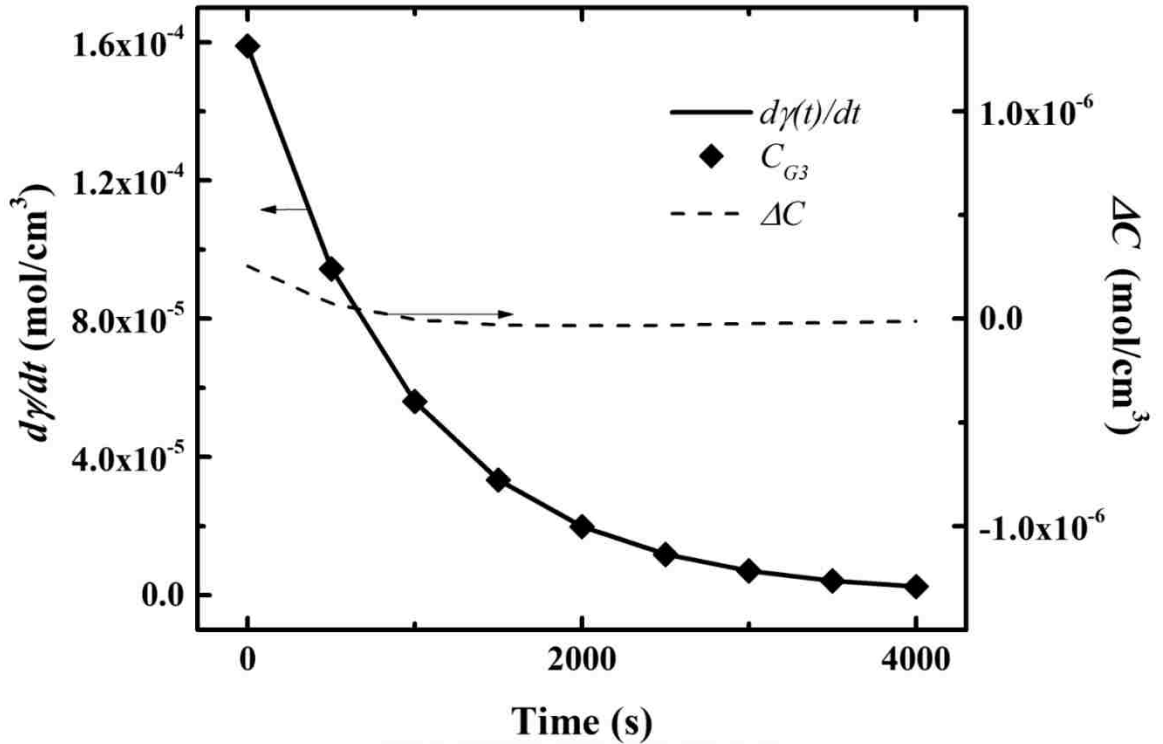


Figure 11. Plot of $d\gamma(t)/dt$ over time overlaid with $C_E(t)$. $d\gamma(t)/dt$ is shown to be equivalent to $C_E(t)$. Notice that the concentration profile closely parallels the concentration of the bulk solution $C_{G3}(t)$. The concentration delta, ΔC , between $C_{G3}(t)$ and $C_E(t)$ is shown as a dashed line.

Plotting the values of $C_E(t)$ shows that the concentration immediately after t_0 is at C_{Ei} (1.587×10^{-4} mol/cm³) which is nearly the same initial concentration of Ge monomer in the bulk solution. The delta between $C_{G3}(t)$ and $C_E(t)$ is minimal, shortly after t_0 . This infers there is little resistance to the Ge monomer diffusion through the BL. Overlaying plots of $C_{G3}(t)$ and $C_E(t)$ in Figure 11 show that the two concentrations closely parallel one another throughout the run. The difference between $C_{G3}(t)$ and $C_E(t)$, ΔC , is plotted with both concentration values in Figure 11. The values for ΔC are more than 2 orders of magnitude less than $C_E(t)$, ranging from 3×10^{-7} mol/cm³ at t_0 to ~ 0 mol/cm³ beyond 500 s during the reaction run. Beyond approximately 500 s in the synthesis, the estimate for $C_{G3}(t)$ is indistinguishable from $C_E(t)$, indicating that the diffusion occurs very rapidly from bulk solution to the surface of the NC. These results highly suggest that the system used for synthesis is not diffusion limited, therefore kinetically limited models must be considered.

Surface Kinetics

Surface kinetics will be described in two steps. First the adsorption and desorption characteristics will be used to create a rate of change for the surface coverage of Ge monomers and organic coordinating ligands (OA in this case). Once the rate expression is known, then it can be incorporated into a growth model to describe the change in radial growth with respect to time.

The adsorption of the Ge monomer to the surface of the NC is proportional to the Ge monomer concentration in equilibrium with the surface, the adsorption rate constant, k_{ad} , and the fraction of open sites. Desorption of the Ge monomer is proportional only to

the fraction of open sites and the desorption rate coefficient (k_{des}). Adsorption of the OA ligands is proportional to the concentration of ligand in solution, the ligand adsorption rate coefficient, k'_{ad} , and the fraction of open Ge sites. Conversely, desorption of the ligands is proportional only to the fraction of Ge sites occupied by the ligands and the ligand desorption rate coefficient, k'_{des} . A rate of fractional site coverage as a function of time is create using a Langmuir-Hinshelwood kinetics site balance of the form,

$$\frac{d\theta_{Ge}}{dt} = k_{ad}C_E(t)\theta_{Ge}(t) - k_{des}\theta_{Ge}(t) - k'_{ad}C_L(t)\theta_{Ge}(t) + k'_{des}\theta_L(t) , \quad (31)$$

where $\theta_{Ge}(t)$ is the fraction of open Ge binding sites on the NC and $\theta_L(t)$ is the fraction of ligand occupied binding sites and $C_L(t)$ is the concentration of ligands in the solution.

Desorption of Ge monomer from the surface of the crystal is assumed to be much smaller than the other terms in Equation (31). Once the NC radius is above the critical radius the growth rate is very high due to the high energy of the NC surface[5]. Once bound with single or multiple atoms of Ge on the surface, it is unlikely for Ge to dissociate from the surface of the Ge NC. Each monolayer of Ge will make the NC more stable thermodynamically and reduce the surface energy and unlikely to proceed in the opposite direction (desorption). Therefore, desorption of Ge monomer from the surface of the NC while growing will be considered insignificant for this calculation. k_{des} is then assumed to be much smaller than the other terms on the right side of Equation (31) and the term $k_{des}\theta_{Ge}(t)$ is eliminated. The ligand concentration changes during the course of the reaction, however, it is a small change in comparison to C_L and assuming it is constant simplifies the site balance equation. The impact of this simplification must be assessed. Using a Ge monomer NC conversion yield of 90 % [10] and assuming that the ligands attach with 100 % binding rate to open Ge sites on the NCs, the change in C_L

over the course of reaction would be $9.1 \times 10^{-6} \text{ mol/cm}^3$. This is more than an order of magnitude smaller than the concentration itself, so this change is not significant, especially when considering that it is unlikely for 100 % of the Ge sites would be occupied with ligands. Since ligands would not be significantly consumed once the growth began, the ligand concentration, C_L , is considered constant throughout the growth of the NC and is represented as \bar{C}_L . Equation (31) with \bar{C}_L substituted and $k_{des}\theta_{Ge}(t)$ removed is rewritten as

$$\frac{d\theta_{Ge}}{dt} = k_{ad}C_E(t)\theta_{Ge}(t) + k'_{des}\theta_L(t) - k'_{ad}\bar{C}_L\theta_{Ge}(t). \quad (32)$$

A substitution was made for $\theta_L = 1 - \theta_{Ge}$ and $C_E(t)$ to simplify the equation to only contain $\theta_{Ge}(t)$ and t variables, resulting in

$$\frac{d\theta_{Ge}}{dt} = k_{ad}C_{Ei}\exp[-t/\tau_c]\theta_{Ge}(t) + k'_{des}(1 - \theta_{Ge}(t)) - k'_{ad}\bar{C}_L\theta_{Ge}(t), \quad (33)$$

which is simplified to

$$\frac{d\theta_{Ge}}{dt} + (k'_{des} + k'_{ad}\bar{C}_L - k_{ad}C_{Ei}\exp[-t/\tau_c])\theta_{Ge}(t) = k'_{des}, \quad (34)$$

which is a non-homogeneous differential equation that must be solved with numerical methods.

Equation (34) can be partially solved analytically by utilizing an integrating factor $P(t)$ which is written as Equation (35).

$$P(t) = k'_{des} + k'_{ad}\bar{C}_L - k_{ad}C_{Ei}\exp[-t/\tau_c] \quad (35)$$

Inserting the integrating factor into Equation (34) and performing the normal steps to solve this differential equation results in the partially evaluated Equation (36).

$$\theta_{Ge}(t) = \frac{k'_{des}}{e^{\int P(t)dt}} \int e^{\int P(t)dt} dt + \frac{C1}{e^{\int P(t)dt}} \quad (36)$$

where $C1$ is the integration constant for the differential equation in Equation (34). When $P(t)$ is substituted for Equation (36) and simplified, the resulting Equation (37) has an integral that is not possible to execute with analytical means.

$$\theta_{Ge}(t) = \frac{k'_{des}}{\exp[k'_{des}t + k'_{ad}\bar{C}_L t + k_{ad}C_{Ei}\tau_c \exp[-t/\tau_c]]} \int \exp[k'_{des}t + k'_{ad}\bar{C}_L t + k_{ad}C_{Ei}\tau_c \exp[-t/\tau_c]] dt + \frac{C1}{\exp[k'_{des}t + k'_{ad}\bar{C}_L t + k_{ad}C_{Ei}\tau_c \exp[-t/\tau_c]]} \quad (37)$$

The unevaluated Equation (38) below, which is an excerpt from Equation (37), is not solvable with analytical methods due to the nesting of exponential terms.

$$\int \exp[k'_{des}t + k'_{ad}\bar{C}_L t + k_{ad}C_{Ei}\tau_c \exp[-t/\tau_c]] dt \quad (38)$$

To calculate a solution for $\theta_{Ge}(t)$ numerically the constants k_{ad} , k'_{ad} and k'_{des} must be defined and an initial value must be defined. Values for k'_{ad} ($2.4 \text{ cm}^3/\text{mol}\cdot\text{s}$) and k'_{des} ($8.2 \times 10^{-6} \text{ s}^{-1}$) for alkanethiols adsorbing to Ge (111) crystal surface obtained experimentally by Kosuri *et al.*[24] are used as an initial approximation for this work due to their similarity to the coordinating ligand used in this synthesis. In the work by Kosuri *et al.*, hexadecanethiol and 1-octadecanethiol are the species that are being studied compared to hexadecylamine and octadecene in this work. The value for k_{ad} ($2.4 \text{ cm}^3/\text{mol}\cdot\text{s}$) is also set at the adsorption coefficient for Ge monomer as a starting point. This number will be optimized later in this work, but this first “guess” will be adequate as an initial estimate. Table 2 shows all the coefficients and values that are used in this estimation. The initial value of $\theta_{Ge}(t)$ is assumed to be 1 at a time of zero seconds. This is an assumption that at time zero, the adsorption of coordinating ligands to the surface of the NC will be sufficiently small to make $\theta_L(t)$ zero. Therefore the surface will be entirely an exposed Ge surface. This is intuitive, since at time zero there will only be a nucleus formed and no radial growth has occurred.

Using the constants defined above and the initial value, the expression of CI can be found. If values of Equation (38) can be calculated with a numerical method, it can be plotted and a value for Equation (38) at $t = 0$ can be determined and entered into Equation (37) also evaluated at $t = 0$ to determine the constant CI .

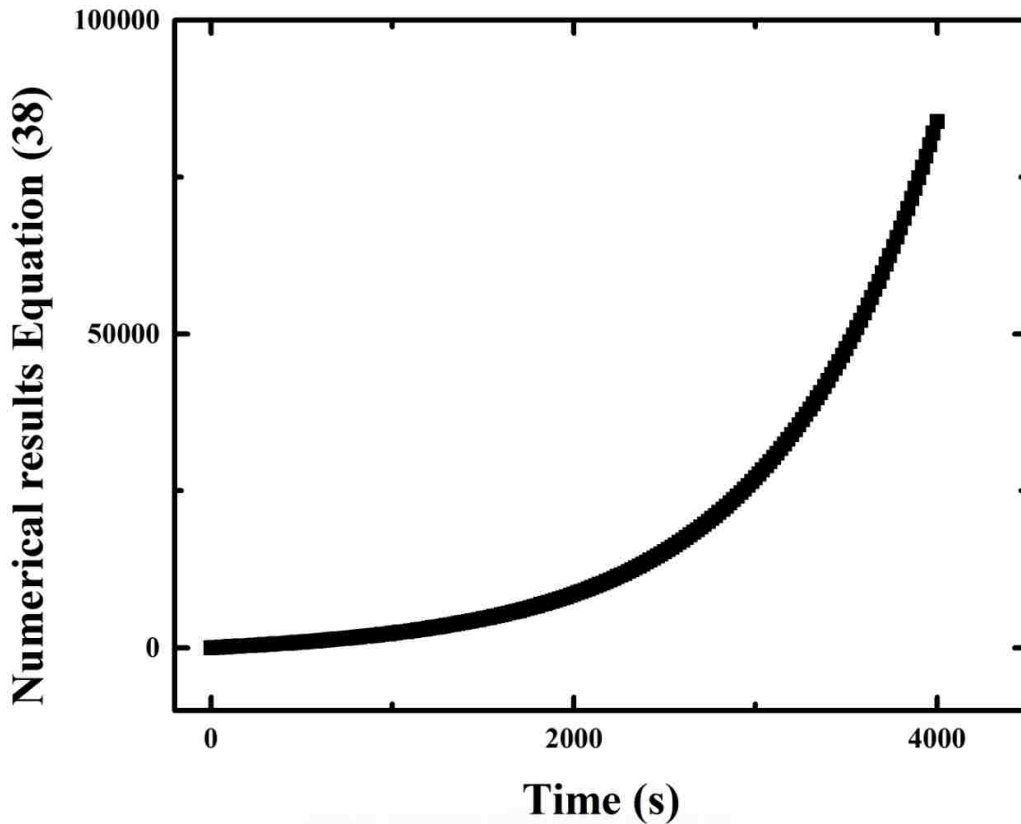


Figure 12: Numerical solution to the integral in Equation (38)

Equation (38) can be integrated numerically with “NIntegrate”, an embedded feature of Mathematica™, which is plotted in (Figure 12). The values are listed in appendix Table A3 when calculated with the Mathematica™ program “ThetaVTime” detailed in Appendix B. When these actions are completed, the value of Equation (38) at

$t = 0$ is also revealed to be zero. When put into Equation (37) evaluated at $t = 0$ the value for $C1$ is shown in Equation (39) below.

$$C1 = e^{k_{ad}C_{Ei}\tau_c} \quad (39)$$

$C1$ is then entered into Equation (37) which yields Equation (40). Equation (40) is written

$$\theta_{Ge}(t) = \frac{k'_{des}}{\exp[k'_{des}t + k'_{ad}\bar{C}_L t + k_{ad}C_{Ei}\tau_c \exp[-t/\tau_c]]} \int_0^t \exp \left[k'_{des}t' + k'_{ad}\bar{C}_L t' + k_{ad}C_{Ei}\tau_c \exp \left[-t'/\tau_c \right] \right] dt' + \frac{e^{k_{ad}C_{Ei}\tau_c}}{\exp[k'_{des}t + k'_{ad}\bar{C}_L t + k_{ad}C_{Ei}\tau_c \exp[-t/\tau_c]]} , \quad (40)$$

where t' is the time variable to be integrated numerically. This can be re-written as

Equation (41), which is simplified, but still requires a numerical solution to $\theta_{Ge}(t)$.

$$\theta_{Ge}(t) = k'_{des} \int_0^t \exp \left[(k'_{des} + k'_{ad}\bar{C}_L)(t' - t) + k_{ad}C_{Ei}\tau_c \exp \left[-(t' + t)/\tau_c \right] \right] dt' + \exp \left[\frac{k_{ad}C_{Ei}\tau_c}{k'_{des}t + k'_{ad}\bar{C}_L t + k_{ad}C_{Ei}\tau_c \exp[-t/\tau_c]} \right] \quad (41)$$

Equation (41) can be evaluated analytically and numerically simultaneously to get numerical values for $\theta_{Ge}(t)$ within the program “ThetaVtime”. However, to develop a model for the radial growth rate, an expression for $\theta_{Ge}(t)$ as a function of time will be used. In order to accomplish this, an approximation of the numerical solution to Equation (34) is needed. The most direct way to achieve this is by generating a Runge Kutta Order 9[25] (RK9) solution to Equation (34) directly and fitting a suitable expression to describe the numerical solution. The results for $\theta_{Ge}(t)$ can be represented as an exponential.

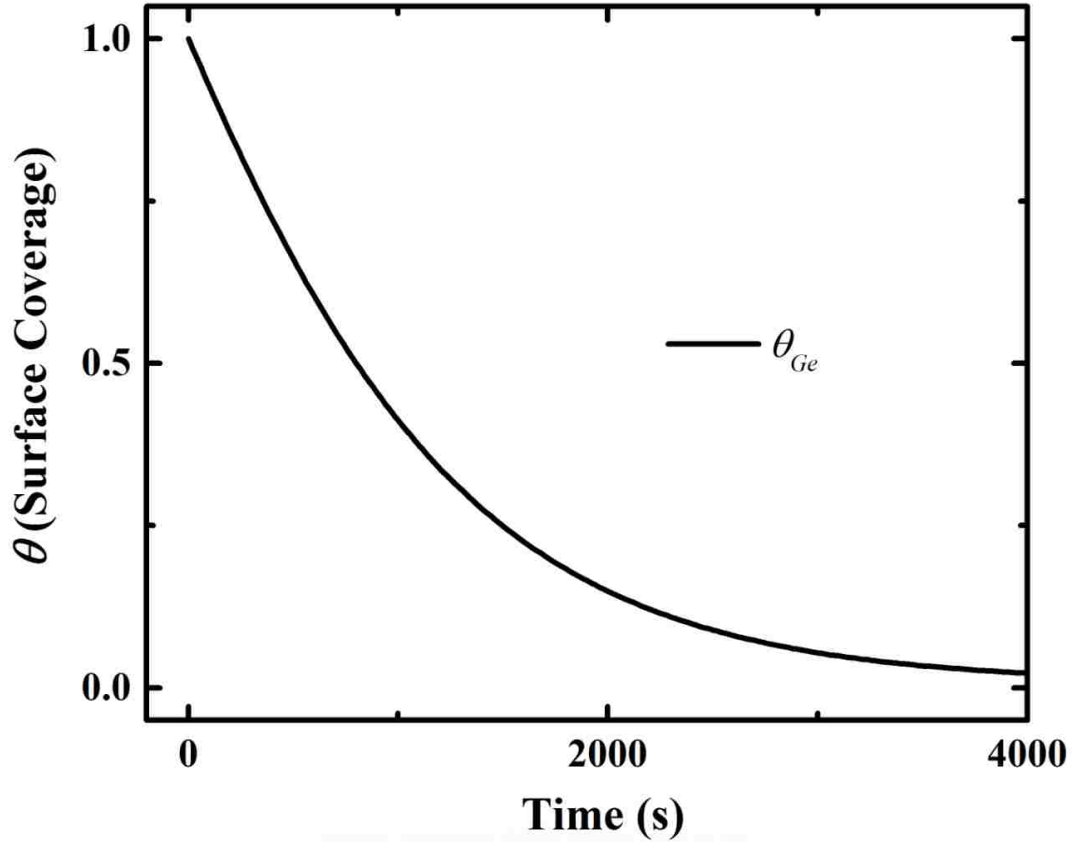


Figure 13: Numerical solution for $\theta_{Ge}(t)$ results from Equation (34).

The numerical solution to $\theta_{Ge}(t)$ is fitted with a single exponential with an expression of the form

$$\theta_{Ge}(t) = D \exp\left[-t/\tau_{\theta_{Ge}}\right] + E, \quad (42)$$

where D (1.06), E (-0.015) and $\tau_{\theta_{Ge}}$ (1108 s) are fitting coefficients for the expression to the numerical solution. The R^2 value for the fit equation is 0.9979 which is presented in Appendix A.

The double exponential equation form fits $\theta_{Ge}(t)$ slightly better than the single exponential form. The differences between the two fit models are more pronounced when the model is optimized in the Optimization section of this Chapter, resulting in an

obvious poor fit for the single exponential. For simplicity, the double exponential form will be used for this initial approximation and the optimized fit to experimental data. The fitted double exponential equation has the form

$$\theta_{Ge}(t) = A \exp\left[-t/\tau_{\theta_{Ge1}}\right] + B \exp\left[-t/\tau_{\theta_{Ge2}}\right] + C, \quad (43)$$

where A (0.5), B (0.543), C (-0.015), $\tau_{\theta_{Ge1}}$ (1108 s) and $\tau_{\theta_{Ge2}}$ (1108 s) are the fitting coefficients for the fit to the numerical solution to $\theta_{Ge}(t)$. When fitted to the numerical solution, Equation (43) has an adjusted R^2 value of 0.9991 which can be seen in Appendix A. When the fitted equation for $\theta_{Ge}(t)$ is inserted back into Equation (34), the numerical results show that the rate of change of θ_{Ge} is negative and increases with time through the NC reaction and flattens to near zero at the end of the run. Therefore, this equation, numerically solved shows the fraction of open Ge surface sites (Figure 14) decreasing over time as the reaction slows. In concept, this result agrees with the experimental data in Figure 2, assuming that as the percentage of open Ge sites decreases, the growth will slow.

If one returns to Equation (41) and solves it with a combination of a numerical method with NIntegrate scripting in Mathematica™ and analytically in the script “ThetaVtime”, a series of numerical result can be generated. If the double exponential expression in Equation (43) is then fitted to this partially analytical solution the fitting coefficients A (0.5), B (0.543), C (-0.015), $\tau_{\theta_{Ge1}}$ (1108 s) and $\tau_{\theta_{Ge2}}$ (1108 s) are the same as the results for the previous method of solving Equation (34) numerically using RK9 directly. Therefore, the two methods for solving the differential equation have the same result numerically. This double exponential expression fitted to the RK9 solution for

$\theta_{Ge}(t)$ will then be useful in the model that will be created in the Optimization section of this chapter.

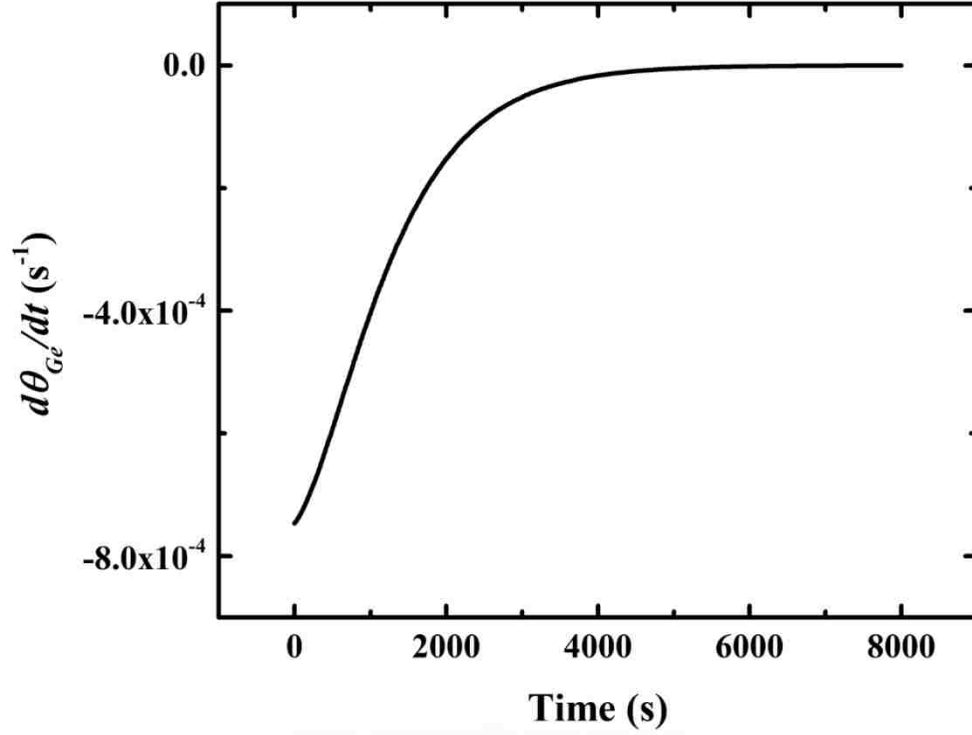


Figure 14: $d\theta_{Ge}/dt$ over reaction timeframe as determined from the RK9 numerical solution to Equation (34). $d\theta_{Ge}/dt$ represents the slope of the expected surface coverage θ_{Ge} vs. time.

The rate of change of ligand coverage, θ_L , can be written the same way as θ_{Ge} . The rate of attachment for ligands is proportional to $\theta_{Ge}(t)$, which is expressed as $1 - \theta_L(t)$, k'_{ad} and C_L . The desorption rate of ligands is proportional to k'_{des} and $\theta_L(t)$. The rate of adsorption of Ge monomers, which removes sites available to ligands, is proportional to k_{ad} , C_E and $\theta_{Ge}(t)$, which is expressed as $1 - \theta_L(t)$. The expression for the rate of change of θ_L is written as

$$\frac{d\theta_L}{dt} = k'_{ad}C_L(t)(1 - \theta_L(t)) - k'_{des}\theta_L(t) - k_{ad}C_E(t)(1 - \theta_L(t)). \quad (44)$$

The previous assumption for a constant C_L is made here as well, therefore C_L is considered constant throughout growth of the NC and is represented as $\overline{C_L}$ and re-written

$$\frac{d\theta_L}{dt} = k'_{ad}\overline{C_L}(1 - \theta_L(t)) - k'_{des}\theta_L(t) - k_{ad}C_E(t)(1 - \theta_L(t)) , \quad (45)$$

which is simplified to the following form.

$$\frac{d\theta_L}{dt} = (-k'_{ad}\overline{C_L} - k'_{des} - k_{ad}C_E(t))\theta_L(t) + (k'_{ad}\overline{C_L} + k_{ad}C_E(t)) \quad (46)$$

The earlier expression for $C_E(t)$ is substituted into this differential equation. Since this is also a non-homogeneous differential equation, it must be solved with numerical methods as well. RK9 as an algorithm in Mathematica™ is also used to obtain the numerical solution to $\theta_L(t)$. Plotting the values for $1 - \theta_L(t)$ becomes a second solution for $\theta_{Ge}(t)$ and a means to compare the solutions for $\theta_{Ge}(t)$ and $\theta_L(t)$. This numerical solution for $1 - \theta_L(t)$ using the ligand site balance with RK9 shows that $1 - \theta_L(t)$ fits an exponential decay of the following form.

$$1 - \theta_L(t) = A1 \exp\left[-\frac{t}{\tau_{\theta_{Gea}}}\right] + B1 \exp\left[-\frac{t}{\tau_{\theta_{Ge2a}}}\right] + C1 \quad (47)$$

where $A1$ (0.5), $B1$ (0.543), $C1$ (-0.015), $\tau_{\theta_{Gea}}$ (1108 s) and $\tau_{\theta_{Ge2a}}$ (1108 s) are the fitting coefficients. The fitting coefficients and equation are identical to the fitted expression for $\theta_{Ge}(t)$ in Equation (34), which confirms that the methods of calculating surface coverage are self-consistent. The results of the numerical solutions for $\theta_{Ge}(t)$ and $\theta_L(t)$ are plotted in Figure 15. Notice that the two solutions are mirror images as expected.

A simplification of the equation can be made to facilitate a confirmation of the numerical solution. To provide an approximation of θ_L , the last term on Equation (44)

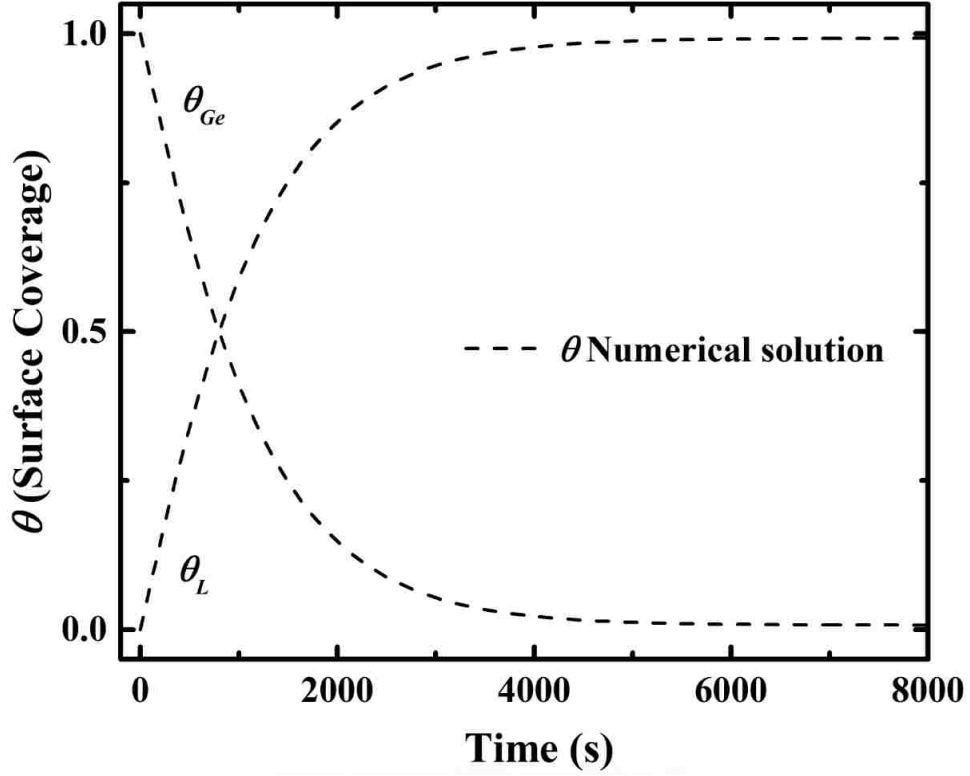


Figure 15. Numerical solutions for open Ge binding sites, $\theta_{Ge}(t)$, and ligand occupied Ge binding sites as a function of time.

will be omitted. By doing so, a path for analytical approximation of the solution is opened. Consider the case of a Ge monomer adsorbing to an open Ge site on the surface of the nanocrystal. The adsorption of another Ge monomer to the surface does not remove the ability of a ligand to adsorb to that site with 100 % certainty, due to the Ge monomer itself becoming another binding site once adsorbed to the crystal surface. Omitting it from the calculation is reasonable for an approximation of surface coverage also because its contribution to θ_L is the smallest of the three terms in Equation (44). The last term is stricken from Equation (44), to reveal an approximate expression for $d\theta_L/dt$,

$$\frac{d\theta_L}{dt} = k'_{ad}\overline{C}_L(1 - \theta_L(t)) - k'_{des}\theta_L(t), \quad (48)$$

which is a homogeneous ODE. Equation (48) is solved to obtain the $\theta_L(t)$ function.

Rearranging terms yields

$$\frac{d\theta_L}{dt} + (k'_{ad}\bar{C}_L + k'_{des})\theta_L(t) = k'_{ad}\bar{C}_L, \quad (49)$$

an ODE of the standard form which is solved by separating variables and using an integrating factor. The integrating factor, $\rho(t)$, has the following form.

$$\rho = \rho(t) = \exp[\int (k'_{ad}\bar{C}_L + k'_{des})dt] \quad (50)$$

Evaluating the integrating factor yields the following expression.

$$\rho = \rho(t) = e^{(k'_{ad}\bar{C}_L + k'_{des})t} \quad (51)$$

Equation (49) is multiplied by the integrating factor to yield the following expression.

$$e^{(k'_{ad}\bar{C}_L + k'_{des})t} \frac{d\theta_L}{dt} + (k'_{ad}\bar{C}_L + k'_{des})\theta_L(t)e^{(k'_{ad}\bar{C}_L + k'_{des})t} = k'_{ad}\bar{C}_L e^{(k'_{ad}\bar{C}_L + k'_{des})t} \quad (52)$$

The equation is simplified by creating constants a and b with the following two expressions in Equations (53) and (54).

$$a = k'_{ad}\bar{C}_L \quad (53)$$

$$b = (k'_{ad}\bar{C}_L + k'_{des}) \quad (54)$$

When a and b are substituted into Equation (52), the resulting expression is Equation (55).

$$e^{bt} \frac{d\theta_L}{dt} + b\theta_L(t)e^{bt} = ae^{bt} \quad (55)$$

Solving the differential Equation (55) by separating the variables θ_L and t and then integrating both sides with respect to their variables results in Equation (56) where c is the integration constant.

$$\theta_L(t)e^{bt} = \frac{a}{b}e^{bt} + c \quad (56)$$

Finding the expression for the constant (c) is done by evaluating Equation (56) at the initial condition; where, $t_0 = 0$ s, $\theta_L(t_0) = 0$. The initial condition is substituted into Equation (56) to yield $c = -a/b$ which is then simplified to Equation (57).

$$\theta_L(t) = \frac{a}{b}(1 - e^{-bt}) \quad (57)$$

Substituting a and b into Equation (57) results in the following equation.

$$\theta_L(t) = \frac{(k'_{ad}\bar{C}_L)}{(k'_{ad}\bar{C}_L + k'_{des})} (1 - e^{-(k'_{ad}\bar{C}_L + k'_{des})t}) \quad (58)$$

Consequently, $\theta_{Ge}(t)$, can be evaluated with Equation (59).

$$\theta_{Ge}(t) = 1 - \frac{(k'_{ad}\bar{C}_L)}{(k'_{ad}\bar{C}_L + k'_{des})} (1 - e^{-(k'_{ad}\bar{C}_L + k'_{des})t}) \quad (59)$$

To represent $\theta_L(t)$ graphically, the constants k'_{ad} and k'_{des} are defined the same as the numerical solutions for $\theta_{Ge}(t)$. Table 2 shows the values for the inputs of Equation (59).

Table 2: Model input parameters for plotting of $\theta_L(t)$ and $\theta_{Ge}(t)$ over time.

| Variable | Value |
|------------------------------------|-----------------------|
| k_{ad} (cm ³ /mol-s) | 2.4 |
| k'_{ad} (cm ³ /mol-s) | 2.4 |
| k'_{des} (s ⁻¹) | 8.20×10 ⁻⁶ |
| C_L (mol/cm ³) | 4.7×10 ⁻⁴ |

The values in Table 2 are substituted into Equation (59), and the result is plotted in Figure 16. Figure 16 also shows the numerical solution to $\theta_L(t)$ and $\theta_{Ge}(t)$. The numerical solution and the analytical estimation agree closely with one another and present the same general solution to $\theta_L(t)$ and $\theta_{Ge}(t)$. This approximation helps prove that the numerically solved and fitted expressions are not grossly different from the best approximation for an analytical solution.

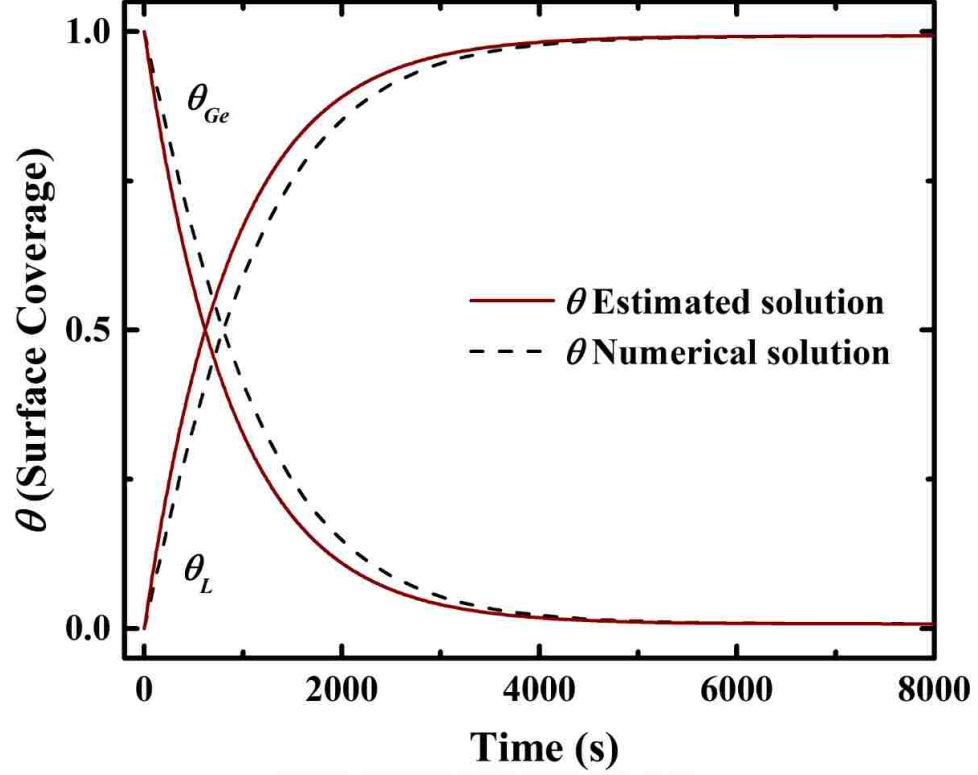


Figure 16. Fractional surface coverage, θ , of the growing Ge NC as a function of time. Ligand coverage is represented by θ_L and open germanium area is represented by θ_{Ge} . The red lines represent the analytical estimation and the dashed lines represent the numerical solution fit.

Substituting into the original ODE for θ_L , results in the following expression for $d\theta_L/dt$ which is represented graphically in Figure 17.

$$\frac{d\theta_L}{dt} = k'_{ad}\bar{C}_L - (k'_{ad}\bar{C}_L + k'_{des}) \frac{(k'_{ad}\bar{C}_L)}{(k'_{ad}\bar{C}_L + k'_{des})} (1 - e^{-(k'_{ad}\bar{C}_L + k'_{des})t}) \quad (60)$$

The analytical estimation of $d\theta_L/dt$ in Figure 17 plotted from Equation (60) agrees with the results in Figure 16. Furthermore, a gross check of $d\theta_L/dt$ in Figure 17 shows that as expected, the increase of θ_L is large at the beginning of the reaction where the surface coverage of ligand is assumed to be at zero. The rate of change of θ_L gradually decreases as the reaction progresses and nears zero after ~ 3000 s. Now that it is

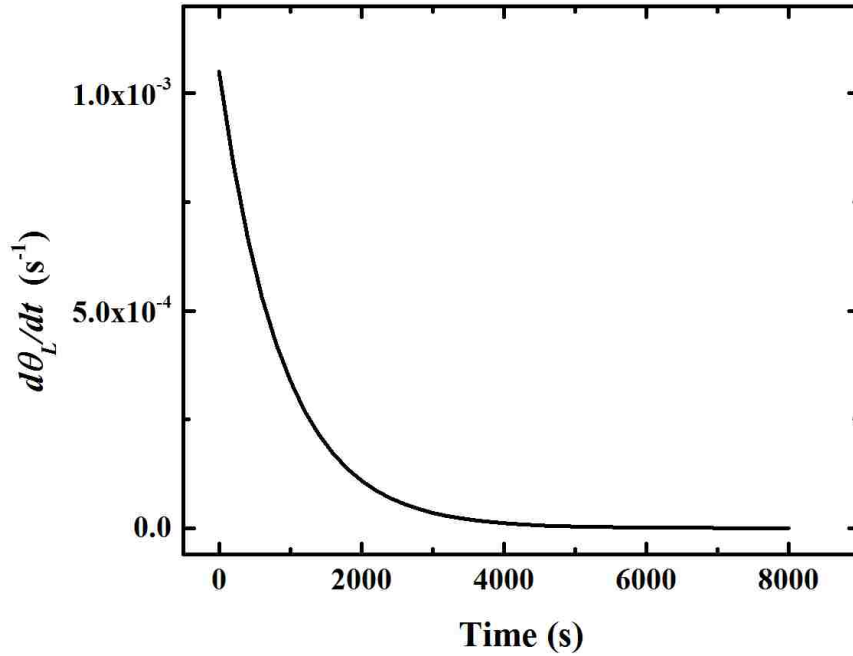


Figure 17: $d\theta_L/dt$ over reaction time as calculated with the analytical approximation. Fitting each value of t used to calculate $\theta_L(t)$, it is evident that the values for $d\theta_L/dt$ accurately represent the slope of $\theta_L(t)$.

established that the numerical solutions for the change in θ_{Ge} and θ_L over time look reasonable with estimates for the adsorption and desorption coefficients substituted, the growth model will be developed with the fitted expression for θ_{Ge} .

Growth Model

To derive an expression for radial growth rate, θ and t must be related to the flow of Ge monomer towards the surface of the NC. The molar flow rate of Ge monomer to the NC (J) in mol/s is related to the radial growth rate of the NC as a function of time is shown in Equation (61);

$$J = \frac{\rho_{Ge}}{MW_{Ge}} 4\pi R_{NC}^2 \frac{dR}{dt} , \quad (61)$$

where ρ_{Ge} (5.323g/cm^3) is crystalline Ge density, MW_{Ge} (72.59 g/mol) is the molecular weight of Ge and R_{NC} is the radius of the NC. Assuming negligible desorption of Ge monomer from the NC, the first term in Equation (32), $4\pi R_{CE}^2 \frac{\rho_{GeA}}{N_A} k_{ad} C_E(t) \theta_{Ge}(t)$, is the adsorption rate for Ge monomer. An expression for flow to the surface area of the NC is written with the rate of adsorption of Ge monomer,

$$J = 4\pi R_{CE}^2 \frac{\rho_{GeA}}{N_A} k_{ad} C_E(t) \theta_{Ge}(t) , \quad (62)$$

where ρ_{GeA} ($6.61 \times 10^{14}\text{ Ge sites/cm}^2$) is the areal surface density of Ge binding sites on the Ge NC, N_A is Avogadro's number and R_{CE} is the radius just above the surface of the NC where the monomer concentration is in equilibrium with the surface of the NC. The value for ρ_{GeA} has been calculated from experimental results by Schlier *et al.*[25]. 100 and 111 Ge crystal orientation site densities were determined from experimental data to be $6.3 \times 10^{14}\text{ Ge sites/cm}^2$ and $7.25 \times 10^{14}\text{ Ge sites/cm}^2$ respectively in the work by Schlier *et al.* The mean of the two experimental values is the estimate for ρ_{GeA} ($6.61 \times 10^{14}\text{ Ge sites/cm}^2$).

Setting flow of Equation (61) and (62) equal produces the following expression.

$$\frac{\rho_{Ge}}{MW_{Ge}} 4\pi R_{NC}^2 \frac{dR}{dt} = \frac{\rho_{GeA}}{N_A} 4\pi R_{CE}^2 k_{ad} C_E(t) \theta_{Ge}(t) \quad (63)$$

In this case, flow to the surface of the NC with radius R_{NC} , and flow through the area of the sphere with radius R_{CE} is considered equivalent due to the infinitely small difference in radius. The small difference results in a negligible difference in the mass balance around the sphere with radius R_{CE} and R_{NC} . Consequently, R_{CE} and R_{NC} are considered equal and are cancelled on opposing side of Equation (63) then simplified to

$$\frac{\rho_{Ge}}{MW_{Ge}} \frac{dR}{dt} = \frac{\rho_{GeA}}{N_A} k_{ad} C_E(t) \theta_{Ge}(t) , \quad (64)$$

which is then re-arranged into a differential equation of standard form,

$$\frac{dR}{dt} = \frac{MW_{Ge}}{\rho_{Ge}} \cdot \frac{\rho_{GeA}}{N_A} k_{ad} C_E(t) \theta_{Ge}(t) , \quad (65)$$

$$\text{and } k_{eff} = \frac{\rho_{GeA}}{N_A} k_{ad} \quad (66)$$

where k_{eff} is the adsorption rate coefficient for the NC. When k_{eff} (2.6×10^{-9} cm/s) is calculated with the approximation for k_{ad} , the value is 11 orders of magnitude less than k_c (305cm/s), further suggesting that the surface kinetics are limiting the growth.

Expressions for $C_E(t)$ and $\theta_{Ge}(t)$ from Equations (30) and (43) respectively are substituted into Equation (67), resulting in

$$\frac{dR}{dt} = \frac{MW_{Ge}}{\rho_{Ge}} \cdot \frac{\rho_{GeA}}{N_A} k_{ad} C_{Ei} e^{-t/\tau_c} (A \exp[-t/\tau_{\theta_{Ge1}}] + B \exp[-t/\tau_{\theta_{Ge2}}] + C) . \quad (67)$$

Next, the variables are separated and integrals are applied from R_0 to R and t_0 to t resulting in

$$\int_{R_0}^R dR = \int_{t_0}^t \frac{\rho_{GeA} MW_{Ge} k_{ad}}{\rho_{Ge} N_A} C_{Ei} e^{\frac{-t}{\tau_c}} \left(A e^{\frac{-t}{\tau_{\theta_{Ge1}}}} + B e^{\frac{-t}{\tau_{\theta_{Ge2}}}} + C \right) dt \quad (68)$$

which is then integrated on both sides and simplified to,

$$R = Q \left[-A \frac{\tau_c \tau_{\theta_{Ge1}}}{(\tau_c + \tau_{\theta_{Ge1}})} e^{\frac{-(\tau_c + \tau_{\theta_{Ge1}})t}{\tau_c \tau_{\theta_{Ge1}}}} - B \frac{\tau_c \tau_{\theta_{Ge2}}}{(\tau_c + \tau_{\theta_{Ge2}})} e^{\frac{-(\tau_c + \tau_{\theta_{Ge2}})t}{\tau_c \tau_{\theta_{Ge2}}}} - C \tau_c e^{-t/\tau_c} \right]_{t_0}^t + R_0 \quad (69)$$

where Q is expressed as

$$Q = \frac{\rho_{GeA} MW_{Ge} k_{ad}}{\rho_{Ge} N_A} C_{Ei} . \quad (70)$$

For optimization, the double exponential fit to the differential equation for $\theta_{Ge}(t)$ is used in order to provide an expression that converges easily in the optimization

program. Equation (69), when evaluated with the initial values from Table 3 does not initially provide a good fit to the experimental data. It is unlikely that the initial values used for the adsorption and desorption coefficients are accurate given the findings of these investigators[26, 27]. The other values (i.e. density, BL thickness and concentrations) are fixed values in this model, therefore, the adsorption and desorption coefficients must be found to optimize the model fit to the experimental data. Empirically, it is evident that the adsorption and desorption coefficient approximations could be much lower than the actual adsorption and desorption coefficients on the NC surface.

Table 3: Initial values for model input parameters.

| Variable | Initial Value |
|---------------------------------------|-----------------------|
| k_{ad} (cm ³ /mol-s) | 2.4 |
| k'_{ad} (cm ³ /mol-s) | 2.4 |
| k'_{des} (s ⁻¹) | 8.2 x10 ⁻⁶ |
| τ_C (s) | 960 |
| C_L (mol/cm ³) | 4.7x10 ⁻⁴ |
| ρ_{Ge} (g/cm ³) | 5.323 |
| MW (g/mol) | 72.59 |
| ρ_{GeA} (sites/cm ²) | 6.61x10 ¹⁴ |
| R_0 (nm) | 0.75 |

The adsorption and desorption coefficients can be tuned to fit the experimental data empirically. The challenge is that three variables, k_{ad} , k'_{ad} and k'_{des} , must be fitted to the experimental data simultaneously while optimizing the fit to the experimental data.

Optimization

The coefficients k_{ad} , k'_{ad} and k'_{des} within Equation (69) were optimized to make $R(t)$ fit to the experimental data. That requires numerical solutions to $\theta_{Ge}(t)$ to produce the fitting parameters A , B , C , $\tau_{\theta_{Ge1}}$ and $\tau_{\theta_{Ge2}}$ which are then used as an input to the growth model, Equation (69). An iterative process for suggesting new values for k_{ad} , k'_{ad} and k'_{des} was used and within the iterative process, the fitting parameters for $\theta_{Ge}(t)$ were calculated then an expression for $R(t)$ was created with the results. The end result is a model for $R(t)$ that is optimized to the experimental data and a script that gives an output of k_{ad} , k'_{ad} and k'_{des} .

Optimization Process

The following scheme which is also illustrated graphically in Figure 18 is used to perform the optimization of $R(t)$. The scripting used in Mathematica™ is available in Appendix B and C.

Outline of “Opt” script developed in Mathematica™ used for optimizing the fit to experimental data:

Step1: The initial values for k_{ad} , k'_{ad} and k'_{des} , from Table 3, are input to Equation (34).

The remaining parameters, C_{Ei} , τ_C , and C_L are also defined in Table 3 and will remain fixed in Equation (34) as follows.

$$\frac{d\theta_{Ge}}{dt} = (k_{ad}C_{Ei}exp[-t/\tau_C] - k'_{des} - k'_{ad}\bar{C}_L)\theta_{Ge} + k'_{des} \quad (34)$$

Step 2: The differential equation is then defined by the initial inputs in step 1. The differential equation for $\theta_{Ge}(t)$ is then solved numerically with RK9. Once Equation (34) is solved, an equation is fit to the numerical solution with the form,

$$\theta_{Ge}(t) = A \exp\left[-t/\tau_{\theta_{Ge}1}\right] + B \exp\left[-t/\tau_{\theta_{Ge}2}\right] + C \quad (43)$$

The coefficients A , B , C , $\tau_{\theta_{Ge}1}$ and $\tau_{\theta_{Ge}2}$ are input to Equation (66), which creates the expression for $R(t)$ used in Step 3. The double exponential method is used for the solution to $\theta_{Ge}(t)$ rather than the partial analytical method. This is done for two reasons; First, the solution results in the same numerical solution when complete, and second, the double exponential solution allows a path to get conversion of the optimization method and return true optimized adsorption and desorption coefficients.

Step 3: The model, Equation (69), is evaluated and the sum of the squares of the residual values (SSR) is calculated with respect to the experimental data. New inputs for the three variables, k_{ad} , k'_{ad} and k'_{des} are generated with the differential evolution algorithm [28, 29] (DEA) within Mathematica™. The DEA minimizes the SSR value by changing k_{ad} , k'_{ad} and k'_{des} to create an array of possible solutions for each such iteration. The best choice in each iteration is selected and then input to the script again. The script is repeated until an endpoint is reached.

Step 4: When the three variables have reached an endpoint, meaning that they have stopped changing with each iteration, the DEA is stopped and final values for k_{ad} , k'_{ad} and k'_{des} are reported in the script.

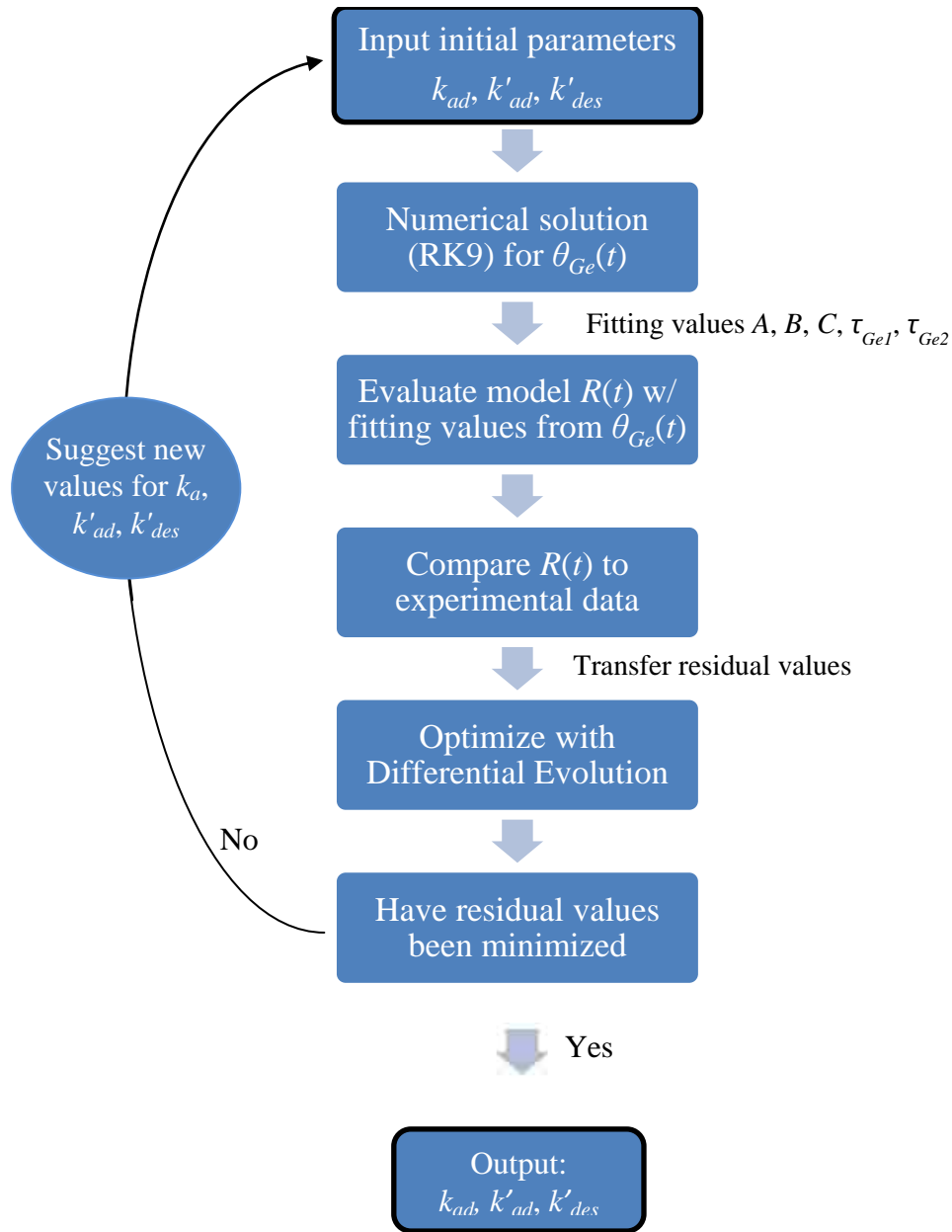


Figure 18. Flow diagram of the method used to find the values k_a , k'_a and k'_{des} . Black borders indicate an input or output.

This creates the best fit to the experimental data. A flow diagram of the process operations is detailed in Figure 18. The fitting coefficients for Equation (43) are reported from a second script named “ThetaVtime” after inputting the final values for k_{ad} , k'_{ad} and k'_{des} . The script “ThetaVtime” performs two functions. It reports the values for the fitting

coefficients in Equation (43) and it provides the graphical output to judge the quality of fit to the experimental data. The values for $\theta_{Ge}(t)$ are plotted as well to make sure the fit to the numerical solution of $\theta_{Ge}(t)$ that is calculated internal to the optimization script is not providing an erroneous fit to the data.

Table 4. Initial and optimized values for model parameters

| Variable | Initial Value | Final Value |
|---------------------------------------|-----------------------|-----------------------|
| k_{ad} (cm ³ /mol-s) | 2.4 | 495 |
| k'_{ad} (cm ³ /mol-s) | 2.4 | 175 |
| k'_{des} (s ⁻¹) | 8.2 x10 ⁻⁶ | 5.1 x10 ⁻² |
| τ_C (s) | 960 | |
| C_L (mol/cm ³) | 4.7x10 ⁻⁴ | |
| ρ_{Ge} (g/cm ³) | 5.323 | |
| MW (g/mol) | 72.59 | |
| ρ_{GeA} (sites/cm ²) | 6.61x10 ¹⁴ | |
| R_0 (nm) | 0.75 | |

Results of Optimization

When optimized, the values for k_{ad} , k'_{ad} and k'_{des} converge to 495 cm³/mol-s, 175 cm³/mol-s and 5.1 x10⁻² respectively. When the converged adsorption and desorption coefficients are found, the fitting coefficients for the numerical solution to $\theta_{Ge}(t)$, A , B , C , $\tau_{\theta_{Ge}}$ and $\tau_{\theta_{Ge2}}$ for $\theta_{Ge}(t)$ result in values 0.382, 0.211, 0.387, 744 s and 168 s respectively with an R² value of 0.9998 at the conditions specified in Table 3. The results of the optimized radial growth fit are illustrated in Figure 19. The sum of the squares of residuals (SSR, as detailed in Appendix C) of the $R(t)$ model is 2.1 nm² and the χ^2 value is 1.79. The R² (0.931) value is reasonable considering only 5 experimental points. When the optimized values for adsorption and desorption are input into ThetaVtime with the

partial analytical solution for $\theta_{Ge}(t)$ (shown in Appendix C), the coefficients A , B , C , $\tau_{\theta_{Ge}}$ and $\tau_{\theta_{Ge2}}$ are identical to the double exponential method and the fit results are the same to the experimental data. Therefore these two methods agree and there will be no difference between the two results, further validating the use of the double exponential method for optimization.

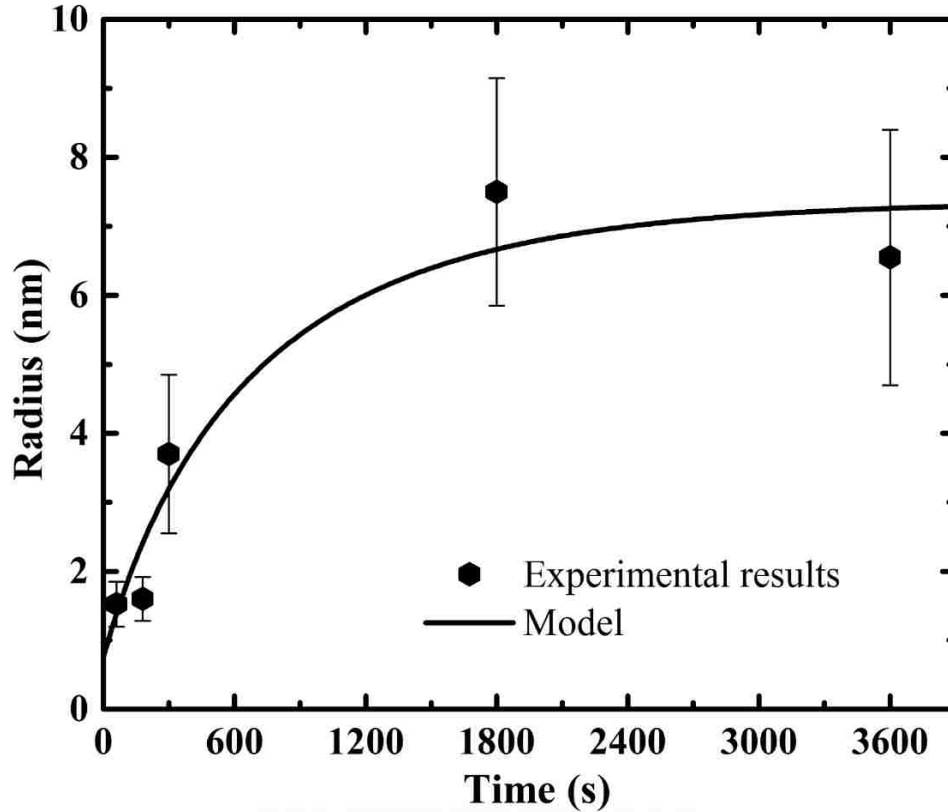


Figure 19. Model for $R(t)$ overlaid with experimental data.

There is a small but meaningful difference from the fit with a single exponential, which can be seen in Figure 20 to the fit with a double exponential in Figure 21. The early growth period before 500 s shows a higher rate of change for $\theta_{Ge}(t)$ than the single exponential fit. Beyond 2000 s, the fit is also showing a smaller rate of change than the numerical solution. The single exponential is a poor fit to the data at the beginning and

the end of the growth, while the double exponential fits well throughout the growth. The R^2 value is 0.994 for the single exponential fit compared to 0.9997 for the double exponential case in Figure 19. The resulting $\theta_{Ge}(t)$ and $\theta_L(t)$ plots for the optimized model are illustrated in Figure 20. The relatively high adsorption coefficients have an obvious impact to the rate of change in $\theta(t)$. The surface coverage changes faster at

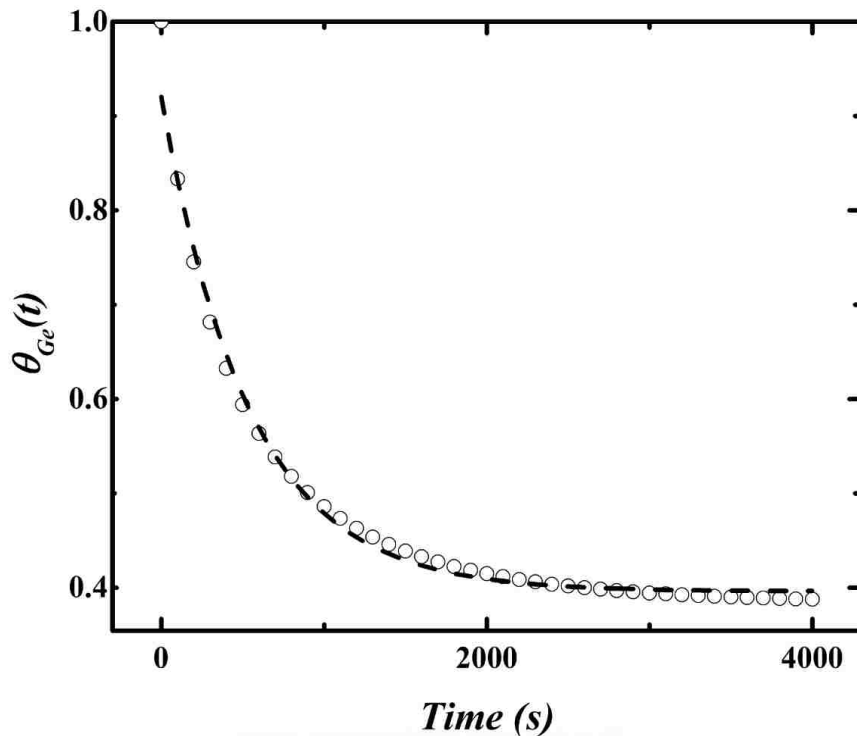


Figure 20. Optimized numerical solution for $\theta_{Ge}(t)$ (circles), with a single exponential fit to the data (dashed line). Notice the fit differences at the beginning and end of growth.

the beginning of growth for both $\theta_{Ge}(t)$ and $\theta_L(t)$ when compared to the initial estimates. The change in $\theta_L(t)$ parallels the radial growth rate closely, showing a small rate of change in $\theta_L(t)$ after approximately 1800 s reaching a steady state at approximately 60 % ligand surface coverage.

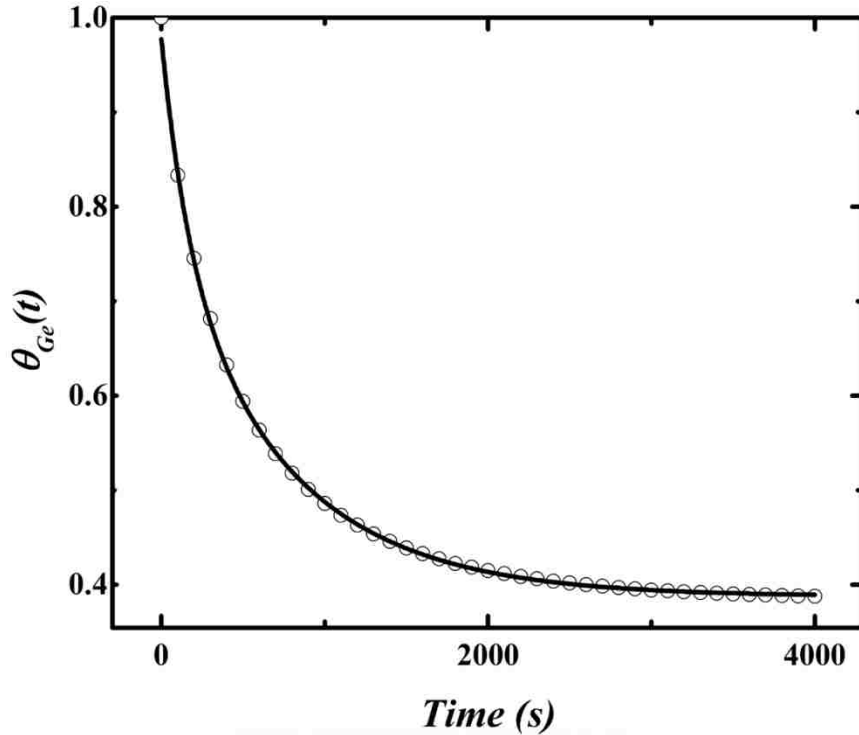


Figure 21. Optimized numerical solution for $\theta_{Ge}(t)$ (circles), with a double exponential fit to the data (solid line). Note the consistent fit throughout the time range.

The two different time constants, $\tau_{\theta_{Ge1}}$ and $\tau_{\theta_{Ge2}}$, fitted with the double exponential expressions indicate that there is a more complex kinetic process occurring. Namely, the double exponential expression indicates that there are two separate kinetic processes at work in this synthesis. One process is happening at a fast rate ($\tau_{\theta_{Ge1}} = 168$ s) at the beginning of the growth and one at a slower rate ($\tau_{\theta_{Ge2}} = 744$ s) for the balance of the NC growth. The faster growth (lower characteristic time constant) at the beginning of the synthesis indicates that there is a higher adsorption coefficient specific to the timeframe from nucleation to ~ 200 s. A smaller adsorption coefficient for the Ge monomer is visually evident in the timeframe up to approximately 2500 s where the radial growth rate lessens considerably up to the end of synthesis approaching 3600 s. The NC radius during this time has a direct impact on the adsorption coefficient, and will reduce it as the NC

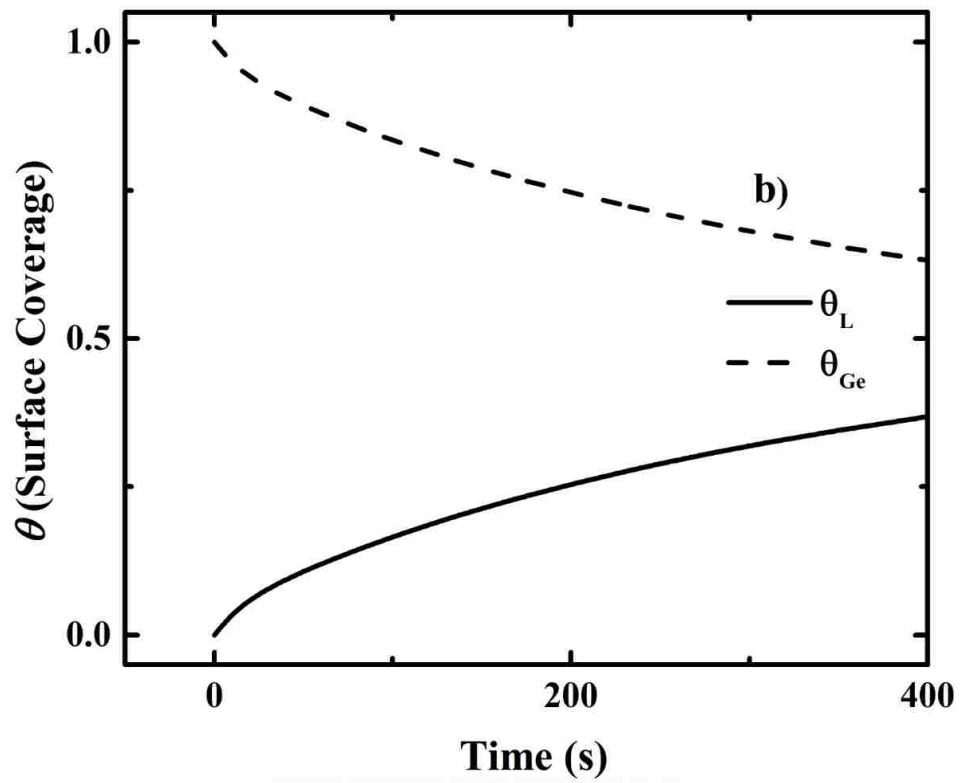
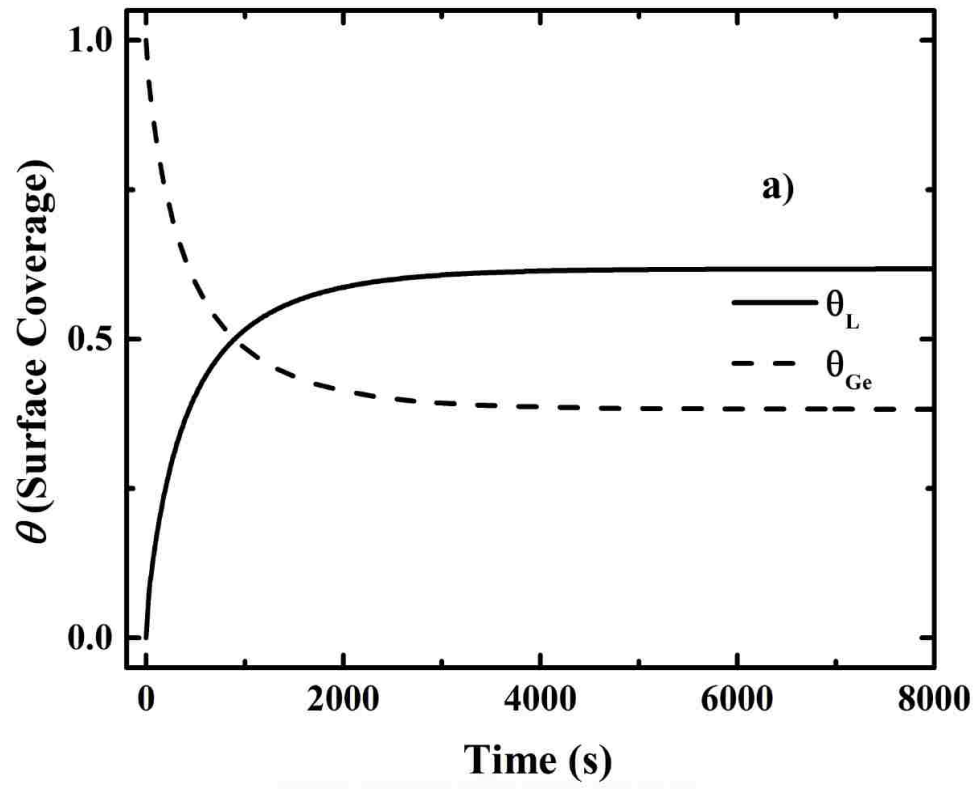


Figure 22. $\theta_L(t)$ and $\theta_{Ge}(t)$ plotted with optimized adsorption and desorption coefficients a) at full scale and b) small t scale to observe behavior at beginning of growth.

radius increases as found by Lu *et al.*[30]. Thus, the adsorption coefficient at the early stages of NC growth is elevated compared to a larger NC or a planar surface and is responsible for the small characteristic time constant. As expected, the adsorption coefficient appears to decrease as the NC increases in size, demonstrated by the larger characteristic time constant for the later part of the growth which agrees with the findings of Lu *et al.*[30]. The specific adsorption coefficients at the beginning and end of growth are not calculated directly, but the overall adsorption coefficients are calculated and they are quite high in comparison to a planar surface.

With the adsorption coefficient of Ge monomer to the NC now known, the new k_{eff} is calculated with the optimized adsorption coefficient. Using the optimized k_{ad} , the new k_{eff} is calculated at 5.4×10^{-7} cm/s which is 9 orders of magnitude below the diffusion mass transfer coefficient. These results for k_{eff} agree with work by Bullen *et al.*[7] indicating that surface adsorption kinetics rate coefficients show much, much smaller rates than the mass transfer coefficient, k_c , calculated earlier in this work. The values for k'_{ad} and k'_{des} also agree quite closely with work published on organic ligand adsorption and desorption to nanocrystals[26]. The very small k_{eff} and the fit of a kinetically limited model for NC growth strongly suggest that the growth of Ge NCs with the solution synthesis is limited by surface kinetics

Chapter 5

Discussion

Model vs. Experimental Data

The sum of the squares of residuals (SSR, as detailed in Appendix C) of the $R(t)$ model compared to the experimental data produces a value of 2.1 nm^2 . Using this method for solving for adsorption and desorption empirically, allows the coefficients to be solved simultaneously with one operation. No prior adsorption coefficient values are needed other than the initial guess. This is beneficial as the values for adsorption and desorption to NCs are not typically available unless obtained through a separate experiment. The fit line produced by Equation (69) and plotted in Figure 17 has a reduced Chi squared (χ^2) value of 1.79 and an R^2 value of 0.931 when compared to the experimental data. This model has a low number of degrees of freedom (DOF) at 1. A fit with a low DOF resulting in a χ^2 of 1.79 is a good fit to the experimental data. If the value were much larger than 1, the fit could be considered poor. A less quantitative measure of fit, but very effective in non-linear fits is examining the residual values. When residual values are plotted by run order and σ in Figure 23, there are no discernible trend. Since there is no gross trend in either time or σ , and the mean of residuals is near zero, the model has demonstrated a good fit to the experimental data.

The model is fit to the experimental data with a differential evolution algorithm (DEA). This allows the three variables, k_{ad} , k'_{ad} and k'_{des} to be fitted simultaneously while processing a series of algorithms contained within the DEA. The numerical solution for

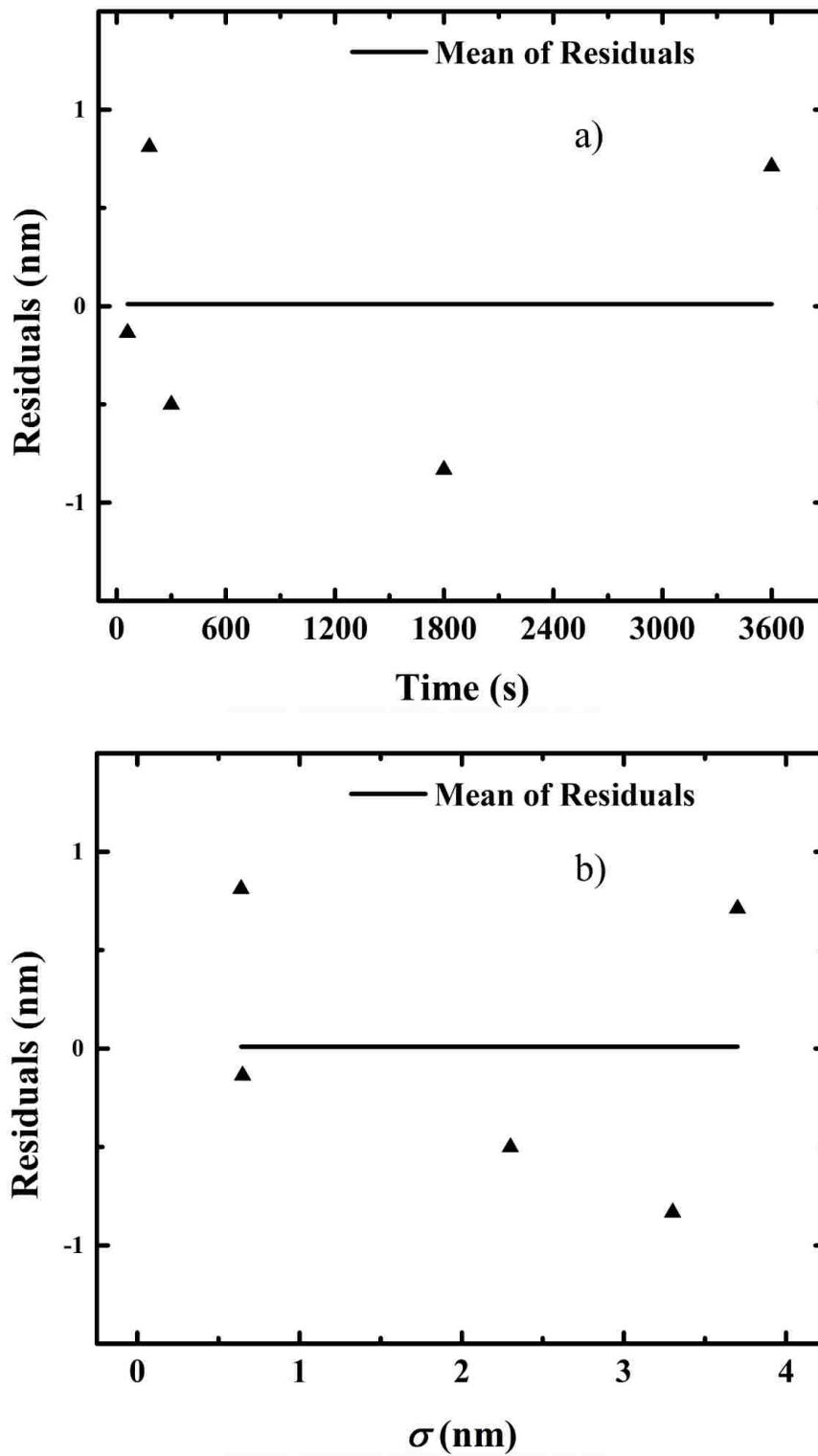


Figure 23. Residual values plotted against a) run order and b) standard deviation. Line on charts is the mean of the residuals, which is nearly zero. There is no obvious trending.

the differential equation calculating $\theta_{Ge}(t)$ was solved using the *Dsolve* algorithm (utilizing RK9) in Mathematica™. From this point forward, a nonlinear fit to the numerical solution was resolved with the *FindFit* algorithm (utilizing the Levenberg-Marquardt Method) in 18 iterations. The solution for the adsorption and desorption coefficients was resolved in 3 iterations of the DEA. Using the *Dsolve* method by fitting the $\theta_{Ge}(t)$ numerical values to a double exponential equation is a more universal method that is less sensitive to the site balance equation than the partial analytical method presented in the text. By using the universal method, different site balance equations can be used and still allow an optimization of the adsorption and desorption coefficients.

These optimized coefficients are 2 orders of magnitude higher than the initial approximation based upon alkanethiol adsorption to a planar Ge surface. This is initially unexpected, however, works by others[26, 27, 31-33] has shown that the adsorption rate coefficients to the surface of NCs decrease as NC radius increases. This would mean that one would expect the adsorption coefficients to be somewhat higher than the planar surface. The adsorption coefficients are indeed higher and agree with this work. Desorption coefficients in the case of organic ligands to the surface of the Ge NC are much larger in comparison to ligand adsorption coefficients to a planar Ge surface. Work by Pan *et al.*[1] indicates that the organic ligands engage in a high rate of exchange with the surface. Indeed, adsorption and desorption coefficients are of the same magnitude as other work for ligand adsorption to NCs[26, 34].

The high adsorption and desorption coefficients are due to the surface free energy differences between planar and NC size radius of curvature. The surface free energy of NC systems has been determined to be higher than a planar surface[30]. If the surface

free energy is higher at a smaller radius of curvature, the high adsorption rate of the NCs is expected. The small radius of curvature of the NC presents a situation with less steric hindrance than the planar case due to a difference in incident angle of adjacent, bound, coordinating ligands. Adsorption of the Ge monomer to the surface lowers the surface energy throughout the growth process (i.e. as the NC radius increases the surface energy decreases, moving towards equilibrium with the solution). This suggests that the NCs in this work will have an adsorption coefficient with respect to Ge monomer that is higher than a planar surface of Ge. There are different mechanisms at work in the observed adsorption rates. First, the difference in surface energy between NC and the planar surface creates a much higher adsorption rate, and adsorption coefficient for Ge monomer to the NCs. Additionally, the subtly different adsorption rates between the beginning of the growth and the remaining growth produce two, large, but relatively different adsorption coefficients for the NC growth. Therefore, the adsorption coefficient result in empirically higher adsorption rates to the NC surface in agreement with other work specific to NCs.

Limitations of Model

In order to accurately calculate the growth rate of an NC *a priori*, the adsorption rate to the surface of the NC must be known from either theoretical or experimental data. In this case, for a Ge NC, the adsorption rate of Ge monomer to the surface of the NC is not known prior to the experiment, or prior to developing the model. Using the coefficients as fitting parameters allows them to be optimized to the experimental data. Having prior knowledge of the adsorption and desorption coefficients may not be

common with regard to some species. Ge adsorption and desorption rates to a Ge NC surface were not found in a literature review so the result had to be determined implicitly from the model after using a similar ligand as an initial approximation. If the coefficients were available, then the process of creating a model could be done *a priori*, predicting the outcome.

Planar adsorption and desorption rates for various materials are more easily obtained. However, they are of only a limited use with this model as the end results for k_{ad} , k'_{ad} and k'_{des} are 2-4 orders of magnitude higher than the values for alkanethiol to Ge adsorption/desorption. A method of predicting the order of magnitude of the coefficients for an NC given the planar coefficients would be useful for generating an initial guess. Adsorption characteristics on an NC like curvature surface would be required prior to the synthesis in order to be a true predictor of the growth rate. In this sense, other Group IV semiconductor materials may have similar adsorption rates when in the NC regime. This would have to be further proven with experimental results. For any species involved in a NC growth synthesis, the adsorption coefficients for an NC surface must be understood before a model would be a successful predictor of growth rate. For instance, an NC synthesis could be conducted at typical conditions to obtain the empirical adsorption and desorption coefficients. Once the adsorption and desorption coefficients are obtained, they can be used to calculate growth rates for other experiments while varying the concentrations.

Possibilities for future study

The model created in this thesis is applicable for the synthesis of spherical Ge NCs, however there is potential for application to other NC morphologies (including nanorods). Each crystal facet of a NC has a different adsorption site density, allowing the potential for manipulating the shape NCs by exploiting these differences. Ligand species as well have different adsorption and desorption coefficients and can be used to selectively occupy binding sites, on different crystal facets to provoke particular morphologies[12, 35-37] from the NC synthesis. Thus, predicting the relative strength of ligand adsorption, can be used to give a measurement of the ligands propensity for producing facet specific growth rates.

Using the model to tune the growth rate of the system described in this thesis is a useful proposition. Changing the system growth rate with careful selection of the precursor initial concentration can produce a system that is self-limiting with respect to NC size. With this model, a calculation *a priori* would allow the system to be targeted prior to the start of any synthesis affording an efficacy to synthesis process. By changing the initial concentration of Ge precursor or ligands, the final size of the NC can be tuned to a size that could be used for applications for Ge fluorescence as demonstrated in Figure 24. For convenient size control, a precursor concentration could be selected to self-limit the synthesis at the prescribed size, rather than relying on the NC growth to be quenched at an exact time. The model will make the initial concentration selection process straightforward and shrink the number of iterations needed for concentration selection.

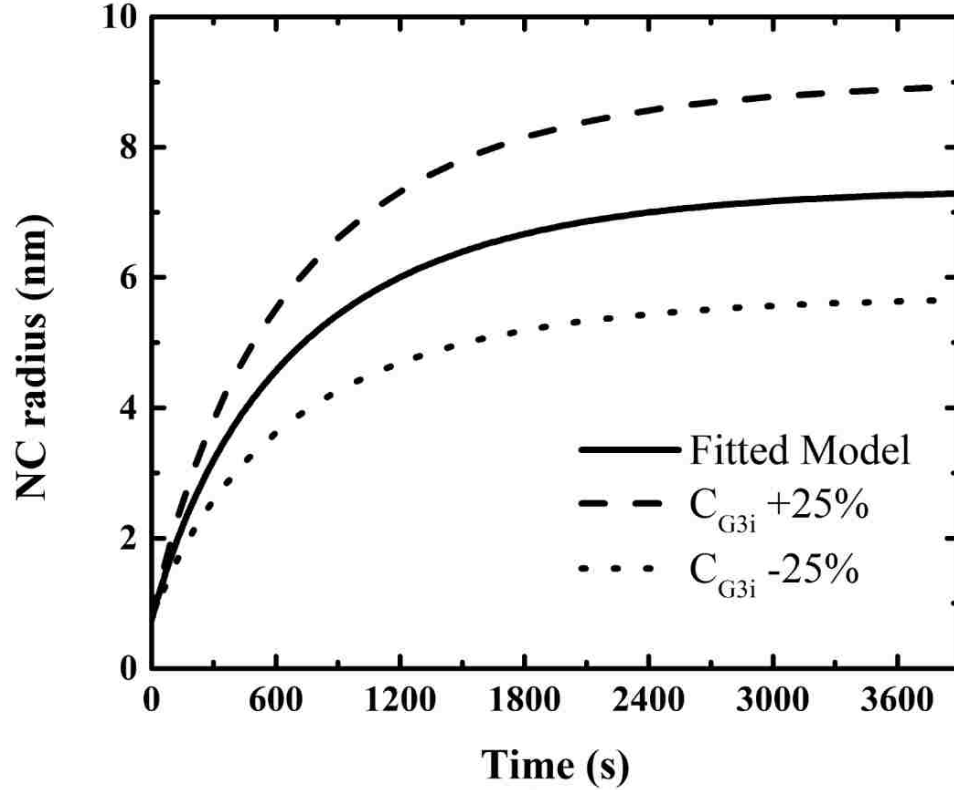


Figure 24: Model for $R(t)$ with different initial Ge monomer concentration C_{G3i} inputs. This data is based upon model data rather than experimental results.

Conclusion

In this thesis, I have presented calculations of the boundary layer thickness and shown that the BL is on the same order of magnitude as the NC. The diffusion constant for Ge monomer in the solution has been calculated and is relatively high due to high temperature of the solution. The calculated BL thickness and diffusion coefficient have significance, as the values result in a very small barrier to convective transport through the BL. The magnitude of the equilibrium concentration, C_E , of Ge monomer is determined with a model of the diffusion from bulk solution to the NC surface. The difference in concentration from the bulk to the surface, the diffusion driving force, was calculated and determined to be very small in comparison to the bulk concentration,

indicating that the diffusion of Ge monomers occurs at a fast rate and is unlikely to provide significant resistance to the Ge NC growth.

A site balance adhering to Langmuir-Hinshelwood kinetics is derived to describe the adsorption and desorption of the Ge monomers and organic ligands in the system. This expression for $\theta_{Ge}(t)$ was derived from a fit to the numerical solution of the binding site balance. With this equation for surface site coverage and expressions generated to describe the molar flux to the surface of the NC, a kinetically limited model for the radial growth rate is developed. Using the adsorption and desorption coefficients as tuning parameters, the radial growth rate equation can be made to optimize the fit to the experimental data. This has the secondary benefit of returning the empirical adsorption and desorption coefficients of the Ge monomer and the coordinating ligands. The adsorption rates of all species in the system are discovered empirically to be 2 or more orders of magnitude higher than the approximate values for planar Ge (111) surface. These results agree with other work involving NCs and ultimately provide an accurate fit to the experimental data gathered for Ge NC synthesis.

The results of this thesis show that there is little resistance to convective transport in the solution synthesis method of Ge NC growth. The small boundary layer size and high diffusion constant contribute to a very small diffusive resistance. Therefore, there is a high probability that this is a kinetically limited system. The growth rate model matches the experimental data and provides strong evidence that the growth is indeed kinetically limited. This has interesting implications for NC growth synthesis. If the surface kinetics controls the growth of the NC, the choice of coordinating ligands and precursor concentrations will have impactful modulation of the growth rate. Future investigations

can focus on modulating the concentrations and adsorption characteristics of the ligands in order to influence NC growth. The different binding site density and surface reactivity of the Ge NC facets can be exploited to selectively bind ligands and possibly create different morphologies. With accurate information on adsorption and desorption coefficients and experimental conditions, a model to determine NC growth, *a priori*, can be created for other systems.

Appendix A

Calculations and Derivations

Calculations for density of 1-Octadecene (OD)

Using the density calculation from Yaws *et al.*[17] below, the density of OD is calculated

$$\rho_{OD} = AB^{-(1-T/C)^n} = (.2405)(.24731)^{-(1-573.15/748)^{.32724}} = .57321 \text{ g/cm}^3 \quad (\text{A1})$$

Where $T = 573\text{K}$, $A = 0.2405$, $B = 0.24731$, $C = 748$ and $n = 0.32724$ as obtained from Yaws *et al.*

Calculations for Boundary Layer thickness

$$Sh = \frac{k_c D}{D_{AB}} = 2 + .6Re^{1/2} Sc^{1/3} \quad (\text{A2})$$

$$Sc = \frac{\nu}{D_{AB}} = \frac{\mu}{\rho D_{AB}} = \frac{.003206 \text{ g} \cdot \text{s} / \text{cm}}{(.57321 \text{ g} / \text{cm}^3)(9.6 \times 10^{-5} \text{ cm}^2 / \text{s})} = 58.3 \quad (\text{A3})$$

By using the Ranz-Marshall correlation again, the mass transfer coefficient of Ge, k_c , was verified using Re , Sc and diameter of the NC, D .

$$k_c = \left[2 + .6Re^{1/2} Sc^{1/3} \right] \cdot \frac{D_{AB}}{D} \quad (\text{A4})$$

$$k_c = \left[2 + .6(4.718 \times 10^{-3})^{1/2} (58.3)^{1/3} \right] \cdot \left(\frac{9.6 \times 10^{-5} \text{ cm}^2 / \text{s}}{7 \times 10^{-7} \text{ cm}} \right) = 296 \text{ cm/s} \quad (\text{A5})$$

Since k_c can be considered equivalent to D_{AB}/δ_c [BSL 695], this can be used to calculate a mass transfer boundary layer for a single nanocrystal within the system.

$$k_c \sim \frac{D_{AB}}{\delta_c} \quad (\text{A6})$$

And therefore, the following equation is written.

$$\delta_c \sim \frac{D_{AB}}{k_c} \quad (\text{A7})$$

Using the above conditions, $\delta_c = 3.24\text{nm}$.

To simplify this model, an assumption is made that there is no reaction over the boundary layer. Therefore the Schmidt number can relate kinematic and concentration boundary layers [22].

$$\frac{\delta_k}{\delta_c} = \frac{\text{kinematic bl}}{\text{mass transfer bl}} = Sc^{1/3} \quad (\text{A8})$$

$$\delta_k = Sc^{1/3} \delta_c \quad (\text{A9})$$

$$\delta_k = Sc^{1/3} \delta_c = (58.3)^{1/3} \cdot 3.09 \times 10^{-7} \text{cm} = 1.2 \times 10^{-6} \text{cm} = 13 \text{nm} \quad (\text{A10})$$

Areal density of Ge binding sites

Values for ρ_{GeA} have been calculated previously from experiments by Schlier *et al.*[25].

100 orientation: $\rho_{GeA100} = 6.3 \times 10^{14} \text{ Ge sites/cm}^2$

111 orientation: $\rho_{GeA111} = 7.25 \times 10^{14} \text{ Ge sites/cm}^2$

Calculating the mean ($\rho_{GeA} = 6.61 \times 10^{14}$ Ge sites/cm²) using the two experimental values using

$$\rho_{GeA} = \frac{(\rho_{GeA100} + \rho_{GeA111})}{2}, \quad (A10)$$

where ρ_{GeA100} is the areal Ge site density on 100 Ge facets, and ρ_{GeA111} is the Ge site density on 111 Ge facets returns an average value for ρ_{GeA} .

Diffusion coefficient Approximation

The diffusion coefficient for Ge in solution is estimated with a method adapted by Sitaraman, Ibrahim and Kuloor[19].

Table A1: Input variables for calculating D_{AB}

| Variable | Value |
|----------------------------------|--------|
| M_s (g/mol) | 252.54 |
| L_s (kJ/mol) | 53.34 |
| L_s (cal/g) | 50.2 |
| L (kJ/mol) | 334.3 |
| L (cal/g) | 1095 |
| μ (cP)[16] | .3206 |
| V_{mGe} (cm ³ /mol) | 16.7 |

$$D_{AB} = 5.4 \times 10^{-8} \left(\frac{M_s^{1/2} L_s^{1/3} T}{\mu_s V_m^{0.5} L^{0.3}} \right)^{0.93} = 5.4 \times 10^{-8} \left(\frac{(252.54 \text{ g/mol})^{1/2} (50.2 \text{ cal/g})^{1/3} (573 \text{ K})}{(.3206 \text{ cP}) (16.7 \text{ cm}^3/\text{mol})^{1/2} (1095 \text{ cal/g})^{0.3}} \right)^{0.93} \quad (A11)$$

$$D_{AB} = 9.6 \times 10^{-5} \text{ cm}^2/\text{s} \quad (A12)$$

Where molar volume (V_m) is calculated below in line A13

$$V_m = V_{mGe} = \frac{MW_{Ge}}{\rho_{Ge}} = \frac{72.59 \text{ g/mol}}{4.3 \text{ g/cm}^3} = 16.7 \text{ cm}^3/\text{mol} \quad (A13)$$

Data supporting the numerical solution for $C_E(t)$

Table A2: Values for $\gamma(t)$, C_{G3} and ΔC used in creation of Figure 10 and Figure 11.

| t (s) | $\gamma(t)$ (mol/cm ²) | $d/dt \gamma(t)$ (mol/cm ³) | C_{G3} (mol/cm ³) | ΔC (mol/cm ³) |
|---------|---------------------------------------|--|------------------------------------|--------------------------------------|
| 0 | 0.0000 | 1.587E-04 | 1.590E-04 | 2.54E-07 |
| 500 | 0.0620 | 9.438E-05 | 9.445E-05 | 7.25E-08 |
| 1000 | 0.0988 | 5.611E-05 | 5.611E-05 | -3.67E-09 |
| 1500 | 0.1206 | 3.336E-05 | 3.333E-05 | -3.00E-08 |
| 2000 | 0.1336 | 1.983E-05 | 1.980E-05 | -3.43E-08 |
| 2500 | 0.1414 | 1.179E-05 | 1.176E-05 | -3.02E-08 |
| 3000 | 0.1459 | 7.010E-06 | 6.986E-06 | -2.38E-08 |
| 3500 | 0.1487 | 4.167E-06 | 4.150E-06 | -1.76E-08 |
| 4000 | 0.1503 | 2.478E-06 | 2.465E-06 | -1.25E-08 |
| 4500 | 0.1512 | 1.473E-06 | 1.464E-06 | -8.66E-09 |
| 5000 | 0.1518 | 8.757E-07 | 8.699E-07 | -5.88E-09 |
| 5500 | 0.1521 | 5.206E-07 | 5.167E-07 | -3.92E-09 |
| 6000 | 0.1523 | 3.095E-07 | 3.069E-07 | -2.59E-09 |
| 6500 | 0.1525 | 1.840E-07 | 1.823E-07 | -1.69E-09 |
| 7000 | 0.1525 | 1.094E-07 | 1.083E-07 | -1.10E-09 |
| 7500 | 0.1526 | 6.504E-08 | 6.434E-08 | -7.05E-10 |
| 8000 | 0.1526 | 3.867E-08 | 3.822E-08 | -4.51E-10 |

Table A3: Values for numerical solution of Equation (38)

| Time (s) | Equation (38) Initial | |
|----------|-----------------------|--------------------------------|
| | Guess | Equation (38) Optimized values |
| 0 | 0.00E+00 | 0.00E+00 |
| 20 | 2.91E+01 | 2.26E+34 |
| 100 | 1.50E+02 | 3.65E+36 |
| 500 | 8.90E+02 | 3.83E+49 |
| 1000 | 2.29E+03 | 4.29E+70 |
| 1500 | 4.61E+03 | 8.59E+94 |
| 2000 | 8.53E+03 | 1.45E+121 |
| 2500 | 1.53E+04 | 3.42E+148 |
| 3000 | 2.71E+04 | 3.84E+176 |
| 3500 | 4.77E+04 | 1.09E+205 |
| 4000 | 8.38E+04 | 5.39E+233 |

Derivation of Equation (28): Expression for $C_E(t)$

The molar flow rate through the boundary layer (BL) is described with an application of Ficks 1st law to this NC system.

$$J_{BL} = 4\pi r^2 D_{AB} \left(\frac{dC_{Ge}}{dr} \right) \Big|_{R < r < R + \delta_c} \quad (A14)$$

The variables can be separated, resulting in

$$J_{BL} \frac{1}{r^2} dr = 4\pi D_{AB} dC_{Ge} \quad . \quad (A15)$$

The equation can then be integrated with respect to r and C_{Ge} . R is integrated from the surface of the NC ($r = R$) to the outside of the BL with thickness δ_c ($r = R + \delta_c$). C_{Ge} is integrated from the concentration of Ge monomer in equilibrium with the surface of the NC (C_E) to the concentration of Ge monomer in the bulk solution (C_{G3}), resulting in

$$J_{BL} \int_R^{R+\delta_c} \frac{1}{r^2} dr = 4\pi D_{AB} \int_{C_E}^{C_{G3}} dC_{Ge} \quad . \quad (A16)$$

Executing the integrals results in the following expression.

$$J_{BL} \left[-\frac{1}{r} \right]_R^{R+\delta_c} = 4\pi D_{AB} [C_{G3}(t) - C_E(t)] \quad (A17)$$

The expression can be expanded to arrive at

$$J_{BL} \left[\frac{1}{R} - \frac{1}{R+\delta_c} \right] = 4\pi D_{AB} [C_{G3}(t) - C_E(t)] \quad . \quad (A18)$$

Terms are simplified from Equation (A18) to obtain the following equation adapted from work by Sugimoto[8].

$$J_{BL} = \frac{4\pi R(R+\delta_c)D_{AB}}{\delta_c} [C_{G3}(t) - C_E(t)] \quad (A19)$$

The molar flowrate in terms of the rate of change in radius (J_E)[8] below is then equated to J_{BL} .

$$J_E = \frac{\rho_{Ge}}{MW_{Ge}} 4\pi R^2 \frac{dR}{dt} \quad (A20)$$

$$\frac{\rho_{Ge}}{MW} 4\pi R^2 \frac{dR}{dt} = \frac{R(R+\delta_c)}{\delta_c} 4\pi D_{AB} [C_{G3}(t) - C_E(t)] \quad (A21)$$

Terms are then rearranged to separate variables arriving at Equation (A22)

$$\frac{\rho_{Ge}}{MW} 4\pi R^2 \left(\frac{\delta_c}{R(R+\delta_c)} \right) dR = 4\pi D_{AB} [C_{G3}(t) - C_E(t)] dt \quad (A22)$$

The left side is integrated from R_0 to $R_0+\Delta R$ which represents the change in radius from R_0 at time t_0 to the new radius, $R_0+\Delta R$ at time t . The right side is then integrated from t_0 to t revealing the expression

$$\int_{R_0}^{R_0+\Delta R} \frac{\rho_{Ge}}{MW} \left(\frac{\delta_c R}{(R+\delta_c)} \right) dR = D_{AB} \int_{t_0}^t [C_{G3}(t) - C_E(t)] dt. \quad (A23)$$

The following is an expression for $C_{G3}(t)$.

$$C_{G3}(t) = C_{Gi} \exp \left[-t / \tau_G \right] \quad (A24)$$

When C_{G3} is inserted into the integral and evaluated, the following expression is obtained.

$$\frac{\rho_{Ge}\delta_c}{MW} (R - \delta_c \ln(R + \delta_c)) \Big|_{R_0}^{R_0+\Delta R} = D_{AB} \left[C_{Gi} \tau_G \left(1 - e^{[-t/\tau_G]} \right) - \int_{t_0}^t C_E(t) dt \right] \quad (A25)$$

It is evident that C_E is the only portion of this expression that is not evaluated. By rearranging terms in the equation, it can expressed as the integral of $C_E(t)$

$$\int_{t_0}^t C_E(t) dt = - \left(\frac{\rho_{Ge}\delta_c}{D_{AB}MW} (R - \delta_c \ln(R + \delta_c)) \Big|_{R_0}^{R_0+\Delta R} - C_{Gi} \left(1 - e^{[-t/\tau_G]} \right) \right) \quad (A26)$$

Derivation of growth rate model for $R(t)$

The molar flow rate of Ge monomer adsorbing to the surface of the NC is described by

$$J = 4\pi R_{CE}^2 \frac{\rho_{GeA}}{N_A} k_{ad} C_E(t) \theta_{Ge}(t) \quad . \quad (A27)$$

The molar flow rate to the surface in terms of the change in R with respect to t is expressed by the following expression.

$$J_E = \frac{\rho_{Ge}}{MW_{Ge}} 4\pi R_{NC}^2 \frac{dR}{dt} \quad (A28)$$

By setting the two equations equal, Equation (A29) can be written.

$$\frac{\rho_{Ge}}{MW_{Ge}} 4\pi R_{NC}^2 \frac{dR}{dt} = \frac{\rho_{GeA}}{N_A} 4\pi R_{CE}^2 k_{ad} C_E(t) \theta_{Ge}(t) \quad (A29)$$

This expression is simplified to result in

$$\frac{\rho_{Ge}}{MW_{Ge}} \frac{dR}{dt} = \frac{\rho_{GeA}}{N_A} k_{ad} C_E(t) \theta_{Ge}(t) \quad . \quad (A30)$$

The variables can now be separated in preparation for integration resulting in Equation (A31).

$$\int dR = \int \frac{MW_{Ge}}{\rho_{Ge}} \cdot \frac{\rho_{GeA}}{N_A} k_{ad} C_E(t) \theta_{Ge}(t) dt \quad (A31)$$

The next step is substituting expressions for $C_E(t)$ and $\theta_{Ge}(t)$ with Equations (A32) and (A33) respectively.

$$C_E(t) = C_{Ei} \exp\left[-t/\tau_c\right] \quad (A32)$$

$$\theta_{Ge}(t) = A \exp\left[-t/\tau_{\theta_{Ge1}}\right] + B \exp\left[-t/\tau_{\theta_{Ge2}}\right] + C \quad (A33)$$

After both expressions are substituted into Equation (A31), the following expression is obtained.

$$\int dR = \int \frac{MW_{Ge}}{\rho_{Ge}} \cdot \frac{\rho_{GeA}}{N_A} k_{ad} C_{Ei} \exp\left[-t/\tau_c\right] \left(\begin{array}{l} A \exp\left[-t/\tau_{\theta_{Ge1}}\right] \\ + B \exp\left[-t/\tau_{\theta_{Ge2}}\right] + C \end{array} \right) dt \quad (A34)$$

The R variable will be integrated from R_0 to R , and t integrated from t_0 to t resulting in the following expression.

$$\int_{R_0}^R dR = \int_{t_0}^t \frac{MW_{Ge}\rho_{Ge}A_{kad}}{\rho_{Ge}N_A} C_{Ei} \exp[-t/\tau_c] \left(\frac{A \exp[-t/\tau_{\theta Ge1}]}{+B \exp[-t/\tau_{\theta Ge2}] + C} \right) dt \quad (A35)$$

The exponential terms are then combined to result in

$$\int_{R_0}^R dR = \int_{t_0}^t \frac{MW_{Ge}\rho_{Ge}A_{kad}}{\rho_{Ge}N_A} C_{Ei} \left(\frac{A e^{(-t/\tau_{\theta Ge1})} e^{(-t/\tau_c)}}{+B e^{(-t/\tau_{\theta Ge2})} e^{(-t/\tau_c)} + C e^{(-t/\tau_c)}} \right) dt \quad (A36)$$

Exponential terms are combined further to facilitate integration, with the following results.

$$\int_{R_0}^R dR = \frac{MW_{Ge}\rho_{Ge}A_{kad}}{\rho_{Ge}N_A} C_{Ei} \int_{t_0}^t \left(\frac{A e^{(-(\tau_c + \tau_{\theta Ge1})t/(\tau_c \tau_{\theta Ge1}))}}{+B e^{(-(\tau_c + \tau_{\theta Ge2})t/(\tau_c \tau_{\theta Ge2}))}} + C e^{(-t/\tau_c)} \right) dt \quad (A37)$$

Both sides of Equation (A37) are then integrated resulting in Equation (A38). The model can now be evaluated from t_0 to t to get $R(t)$.

$$R = Q \left[-A \frac{\tau_c \tau_{\theta Ge1}}{(\tau_c + \tau_{\theta Ge1})} e^{\frac{-(\tau_c + \tau_{\theta Ge1})t}{\tau_c \tau_{\theta Ge1}}} - B \frac{\tau_c \tau_{\theta Ge2}}{(\tau_c + \tau_{\theta Ge2})} e^{\frac{-(\tau_c + \tau_{\theta Ge2})t}{\tau_c \tau_{\theta Ge2}}} - C \tau_c e^{-t/\tau_c} \right]_{t_0}^t + R_0 \quad (A38)$$

$$Q = \frac{MW_{Ge}\rho_{Ge}A_{kad}}{\rho_{Ge}N_A} C_{Ei} \quad (A39)$$

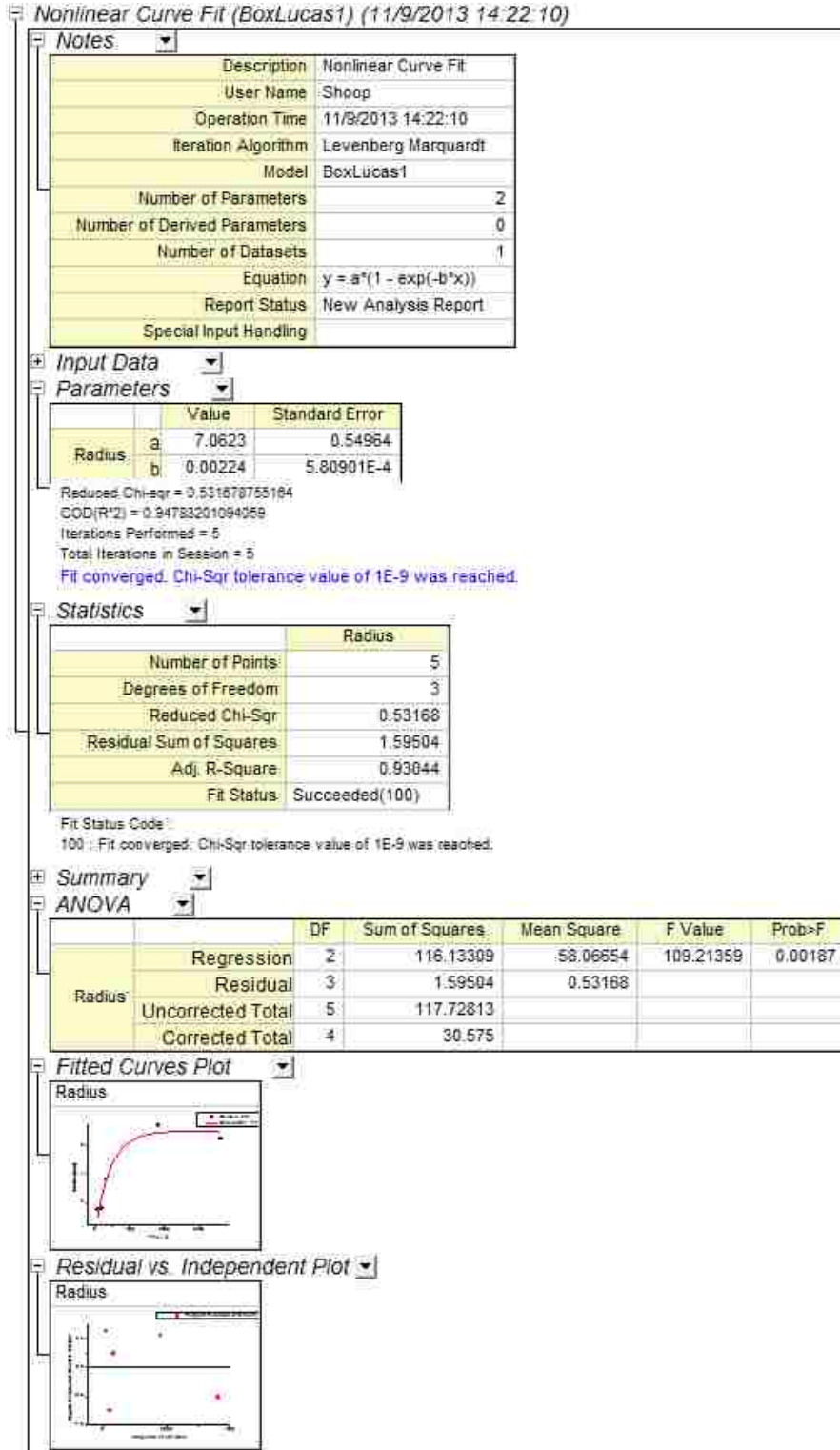


Figure A1. Empirical fit of single exponential to the experimental data for Figure 3 in main text.

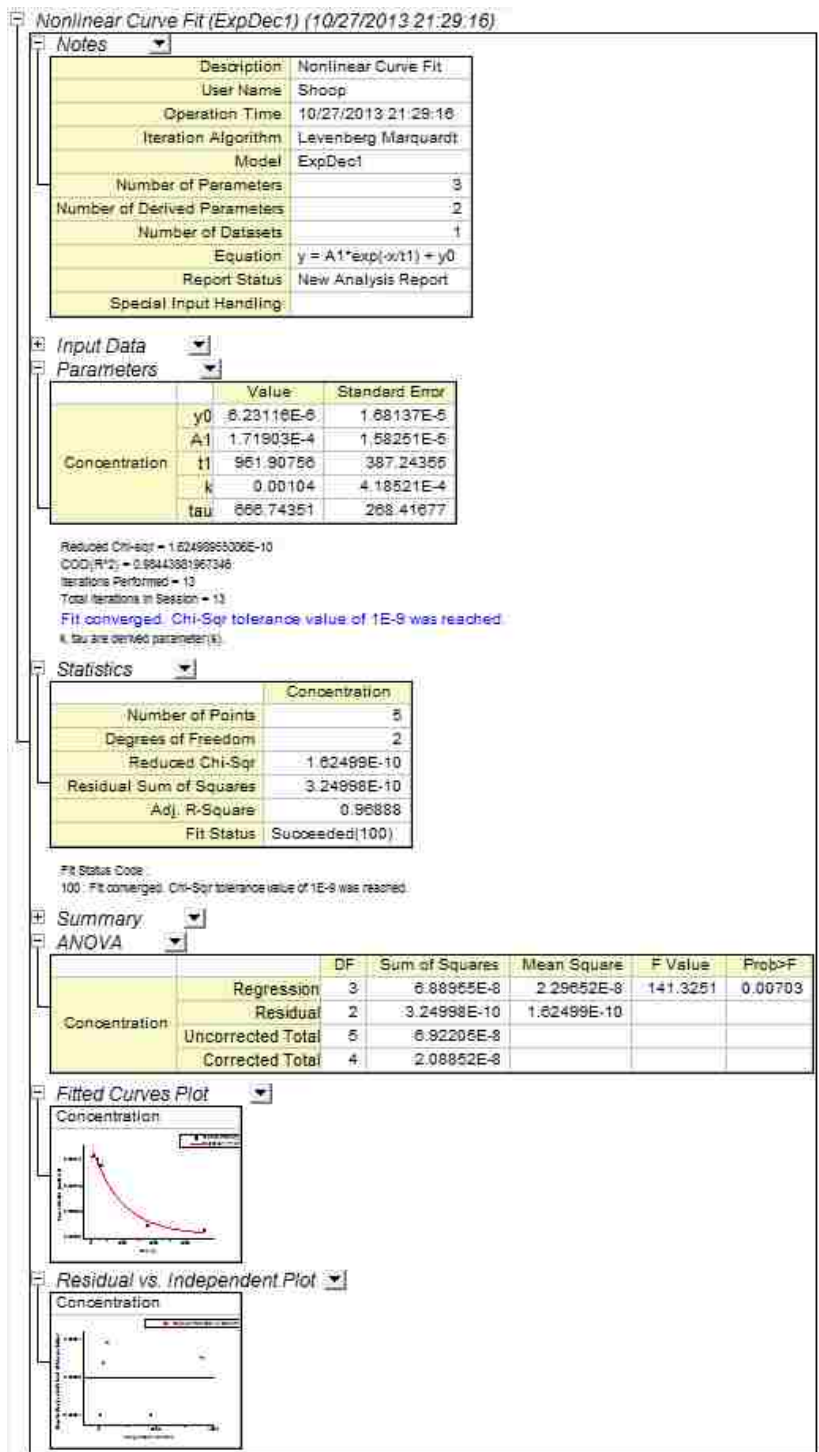


Figure A2. Fit to estimates of C_{G3} used to calculate the characteristic time constant τ_G used to describe the behavior of C_{G3} with respect to time.

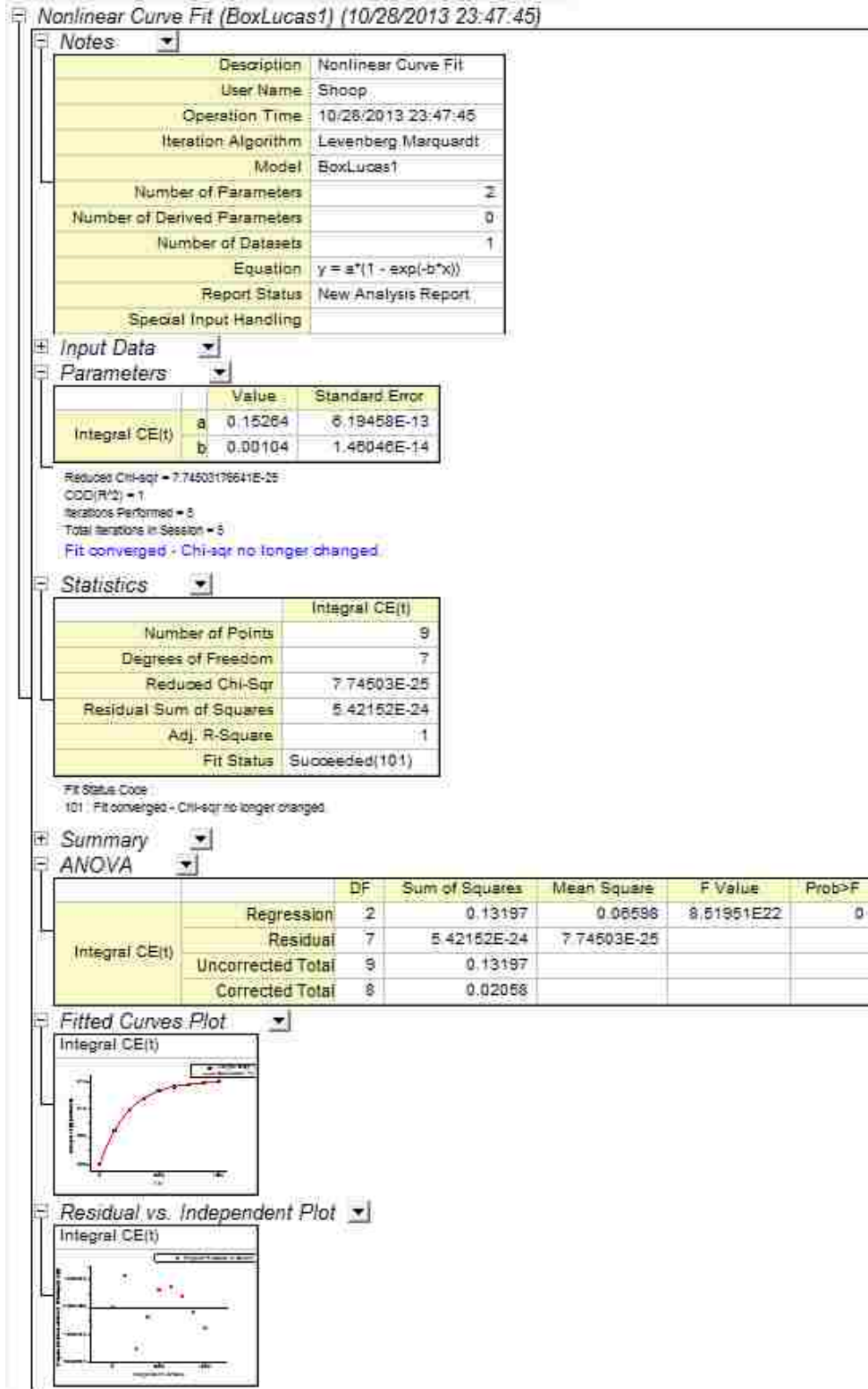


Figure A3. Empirical fit to the numerical solution to $\int C_E(t)dt = \gamma(t)$

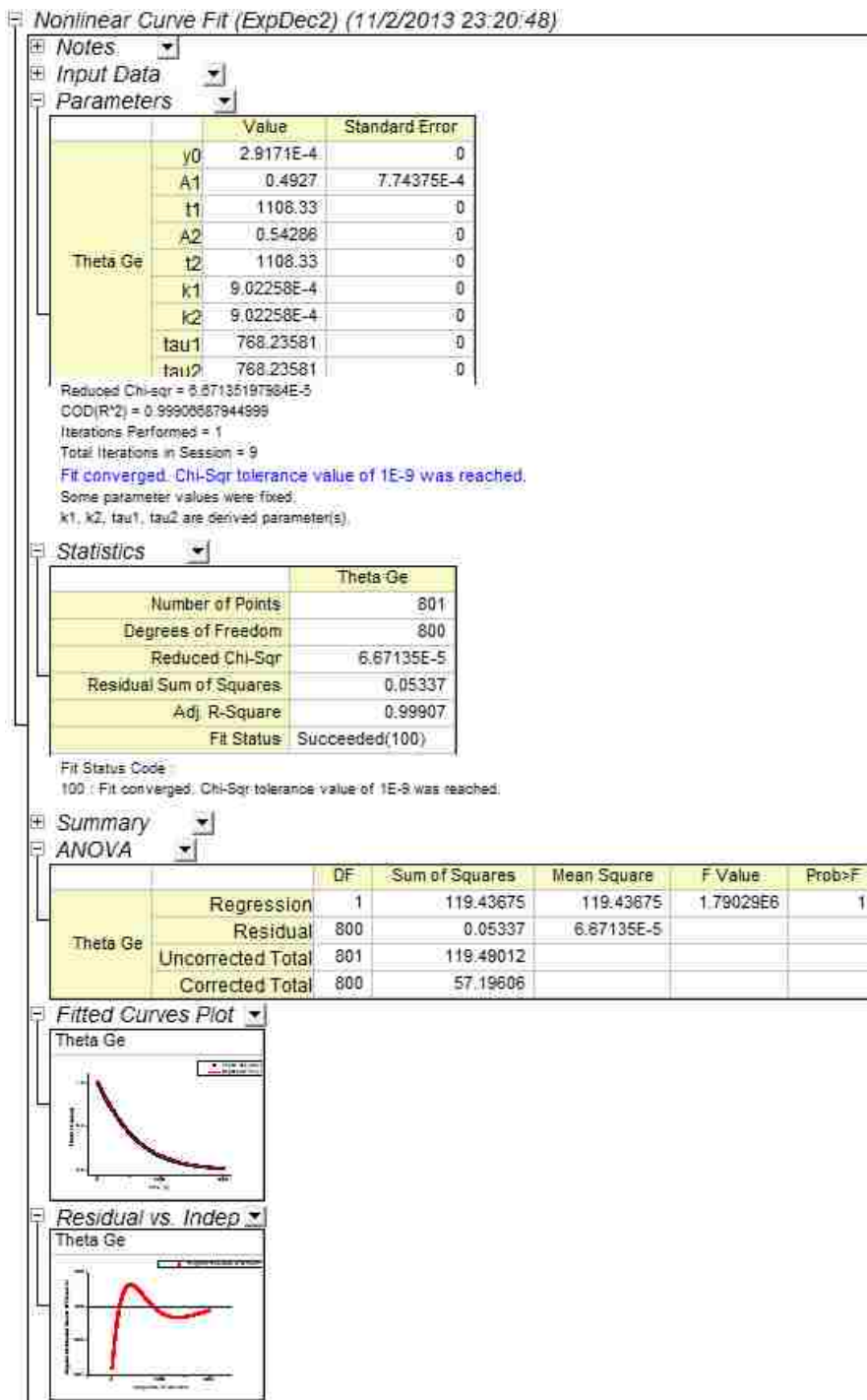


Figure A4. Empirical fit to numerical solution for $\theta_{Ge}(t)$ with double exponential containing initial approximation values for k_{ad} , k'_{ad} and k'_{des} . This fit is a verification done parallel to the fit done in the Mathematica™ script purely to obtain the goodness of fit metrics.

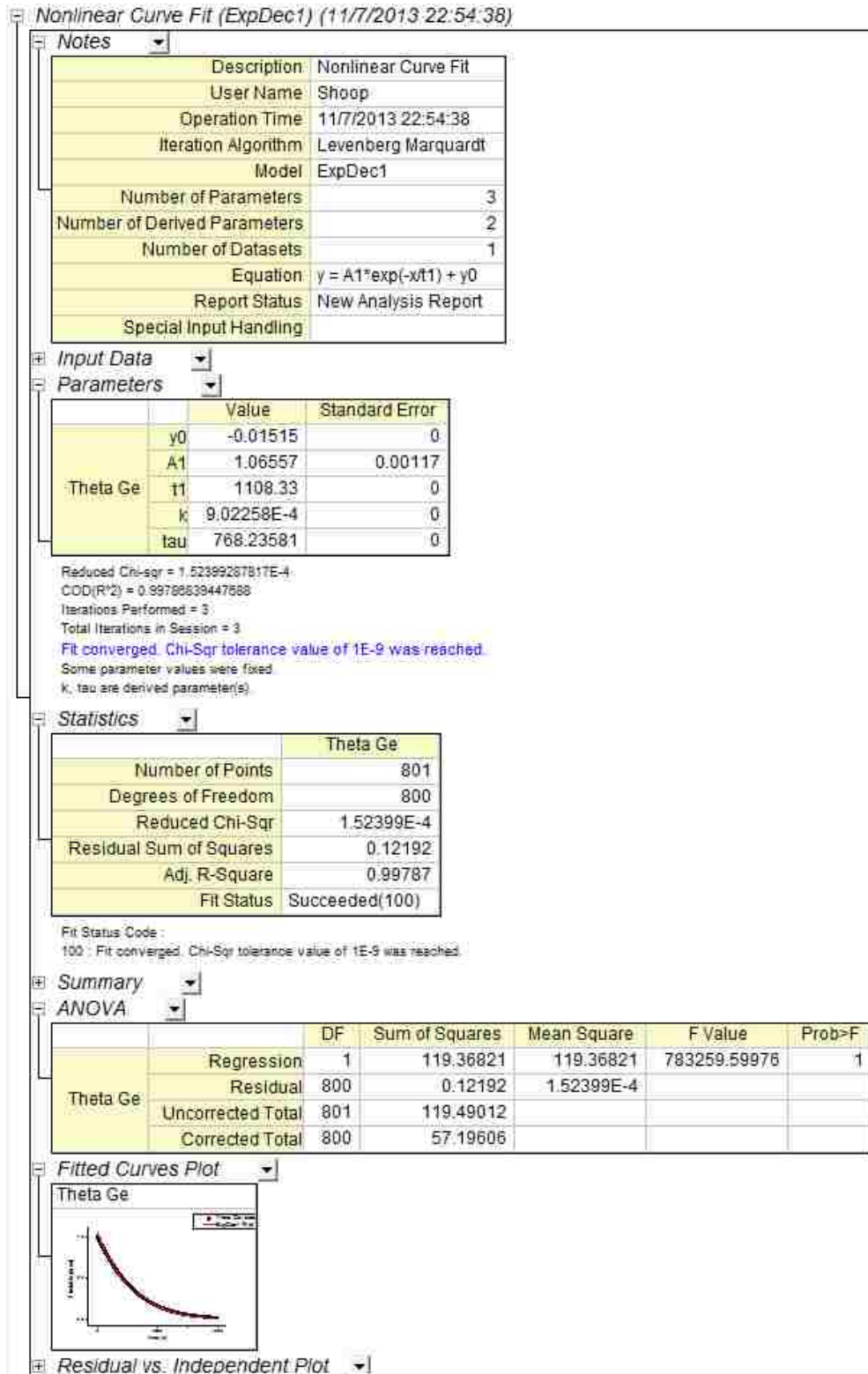


Figure A5. Empirical fit to numerical solution for $\theta_{Ge}(t)$ with single exponential containing initial approximation values for k_{ad} , k'_{ad} and k'_{des} . This fit is a verification done parallel to the fit done in the Mathematica™ script purely to obtain the goodness of fit metrics.

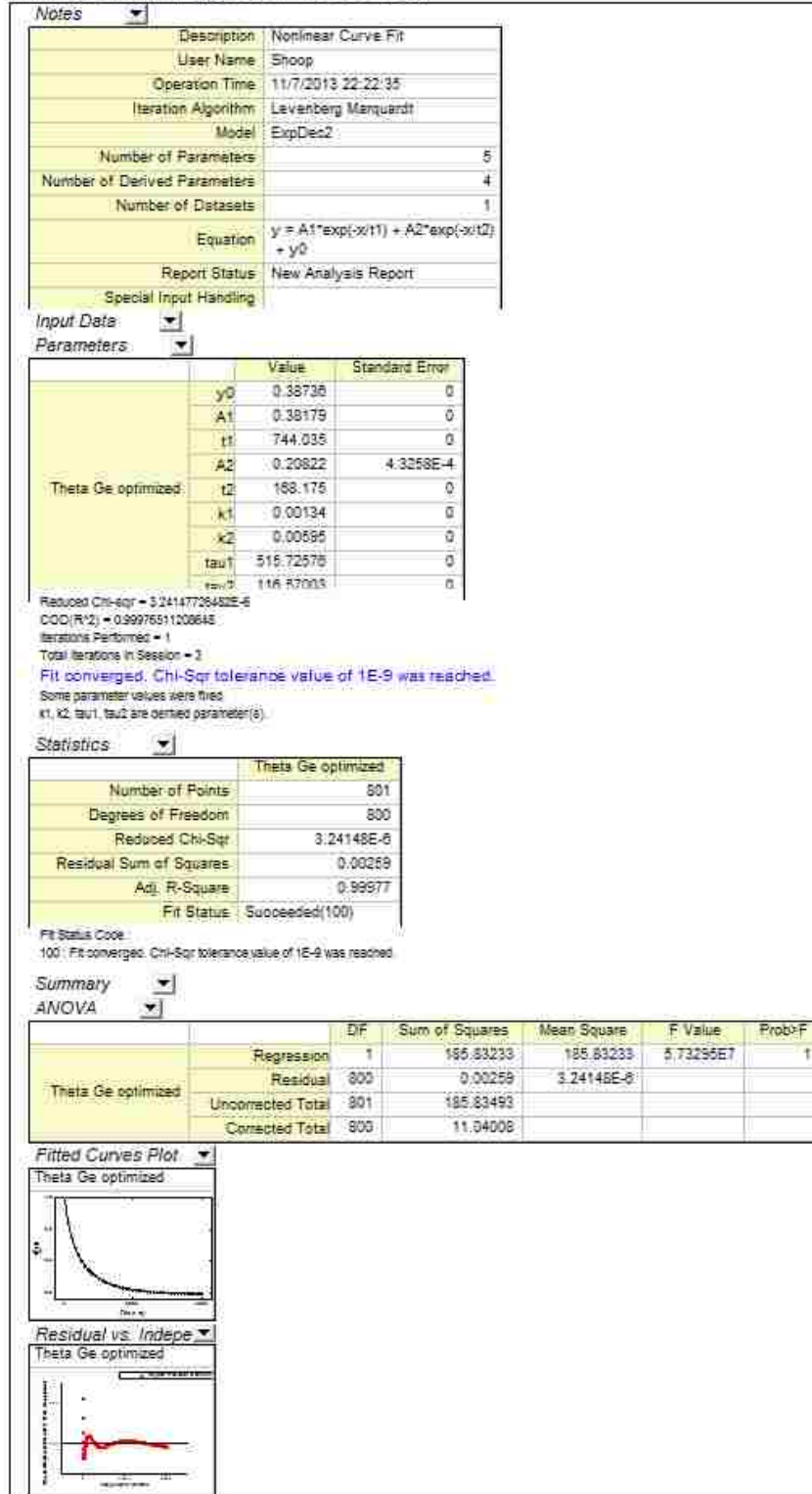


Figure A6. Empirical fit to numerical solution for $\theta_{Ge}(t)$ with single double exponential to optimized values for k_{ad} , k'_{ad} and k'_{des} . This fit is a verification done parallel to the fit done in the Mathematica™ script purely to obtain the goodness of fit metrics.

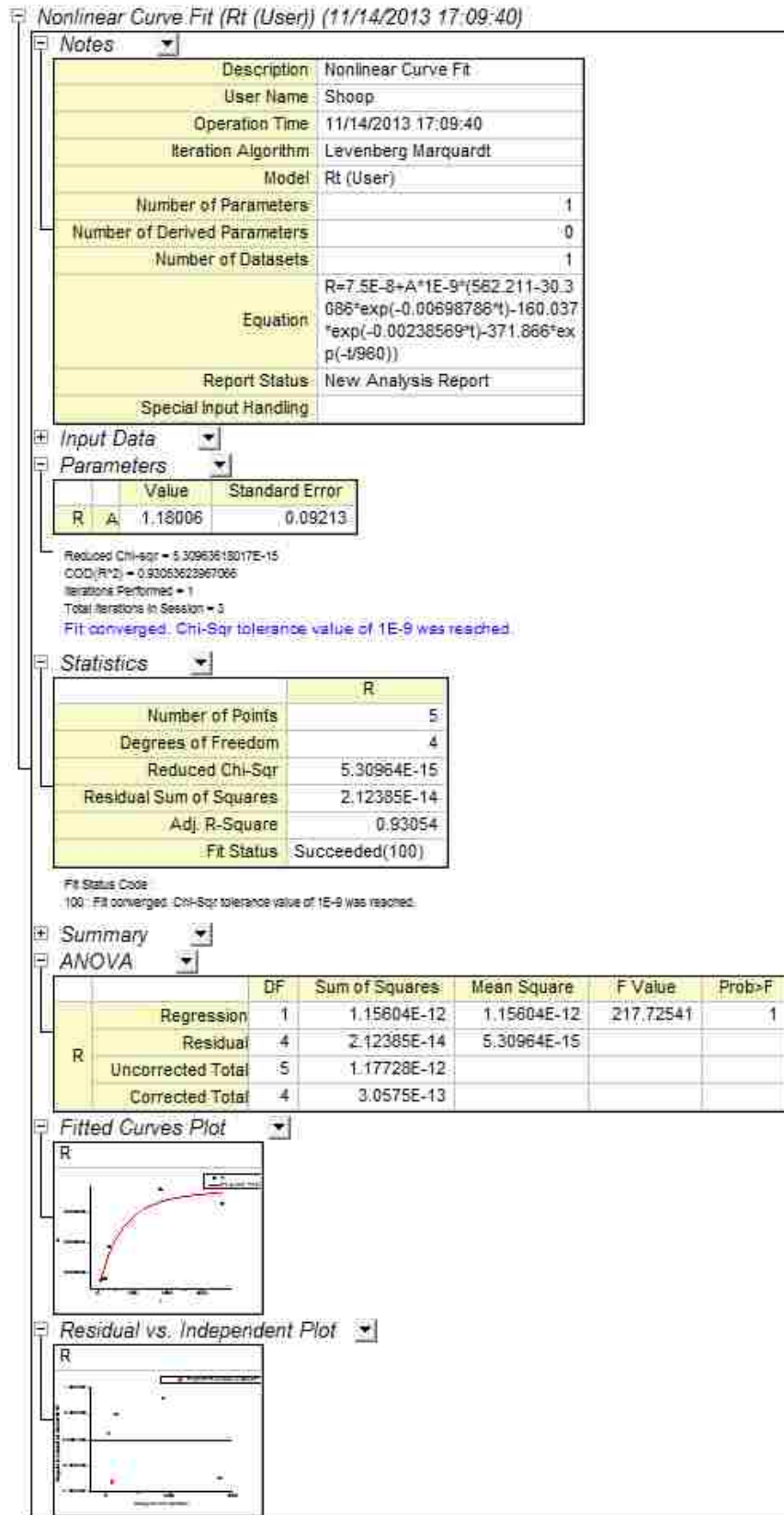


Figure A7. R^2 determination for the $R(t)$ model fit to experimental data. $R^2 = .931$

Appendix B

Numerical solutions of $\theta(t)$ for Ge and Ligands

The Mathematica™ script in this appendix is used to find the numerical solution to $\theta_{Ge}(t)$ and $\theta_L(t)$. The output is the fitting parameters A_g , B_g , C_g , τ_{G1} , and τ_{G2} for the model “modelg”. The script and output are calculated with the initial estimates for the adsorption and desorption coefficients. The output of this solution can be found in Figure 15.

Definitions

The values in the thesis text are not identical to the representations in the Mathematica™ scripts. Therefore, a key for relating the two has been provided in Table B1.

Table B1. Table relating Mathematica script variable to the Thesis text variable.

| Mathematica™ Script variable | Thesis Text |
|---------------------------------|--|
| ka1 | k_a |
| ka2 | k'_a |
| kdes | k'_{des} |
| csat | C_{Ei} |
| cl | C_L |
| pgea | ρ_{GeA} areal density of Ge binding sites |
| pge | ρ_{Ge} (density of Ge) |
| mw | MW_{Ge} Molecular weight of Ge |

| | |
|-----------|--|
| na | N_A Avagadro's number |
| τ_c | τ_c |
| Ag | A (in double exponential fit to $\theta_{Ge}(t)$) |
| Bg | B (in double exponential fit to $\theta_{Ge}(t)$) |
| Cg | C (in double exponential fit to $\theta_{Ge}(t)$) |
| τ_g | τ_{Ge1} (in double exponential fit to $\theta_{Ge}(t)$) |
| τ_g2 | τ_{Ge2} (in double exponential fit to $\theta_{Ge}(t)$) |
| Mtime | <i>Substitute value for maximum integration limit in numerical integration for Equation (38)</i> |

Mathematica™ script “ThetaVtime” using double exponential to solve differential equation for $\theta_{Ge}(t)$.

```
In[100]:=Clear[ka1, csat, kdes, ka2, cl, a, n, pgea, pge, mw, na,  $\tau_c$ ]
```

```
In[101]:=ka1=2.4
          csat=1.59*^-4
          kdes=8.2*^-6
          ka2=2.4
          cl=4.7*^-4
          n=1
          pgea=6.61*^14
          pge=5.323
          mw=72.59
          na=6.022*^23
           $\tau_c$ =960
          g=NDSolve[{y'[t]-(ka1*csat*E^(-t/ $\tau_c$ )-kdes-ka2*cl)*y[t] $\square$ kdes,y[0] $\square$ 1},y,{t,0,5000}]
```

```
Out[101]:=2.4
```

```
Out[102]:=0.000159
```

```
Out[103]:=8.2 $\times$ 10-6
```

Out[104]:=2.4

Out[105]:=0.00047

Out[106]:=1

Out[107]:=6.61×10¹⁴

Out[108]:=5.323

Out[109]:=72.59

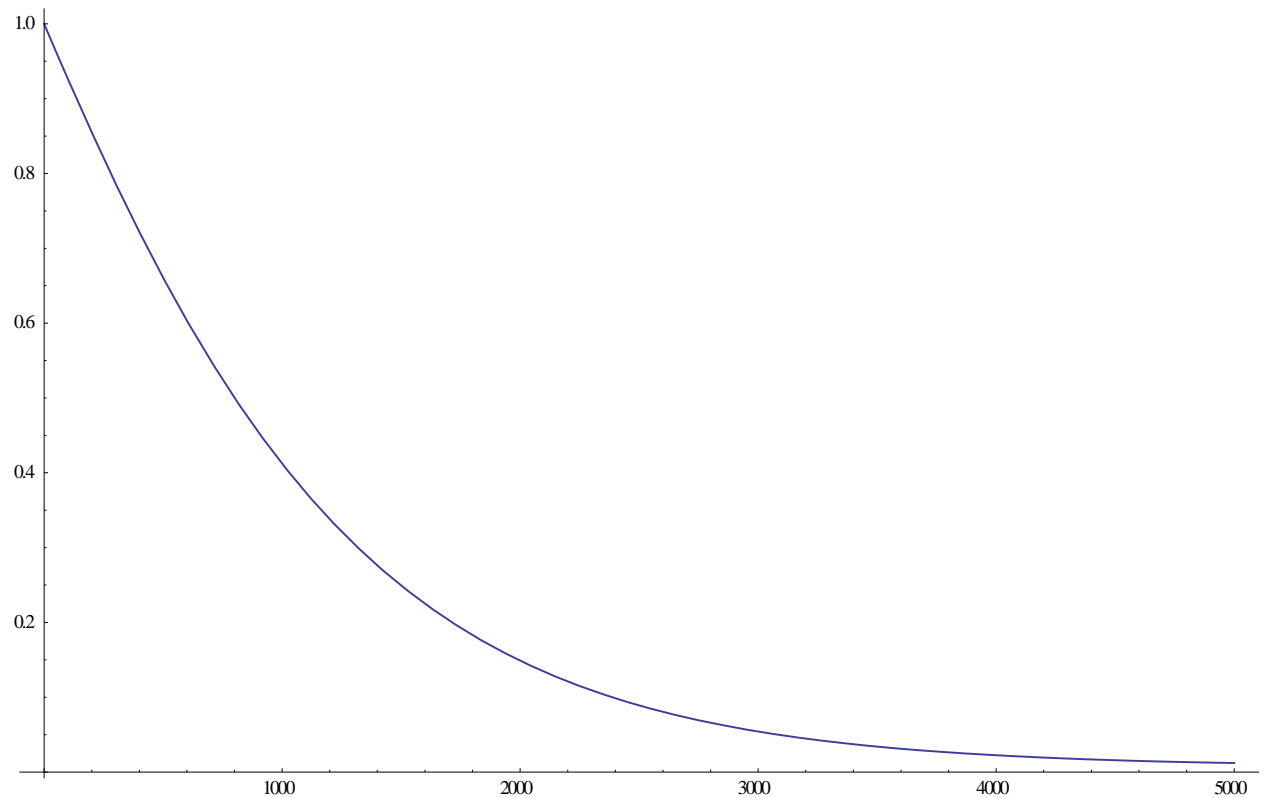
Out[110]:=6.022×10²³

Out[111]:=960

Out[112]:={y→InterpolatingFunction[{{0.,5000.}},<>]}

In[113]:=Plot[{Evaluate[{y[t]}/.g]}, {t, 0,5000}, PlotRange → Full]

Out[113]:=



In[114]:=datag=Table[{t,N[y[t]/.g]}, {t,0,4000,20}]

datag2=Flatten[datag]

datag3=Partition[datag2,2]

Out[114]:=

```

{{0,{1}}, {20,{0.985106}}, {40,{0.970286}}, {60,{0.955545}}, {80,{0.94089}}, {100,{0.926327}}, {120,{
0.911861}}, {140,{0.897497}}, {160,{0.883241}}, {180,{0.869097}}, {200,{0.85507}}, {220,{0.841163}},
{240,{0.82738}}, {260,{0.813725}}, {280,{0.8002}}, {300,{0.78681}}, {320,{0.773557}}, {340,{0.760443
}}, {360,{0.747471}}, {380,{0.734642}}, {400,{0.721959}}, {420,{0.709424}}, {440,{0.697037}}, {460,{0.
684801}}, {480,{0.672716}}, {500,{0.660784}}, {520,{0.649005}}, {540,{0.63738}}, {560,{0.625909}}, {5
80,{0.614593}}, {600,{0.603432}}, {620,{0.592426}}, {640,{0.581576}}, {660,{0.57088}}, {680,{0.56034
}}, {700,{0.549954}}, {720,{0.539722}}, {740,{0.529644}}, {760,{0.519719}}, {780,{0.509946}}, {800,{0.
500325}}, {820,{0.490854}}, {840,{0.481533}}, {860,{0.472361}}, {880,{0.463336}}, {900,{0.454459}}, {
920,{0.445726}}, {940,{0.437138}}, {960,{0.428693}}, {980,{0.42039}}, {1000,{0.412227}}, {1020,{0.40
4203}}, {1040,{0.396316}}, {1060,{0.388566}}, {1080,{0.38095}}, {1100,{0.373468}}, {1120,{0.366117}
}, {1140,{0.358896}}, {1160,{0.351804}}, {1180,{0.344839}}, {1200,{0.337999}}, {1220,{0.331283}}, {12
40,{0.324689}}, {1260,{0.318216}}, {1280,{0.311862}}, {1300,{0.305625}}, {1320,{0.299504}}, {1340,{0
.293496}}, {1360,{0.287602}}, {1380,{0.281818}}, {1400,{0.276143}}, {1420,{0.270575}}, {1440,{0.2651
14}}, {1460,{0.259757}}, {1480,{0.254502}}, {1500,{0.249349}}, {1520,{0.244295}}, {1540,{0.239339}},
{1560,{0.23448}}, {1580,{0.229715}}, {1600,{0.225043}}, {1620,{0.220464}}, {1640,{0.215974}}, {1660,
{0.211573}}, {1680,{0.207259}}, {1700,{0.20303}}, {1720,{0.198886}}, {1740,{0.194825}}, {1760,{0.190
845}}, {1780,{0.186945}}, {1800,{0.183123}}, {1820,{0.179378}}, {1840,{0.175709}}, {1860,{0.172115}
}, {1880,{0.168593}}, {1900,{0.165143}}, {1920,{0.161764}}, {1940,{0.158453}}, {1960,{0.15521}}, {198
0,{0.152034}}, {2000,{0.148923}}, {2020,{0.145877}}, {2040,{0.142893}}, {2060,{0.139971}}, {2080,{0.
137109}}, {2100,{0.134307}}, {2120,{0.131563}}, {2140,{0.128876}}, {2160,{0.126245}}, {2180,{0.1236
69}}, {2200,{0.121147}}, {2220,{0.118677}}, {2240,{0.11626}}, {2260,{0.113893}}, {2280,{0.111577}}, {
2300,{0.109309}}, {2320,{0.107088}}, {2340,{0.104915}}, {2360,{0.102788}}, {2380,{0.100706}}, {2400,
{0.0986676}}, {2420,{0.0966727}}, {2440,{0.0947203}}, {2460,{0.0928094}}, {2480,{0.0909393}}, {2500
,{0.089109}}, {2520,{0.0873178}}, {2540,{0.0855648}}, {2560,{0.0838494}}, {2580,{0.0821707}}, {2600,
{0.0805281}}, {2620,{0.0789206}}, {2640,{0.0773477}}, {2660,{0.0758085}}, {2680,{0.0743025}}, {2700
,{0.0728289}}, {2720,{0.0713871}}, {2740,{0.0699764}}, {2760,{0.0685962}}, {2780,{0.0672457}}, {280
0,{0.0659245}}, {2820,{0.0646318}}, {2840,{0.0633672}}, {2860,{0.0621299}}, {2880,{0.0609195}}, {29
00,{0.0597354}}, {2920,{0.0585769}}, {2940,{0.0574437}}, {2960,{0.0563351}}, {2980,{0.0552506}}, {3
000,{0.0541897}}, {3020,{0.0531519}}, {3040,{0.0521368}}, {3060,{0.0511438}}, {3080,{0.0501725}}, {
3100,{0.0492224}}, {3120,{0.048293}}, {3140,{0.0473839}}, {3160,{0.0464948}}, {3180,{0.0456251}}, {
3200,{0.0447745}}, {3220,{0.0439425}}, {3240,{0.0431287}}, {3260,{0.0423328}}, {3280,{0.0415542}},
{3300,{0.0407928}}, {3320,{0.0400482}}, {3340,{0.0393199}}, {3360,{0.0386076}}, {3380,{0.037911}},
{3400,{0.0372296}}, {3420,{0.0365633}}, {3440,{0.0359116}}, {3460,{0.0352743}}, {3480,{0.034651}},
{3500,{0.0340414}}, {3520,{0.0334454}}, {3540,{0.0328624}}, {3560,{0.0322923}}, {3580,{0.0317348}},
{3600,{0.0311895}}, {3620,{0.0306563}}, {3640,{0.0301349}}, {3660,{0.0296251}}, {3680,{0.0291265}},
{3700,{0.0286389}}, {3720,{0.0281621}}, {3740,{0.0276958}}, {3760,{0.0272399}}, {3780,{0.026794}},
{3800,{0.026358}}, {3820,{0.0259317}}, {3840,{0.0255148}}, {3860,{0.0251072}}, {3880,{0.0247086}},
{3900,{0.0243188}}, {3920,{0.0239376}}, {3940,{0.0235649}}, {3960,{0.0232005}}, {3980,{0.0228442
}}, {4000,{0.0224958}}}}

```

Out[115]:=

```

{0,1.,20,0.985106,40,0.970286,60,0.955545,80,0.94089,100,0.926327,120,0.911861,140,0.897497,160,0.8
83241,180,0.869097,200,0.85507,220,0.841163,240,0.82738,260,0.813725,280,0.8002,300,0.78681,320,0.
773557,340,0.760443,360,0.747471,380,0.734642,400,0.721959,420,0.709424,440,0.697037,460,0.68480
1,480,0.672716,500,0.660784,520,0.649005,540,0.63738,560,0.625909,580,0.614593,600,0.603432,620,0.
592426,640,0.581576,660,0.57088,680,0.56034,700,0.549954,720,0.539722,740,0.529644,760,0.519719,7
80,0.509946,800,0.500325,820,0.490854,840,0.481533,860,0.472361,880,0.463336,900,0.454459,920,0.4
45726,940,0.437138,960,0.428693,980,0.42039,1000,0.412227,1020,0.404203,1040,0.396316,1060,0.388
566,1080,0.38095,1100,0.373468,1120,0.366117,1140,0.358896,1160,0.351804,1180,0.344839,1200,0.33
7999,1220,0.331283,1240,0.324689,1260,0.318216,1280,0.311862,1300,0.305625,1320,0.299504,1340,0.
293496,1360,0.287602,1380,0.281818,1400,0.276143,1420,0.270575,1440,0.265114,1460,0.259757,1480,
0.254502,1500,0.249349,1520,0.244295,1540,0.239339,1560,0.23448,1580,0.229715,1600,0.225043,1620
,0.220464,1640,0.215974,1660,0.211573,1680,0.207259,1700,0.20303,1720,0.198886,1740,0.194825,176
0,0.190845,1780,0.186945,1800,0.183123,1820,0.179378,1840,0.175709,1860,0.172115,1880,0.168593,1
900,0.165143,1920,0.161764,1940,0.158453,1960,0.15521,1980,0.152034,2000,0.148923,2020,0.145877,
2040,0.142893,2060,0.139971,2080,0.137109,2100,0.134307,2120,0.131563,2140,0.128876,2160,0.12624

```

5,2180,0.123669,2200,0.121147,2220,0.118677,2240,0.11626,2260,0.113893,2280,0.111577,2300,0.109309,2320,0.107088,2340,0.104915,2360,0.102788,2380,0.100706,2400,0.0986676,2420,0.0966727,2440,0.0947203,2460,0.0928094,2480,0.0909393,2500,0.089109,2520,0.0873178,2540,0.0855648,2560,0.0838494,2580,0.0821707,2600,0.0805281,2620,0.0789206,2640,0.0773477,2660,0.0758085,2680,0.0743025,2700,0.0728289,2720,0.0713871,2740,0.0699764,2760,0.0685962,2780,0.0672457,2800,0.0659245,2820,0.0646318,2840,0.0633672,2860,0.0621299,2880,0.0609195,2900,0.0597354,2920,0.0585769,2940,0.0574437,2960,0.0563351,2980,0.0552506,3000,0.0541897,3020,0.0531519,3040,0.0521368,3060,0.0511438,3080,0.0501725,3100,0.0492224,3120,0.048293,3140,0.0473839,3160,0.0464948,3180,0.0456251,3200,0.0447745,3220,0.0439425,3240,0.0431287,3260,0.0423328,3280,0.0415542,3300,0.0407928,3320,0.0400482,3340,0.0393199,3360,0.0386076,3380,0.037911,3400,0.0372296,3420,0.0365633,3440,0.0359116,3460,0.0352743,3480,0.034651,3500,0.0340414,3520,0.0334454,3540,0.0328624,3560,0.0322923,3580,0.0317348,3600,0.0311895,3620,0.0306563,3640,0.0301349,3660,0.0296251,3680,0.0291265,3700,0.0286389,3720,0.0281621,3740,0.0276958,3760,0.0272399,3780,0.026794,3800,0.026358,3820,0.0259317,3840,0.0255148,3860,0.0251072,3880,0.0247086,3900,0.0243188,3920,0.0239376,3940,0.0235649,3960,0.0232005,3980,0.0228442,4000,0.0224958}

Out[116]:=

```
{ {0,1}, {20,0.985106}, {40,0.970286}, {60,0.955545}, {80,0.94089}, {100,0.926327}, {120,0.911861}, {140,0.897497}, {160,0.883241}, {180,0.869097}, {200,0.85507}, {220,0.841163}, {240,0.82738}, {260,0.813725}, {280,0.8002}, {300,0.78681}, {320,0.773557}, {340,0.760443}, {360,0.747471}, {380,0.734642}, {400,0.721959}, {420,0.709424}, {440,0.697037}, {460,0.684801}, {480,0.672716}, {500,0.660784}, {520,0.649005}, {540,0.63738}, {560,0.625909}, {580,0.614593}, {600,0.603432}, {620,0.592426}, {640,0.581576}, {660,0.57088}, {680,0.56034}, {700,0.549954}, {720,0.539722}, {740,0.529644}, {760,0.519719}, {780,0.509946}, {800,0.500325}, {820,0.490854}, {840,0.481533}, {860,0.472361}, {880,0.463336}, {900,0.454459}, {920,0.445726}, {940,0.437138}, {960,0.428693}, {980,0.42039}, {1000,0.412227}, {1020,0.404203}, {1040,0.396316}, {1060,0.388566}, {1080,0.38095}, {1100,0.373468}, {1120,0.366117}, {1140,0.358896}, {1160,0.351804}, {1180,0.344839}, {1200,0.337999}, {1220,0.331283}, {1240,0.324689}, {1260,0.318216}, {1280,0.311862}, {1300,0.305625}, {1320,0.299504}, {1340,0.293496}, {1360,0.287602}, {1380,0.281818}, {1400,0.276143}, {1420,0.270575}, {1440,0.265114}, {1460,0.259757}, {1480,0.254502}, {1500,0.249349}, {1520,0.244295}, {1540,0.239339}, {1560,0.23448}, {1580,0.229715}, {1600,0.225043}, {1620,0.220464}, {1640,0.215974}, {1660,0.211573}, {1680,0.207259}, {1700,0.20303}, {1720,0.198886}, {1740,0.194825}, {1760,0.190845}, {1780,0.186945}, {1800,0.183123}, {1820,0.179378}, {1840,0.175709}, {1860,0.172115}, {1880,0.168593}, {1900,0.165143}, {1920,0.161764}, {1940,0.158453}, {1960,0.15521}, {1980,0.152034}, {2000,0.148923}, {2020,0.145877}, {2040,0.142893}, {2060,0.139971}, {2080,0.137109}, {2100,0.134307}, {2120,0.131563}, {2140,0.128876}, {2160,0.126245}, {2180,0.123669}, {2200,0.121147}, {2220,0.118677}, {2240,0.11626}, {2260,0.113893}, {2280,0.111577}, {2300,0.109309}, {2320,0.107088}, {2340,0.104915}, {2360,0.102788}, {2380,0.100706}, {2400,0.0986676}, {2420,0.0966727}, {2440,0.0947203}, {2460,0.0928094}, {2480,0.0909393}, {2500,0.089109}, {2520,0.0873178}, {2540,0.0855648}, {2560,0.0838494}, {2580,0.0821707}, {2600,0.0805281}, {2620,0.0789206}, {2640,0.0773477}, {2660,0.0758085}, {2680,0.0743025}, {2700,0.0728289}, {2720,0.0713871}, {2740,0.0699764}, {2760,0.0685962}, {2780,0.0672457}, {2800,0.0659245}, {2820,0.0646318}, {2840,0.0633672}, {2860,0.0621299}, {2880,0.0609195}, {2900,0.0597354}, {2920,0.0585769}, {2940,0.0574437}, {2960,0.0563351}, {2980,0.0552506}, {3000,0.0541897}, {3020,0.0531519}, {3040,0.0521368}, {3060,0.0511438}, {3080,0.0501725}, {3100,0.0492224}, {3120,0.048293}, {3140,0.0473839}, {3160,0.0464948}, {3180,0.0456251}, {3200,0.0447745}, {3220,0.0439425}, {3240,0.0431287}, {3260,0.0423328}, {3280,0.0415542}, {3300,0.0407928}, {3320,0.0400482}, {3340,0.0393199}, {3360,0.0386076}, {3380,0.037911}, {3400,0.0372296}, {3420,0.0365633}, {3440,0.0359116}, {3460,0.0352743}, {3480,0.034651}, {3500,0.0340414}, {3520,0.0334454}, {3540,0.0328624}, {3560,0.0322923}, {3580,0.0317348}, {3600,0.0311895}, {3620,0.0306563}, {3640,0.0301349}, {3660,0.0296251}, {3680,0.0291265}, {3700,0.0286389}, {3720,0.0281621}, {3740,0.0276958}, {3760,0.0272399}, {3780,0.026794}, {3800,0.026358}, {3820,0.0259317}, {3840,0.0255148}, {3860,0.0251072}, {3880,0.0247086}, {3900,0.0243188}, {3920,0.0239376}, {3940,0.0235649}, {3960,0.0232005}, {3980,0.0228442}, {4000,0.0224958} }
```

In[117]:= { modelg=Ag*Exp[-t/τg]+Bg*Exp[-t/τg2]+cg

gsol=FindFit[datag3,modelg,{ {Ag,.3}, {τg,2000}, {Bg,.3}, {τg2,2000}, {cg,.004}],t]

```

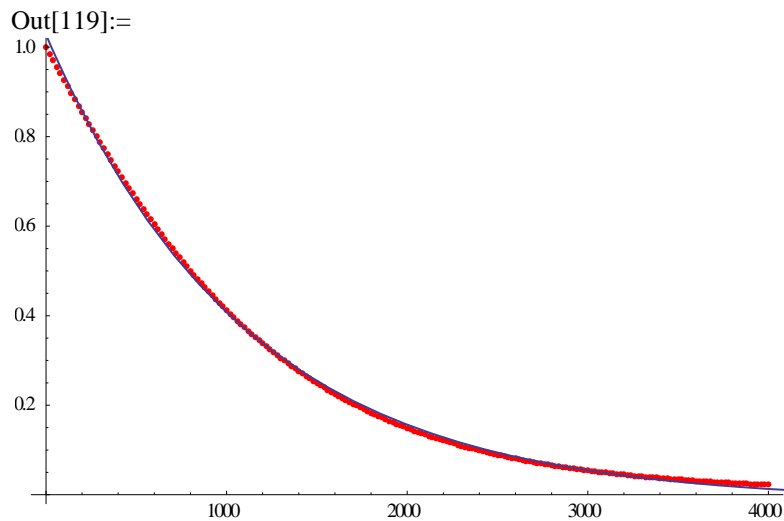
Out[117]:= {{cg+Ag : [ t/g +Bg : [ t/g2
Out[118]:= {Ag → 0.500515, τg → 1108.33, Bg → 0.542862, τg2 → 1108.33, cg →
-0.0151544}

```

```

In[119]:= Show[ListPlot[datag3, PlotStyle→Red,PlotRange→Full], Plot[{Evaluate[modelg/.gsol]}, {t, 0,
7000},PlotRange→Full]]

```



Mathematica™ script “ThetaVtime” using partial analytical method to solve differential equation for $\theta_{Ge}(t)$.

```

In[100]:= Clear[ka1, csat, kdes, ka2, cl, a, n, pgea, pge, mw, na, τc]

```

```

In[101]:= ka1=2.4
          csat=1.59*^-4
          kdes=8.2*^-6
          ka2=2.4
          cl=4.7*^-4
          n=1
          pgea=6.61*^14
          pge=5.323
          mw=72.59
          na=6.022*^23
          τc=960

```

```

g[t_]:=kdes*(NIntegrate[(Exp[(kdes*x+ka2*cl*x+ka1*csat*tc*Exp[-
x/tc])]/(Exp[(kdes*t+ka2*cl*t+ka1*csat*tc*Exp[-
t/tc])]),{x,0,mtime}))+Exp[(ka1*csat*tc)]/Exp[(kdes*t+ka2*cl*t+ka1*csat*tc*Exp[-t/tc])]
Out[101]:=2.4
Out[102]:=0.000159

Out[103]:=8.2×10-6

Out[104]:=2.4

Out[105]:=0.00047

Out[106]:=1

Out[107]:=6.61×1014

Out[108]:=5.323

Out[109]:=72.59

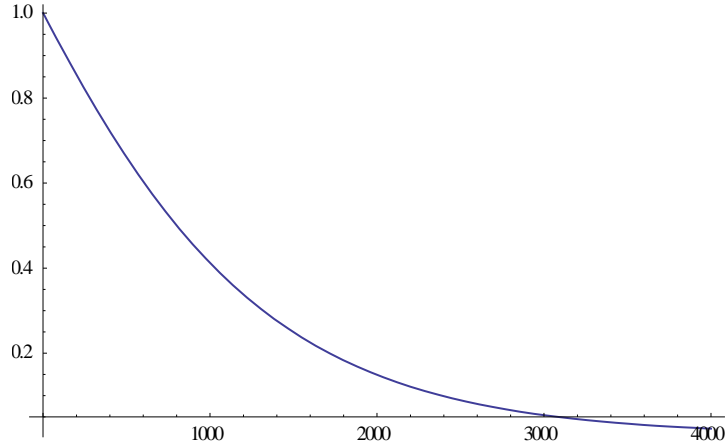
Out[110]:=6.022×1023

Out[111]:=960

```

```
In[113]:=Plot[{N[g[mtime]]}, {mtime, 0,4000}, PlotRange -> Full]
```

```
Out[113]:=
```



```

In[114]:=datag=Table[{mtime, N[g[mtime]]}, {mtime, 0,4000,20}]
datag2=Flatten[datag]

datag3=Partition[datag2,2]

```

```

Out[114]:=
{{0,1.}, {20,0.985106}, {40,0.970286}, {60,0.955545}, {80,0.94089}, {100,0.926327}, {120,0.911861}, {140,
0.897497}, {160,0.883241}, {180,0.869097}, {200,0.85507}, {220,0.841163}, {240,0.82738}, {260,0.813725
}, {280,0.8002}, {300,0.78681}, {320,0.773557}, {340,0.760443}, {360,0.747471}, {380,0.734642}, {400,0.7
21959}, {420,0.709424}, {440,0.697037}, {460,0.684801}, {480,0.672716}, {500,0.660784}, {520,0.649005
}, {540,0.637379}, {560,0.625909}, {580,0.614593}, {600,0.603432}, {620,0.592426}, {640,0.581576}, {660
,0.57088}, {680,0.56034}, {700,0.549954}, {720,0.539722}, {740,0.529644}, {760,0.519719}, {780,0.50994

```

6},{800,0.500325},{820,0.490854},{840,0.481533},{860,0.472361},{880,0.463336},{900,0.454459},{920,0.445726},{940,0.437138},{960,0.428693},{980,0.42039},{1000,0.412227},{1020,0.404203},{1040,0.396316},{1060,0.388566},{1080,0.38095},{1100,0.373468},{1120,0.366117},{1140,0.358896},{1160,0.351804},{1180,0.344839},{1200,0.337999},{1220,0.331283},{1240,0.324689},{1260,0.318216},{1280,0.311862},{1300,0.305625},{1320,0.299504},{1340,0.293496},{1360,0.287602},{1380,0.281818},{1400,0.276143},{1420,0.270575},{1440,0.265114},{1460,0.259757},{1480,0.254502},{1500,0.249349},{1520,0.244295},{1540,0.239339},{1560,0.23448},{1580,0.229715},{1600,0.225043},{1620,0.220464},{1640,0.215974},{1660,0.211573},{1680,0.207259},{1700,0.20303},{1720,0.198886},{1740,0.194825},{1760,0.190845},{1780,0.186945},{1800,0.183123},{1820,0.179378},{1840,0.175709},{1860,0.172115},{1880,0.168593},{1900,0.165143},{1920,0.161764},{1940,0.158453},{1960,0.15521},{1980,0.152034},{2000,0.148923},{2020,0.145877},{2040,0.142893},{2060,0.139971},{2080,0.137109},{2100,0.134307},{2120,0.131563},{2140,0.128876},{2160,0.126245},{2180,0.123669},{2200,0.121147},{2220,0.118678},{2240,0.11626},{2260,0.113893},{2280,0.111577},{2300,0.109309},{2320,0.107088},{2340,0.104915},{2360,0.102788},{2380,0.100706},{2400,0.0986676},{2420,0.0966728},{2440,0.0947203},{2460,0.0928095},{2480,0.0909393},{2500,0.089109},{2520,0.0873178},{2540,0.0855649},{2560,0.0838495},{2580,0.0821708},{2600,0.0805281},{2620,0.0789206},{2640,0.0773477},{2660,0.0758085},{2680,0.0743025},{2700,0.072829},{2720,0.0713871},{2740,0.0699764},{2760,0.0685962},{2780,0.0672457},{2800,0.0659245},{2820,0.0646319},{2840,0.0633672},{2860,0.0621299},{2880,0.0609195},{2900,0.0597354},{2920,0.058577},{2940,0.0574437},{2960,0.0563351},{2980,0.0552506},{3000,0.0541897},{3020,0.053152},{3040,0.0521368},{3060,0.0511438},{3080,0.0501725},{3100,0.0492224},{3120,0.048293},{3140,0.047384},{3160,0.0464949},{3180,0.0456252},{3200,0.0447745},{3220,0.0439425},{3240,0.0431287},{3260,0.0423328},{3280,0.0415543},{3300,0.0407929},{3320,0.0400482},{3340,0.0393199},{3360,0.0386076},{3380,0.037911},{3400,0.0372296},{3420,0.0365633},{3440,0.0359116},{3460,0.0352743},{3480,0.034651},{3500,0.0340415},{3520,0.0334454},{3540,0.0328624},{3560,0.0322923},{3580,0.0317348},{3600,0.0311896},{3620,0.0306564},{3640,0.030135},{3660,0.0296251},{3680,0.0291265},{3700,0.0286389},{3720,0.0281621},{3740,0.0276958},{3760,0.0272399},{3780,0.0267941},{3800,0.0263581},{3820,0.0259317},{3840,0.0255149},{3860,0.0251072},{3880,0.0247086},{3900,0.0243188},{3920,0.0239377},{3940,0.023565},{3960,0.0232006},{3980,0.0228442},{4000,0.0224958}}

Out[115]:=

{0,1.,20,0.985106,40,0.970286,60,0.955545,80,0.94089,100,0.926327,120,0.911861,140,0.897497,160,0.883241,180,0.869097,200,0.85507,220,0.841163,240,0.82738,260,0.813725,280,0.8002,300,0.78681,320,0.773557,340,0.760443,360,0.747471,380,0.734642,400,0.721959,420,0.709424,440,0.697037,460,0.68480,480,0.672716,500,0.660784,520,0.649005,540,0.637379,560,0.625909,580,0.614593,600,0.603432,620,0.592426,640,0.581576,660,0.57088,680,0.56034,700,0.549954,720,0.539722,740,0.529644,760,0.519719,780,0.509946,800,0.500325,820,0.490854,840,0.481533,860,0.472361,880,0.463336,900,0.454459,920,0.445726,940,0.437138,960,0.428693,980,0.42039,1000,0.412227,1020,0.404203,1040,0.396316,1060,0.388566,1080,0.38095,1100,0.373468,1120,0.366117,1140,0.358896,1160,0.351804,1180,0.344839,1200,0.337999,1220,0.331283,1240,0.324689,1260,0.318216,1280,0.311862,1300,0.305625,1320,0.299504,1340,0.293496,1360,0.287602,1380,0.281818,1400,0.276143,1420,0.270575,1440,0.265114,1460,0.259757,1480,0.254502,1500,0.249349,1520,0.244295,1540,0.239339,1560,0.23448,1580,0.229715,1600,0.225043,1620,0.220464,1640,0.215974,1660,0.211573,1680,0.207259,1700,0.20303,1720,0.198886,1740,0.194825,1760,0.190845,1780,0.186945,1800,0.183123,1820,0.179378,1840,0.175709,1860,0.172115,1880,0.168593,1900,0.165143,1920,0.161764,1940,0.158453,1960,0.15521,1980,0.152034,2000,0.148923,2020,0.145877,2040,0.142893,2060,0.139971,2080,0.137109,2100,0.134307,2120,0.131563,2140,0.128876,2160,0.126245,2180,0.123669,2200,0.121147,2220,0.118678,2240,0.11626,2260,0.113893,2280,0.111577,2300,0.109309,2320,0.107088,2340,0.104915,2360,0.102788,2380,0.100706,2400,0.0986676,2420,0.0966728,2440,0.0947203,2460,0.0928095,2480,0.0909393,2500,0.089109,2520,0.0873178,2540,0.0855649,2560,0.0838495,2580,0.0821708,2600,0.0805281,2620,0.0789206,2640,0.0773477,2660,0.0758085,2680,0.0743025,2700,0.072829,2720,0.0713871,2740,0.0699764,2760,0.0685962,2780,0.0672457,2800,0.0659245,2820,0.0646319,2840,0.0633672,2860,0.0621299,2880,0.0609195,2900,0.0597354,2920,0.058577,2940,0.0574437,2960,0.0563351,2980,0.0552506,3000,0.0541897,3020,0.053152,3040,0.0521368,3060,0.0511438,3080,0.0501725,3100,0.0492224,3120,0.048293,3140,0.047384,3160,0.0464949,3180,0.0456252,3200,0.0447745,3220,0.0439425,3240,0.0431287,3260,0.0423328,3280,0.0415543,3300,0.0407929,3320,0.0400482,3340,0.0393199,3360,0.0386076,3380,0.037911,3400,0.0372296,3420,0.0365633,3440,0.0359116,3460,0.0352743,3480,0.034651,3500,0.0340415,3520,0.0334454,3540,0.0328624,3560,0.0322923,3580,0.0317348,3600,0.0311896,3620,0.0306564,3640,0.030135,3660,0.0296251,3680,0.0291265,3700,0.0286389,3720,0.0281621,3740,0.0276958,3760,0.0272399,3780,0.0267941,3800,0.0263581,3820,0.0259317,3840,0.0255149,3860,0.0251072,3880,0.0247086,3900,0.0243188,3920,0.0239377,3940,0.023565,3960,0.0232006,3980,0.0228442,4000,0.0224958}}

```
00,0.0311896,3620,0.0306564,3640,0.030135,3660,0.0296251,3680,0.0291265,3700,0.0286389,3720,0.0281621,3740,0.0276958,3760,0.0272399,3780,0.0267941,3800,0.0263581,3820,0.0259317,3840,0.0255149,3860,0.0251072,3880,0.0247086,3900,0.0243188,3920,0.0239377,3940,0.023565,3960,0.0232006,3980,0.0228442,4000,0.0224958}
```

```
Out[116]:=
```

```
{ {0,1.}, {20,0.985106}, {40,0.970286}, {60,0.955545}, {80,0.94089}, {100,0.926327}, {120,0.911861}, {140,0.897497}, {160,0.883241}, {180,0.869097}, {200,0.85507}, {220,0.841163}, {240,0.82738}, {260,0.813725}, {280,0.8002}, {300,0.78681}, {320,0.773557}, {340,0.760443}, {360,0.747471}, {380,0.734642}, {400,0.721959}, {420,0.709424}, {440,0.697037}, {460,0.684801}, {480,0.672716}, {500,0.660784}, {520,0.649005}, {540,0.637379}, {560,0.625909}, {580,0.614593}, {600,0.603432}, {620,0.592426}, {640,0.581576}, {660,0.57088}, {680,0.56034}, {700,0.549954}, {720,0.539722}, {740,0.529644}, {760,0.519719}, {780,0.509946}, {800,0.500325}, {820,0.490854}, {840,0.481533}, {860,0.472361}, {880,0.463336}, {900,0.454459}, {920,0.445726}, {940,0.437138}, {960,0.428693}, {980,0.42039}, {1000,0.412227}, {1020,0.404203}, {1040,0.396316}, {1060,0.388566}, {1080,0.38095}, {1100,0.373468}, {1120,0.366117}, {1140,0.358896}, {1160,0.351804}, {1180,0.344839}, {1200,0.337999}, {1220,0.331283}, {1240,0.324689}, {1260,0.318216}, {1280,0.311862}, {1300,0.305625}, {1320,0.299504}, {1340,0.293496}, {1360,0.287602}, {1380,0.281818}, {1400,0.276143}, {1420,0.270575}, {1440,0.265114}, {1460,0.259757}, {1480,0.254502}, {1500,0.249349}, {1520,0.244295}, {1540,0.239339}, {1560,0.23448}, {1580,0.229715}, {1600,0.225043}, {1620,0.220464}, {1640,0.215974}, {1660,0.211573}, {1680,0.207259}, {1700,0.20303}, {1720,0.198886}, {1740,0.194825}, {1760,0.190845}, {1780,0.186945}, {1800,0.183123}, {1820,0.179378}, {1840,0.175709}, {1860,0.172115}, {1880,0.168593}, {1900,0.165143}, {1920,0.161764}, {1940,0.158453}, {1960,0.15521}, {1980,0.152034}, {2000,0.148923}, {2020,0.145877}, {2040,0.142893}, {2060,0.139971}, {2080,0.137109}, {2100,0.134307}, {2120,0.131563}, {2140,0.128876}, {2160,0.126245}, {2180,0.123669}, {2200,0.121147}, {2220,0.118678}, {2240,0.11626}, {2260,0.113893}, {2280,0.111577}, {2300,0.109309}, {2320,0.107088}, {2340,0.104915}, {2360,0.102788}, {2380,0.100706}, {2400,0.0986676}, {2420,0.0966728}, {2440,0.0947203}, {2460,0.0928095}, {2480,0.0909393}, {2500,0.089109}, {2520,0.0873178}, {2540,0.0855649}, {2560,0.0838495}, {2580,0.0821708}, {2600,0.0805281}, {2620,0.0789206}, {2640,0.0773477}, {2660,0.0758085}, {2680,0.0743025}, {2700,0.072829}, {2720,0.0713871}, {2740,0.0699764}, {2760,0.0685962}, {2780,0.0672457}, {2800,0.0659245}, {2820,0.0646319}, {2840,0.0633672}, {2860,0.0621299}, {2880,0.0609195}, {2900,0.0597354}, {2920,0.058577}, {2940,0.0574437}, {2960,0.0563351}, {2980,0.0552506}, {3000,0.0541897}, {3020,0.053152}, {3040,0.0521368}, {3060,0.0511438}, {3080,0.0501725}, {3100,0.0492224}, {3120,0.048293}, {3140,0.047384}, {3160,0.0464949}, {3180,0.0456252}, {3200,0.0447745}, {3220,0.0439425}, {3240,0.0431287}, {3260,0.0423328}, {3280,0.0415543}, {3300,0.0407929}, {3320,0.0400482}, {3340,0.0393199}, {3360,0.0386076}, {3380,0.037911}, {3400,0.0372296}, {3420,0.0365633}, {3440,0.0359116}, {3460,0.0352743}, {3480,0.034651}, {3500,0.0340415}, {3520,0.0334454}, {3540,0.0328624}, {3560,0.0322923}, {3580,0.0317348}, {3600,0.0311896}, {3620,0.0306564}, {3640,0.030135}, {3660,0.0296251}, {3680,0.0291265}, {3700,0.0286389}, {3720,0.0281621}, {3740,0.0276958}, {3760,0.0272399}, {3780,0.0267941}, {3800,0.0263581}, {3820,0.0259317}, {3840,0.0255149}, {3860,0.0251072}, {3880,0.0247086}, {3900,0.0243188}, {3920,0.0239377}, {3940,0.023565}, {3960,0.0232006}, {3980,0.0228442}, {4000,0.0224958} }
```

```
In[117]:= { {modelg=Ag*Exp[-t/τg]+Bg*Exp[-t/τg2]+cg
```

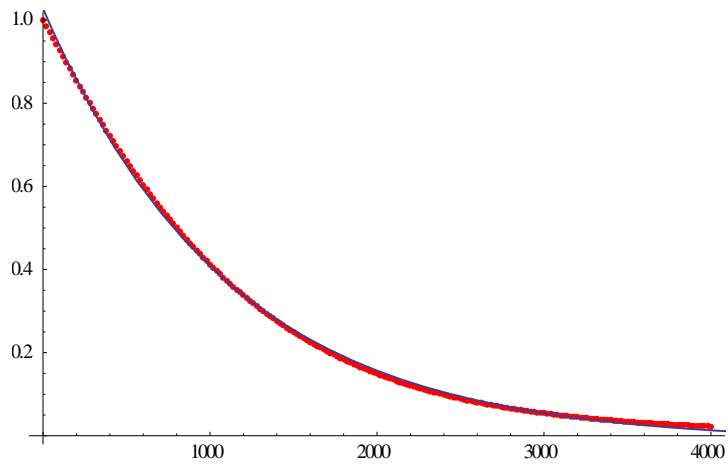
```
gsol=FindFit[datag3,modelg,{ {Ag,.3}, {τg,2000}, {Bg,.3}, {τg2,2000}, {cg,.004} },t]
```

```
Out[117]:= { {cg+Ag Exp[-t/τg]+Bg Exp[-t/τg2]
```

```
Out[118]:= {Ag → 0.542745, τg → 1108.33, Bg → 0.500632, τg2 → 1108.33, cg → -0.0151543}
```

```
In[119]:= Show[ListPlot[datag3, PlotStyle→Red,PlotRange→Full], Plot[{Evaluate[modelg/gsol]}, {t, 0, 7000},PlotRange→Full]]
```

```
Out[119]:=
```

Appendix C Model Optimization Detail

This Appendix contains the Mathematica™ Code for the Optimization of k_{ad} , k'_{ad} and k'_{des} as fit to the model in this thesis. The values of k_{ad} , k'_{ad} and k'_{des} are changed using a Differential Evolution algorithm in Mathematica™ to minimize the sum of squares of the residual values of Model versus experimental mean data. Experimental data is represented in cm. The output is the optimized values for parameters k_{ad} , k'_{ad} and k'_{des} . The results of the growth rate model with the optimized values for k_{ad} , k'_{ad} and k'_{des} can be found in Figure 19.

Definitions

The values in the thesis text are not identical to the representations in the Mathematica™ scripts. Therefore, a key for relating the two has been provided in Table C1.

Table C1. Table relating Mathematica™ script variable to the Thesis text variable.

| Mathematica™ Script variable | Thesis Text |
|---------------------------------|-------------|
| ka1 | k_a |
| ka2 | k'_a |
| kdes | k'_{des} |
| csat | C_{Ei} |
| cl | C_L |

| | |
|-----------|---|
| pgea | ρ_{GeA} areal density of Ge binding sites |
| pge | ρ_{Ge} (density of Ge) |
| mw | MW_{Ge} Molecular weight of Ge |
| na | N_A Avagadro's number |
| τc | τ_c |
| n | number of iterations of Differential Evolution |
| Ag | A (in double exponential fit to $\theta_{Ge}(t)$) |
| Bg | B (in double exponential fit to $\theta_{Ge}(t)$) |
| Cg | C (in double exponential fit to $\theta_{Ge}(t)$) |
| τg | τ_{Ge1} (in double exponential fit to $\theta_{Ge}(t)$) |
| $\tau g2$ | τ_{Ge2} (in double exponential fit to $\theta_{Ge}(t)$) |

Mathematica™ script “Opt”

```
In[100]:= Clear[csat, cl, n, pgea, pge, mw, na, t,  $\tau c$ , ka1, ka2, kdes, opt, n]
```

```
In[101]:= n=0
opt[ka1_?NumericQ,ka2_?NumericQ,kdes_?NumericQ]:=(csat=1.59*^-4;cl=4.7*^-4;n=1;pgea=6.61*^14;pge=5.323;mw=72.59;na=6.022*^23; $\tau c$ =960;g=NDSolve[{y'[t]-((ka1)*csat*E^(-t/ $\tau c$ )-(kdes)-(ka2)*cl)*y[t]□(kdes),y[0]□1},y,{t,0,5000}];datag=Table[{t,N[y[t]/.g]},{t,0,4000,20}];datag2=Flatten[datag];datag3=Partition[datag2,2];modelg=Ag*Exp[-t/ $\tau g$ ]+Bg*Exp[-t/ $\tau g2$ ]+cg;gsol=FindFit[datag3,modelg,{{Ag,.1},{ $\tau g$ ,100},{Bg,.8},{ $\tau g2$ ,200},{cg,.004}},t];Resid=(Abs[1.525*^-7-N[((ka1)*pgea*mw*csat)/(pge*na)*((-
```

```

Evaluate[Ag/.gsol]*((τc*Evaluate[τg/.gsol])/(τc+Evaluate[τg/.gsol]))*Exp[-
(τc+Evaluate[τg/.gsol])*60/(τc*Evaluate[τg/.gsol])]-
Evaluate[Bg/.gsol]*((τc*Evaluate[τg2/.gsol])/(τc+Evaluate[τg2/.gsol]))*Exp[-
(τc+Evaluate[τg2/.gsol])*60/(τc*Evaluate[τg2/.gsol])]-Evaluate[cg/.gsol]*τc*Exp[-60/τc]- (-
Evaluate[Ag/.gsol]*((τc*Evaluate[τg/.gsol])/(τc+Evaluate[τg/.gsol]))-
Evaluate[Bg/.gsol]*((τc*Evaluate[τg2/.gsol])/(τc+Evaluate[τg2/.gsol]))-Evaluate[cg/.gsol]*τc)) +7.5*^-8
]]^2+(Abs[1.6*^-7-N[((ka1)*pgea*mw*csat)/(pge*na)*((-
Evaluate[Ag/.gsol]*((τc*Evaluate[τg/.gsol])/(τc+Evaluate[τg/.gsol]))*Exp[-
(τc+Evaluate[τg/.gsol])*180/(τc*Evaluate[τg/.gsol])]-
Evaluate[Bg/.gsol]*((τc*Evaluate[τg2/.gsol])/(τc+Evaluate[τg2/.gsol]))*Exp[-
(τc+Evaluate[τg2/.gsol])*180/(τc*Evaluate[τg2/.gsol])]-Evaluate[cg/.gsol]*τc*Exp[-180/τc])- (-
Evaluate[Ag/.gsol]*((τc*Evaluate[τg/.gsol])/(τc+Evaluate[τg/.gsol]))-
Evaluate[Bg/.gsol]*((τc*Evaluate[τg2/.gsol])/(τc+Evaluate[τg2/.gsol]))-Evaluate[cg/.gsol]*τc)) +7.5*^-8
]]^2+(Abs[3.7*^-7-N[((ka1)*pgea*mw*csat)/(pge*na)*((-
Evaluate[Ag/.gsol]*((τc*Evaluate[τg/.gsol])/(τc+Evaluate[τg/.gsol]))*Exp[-
(τc+Evaluate[τg/.gsol])*300/(τc*Evaluate[τg/.gsol])]-
Evaluate[Bg/.gsol]*((τc*Evaluate[τg2/.gsol])/(τc+Evaluate[τg2/.gsol]))*Exp[-
(τc+Evaluate[τg2/.gsol])*300/(τc*Evaluate[τg2/.gsol])]-Evaluate[cg/.gsol]*τc*Exp[-300/τc])- (-
Evaluate[Ag/.gsol]*((τc*Evaluate[τg/.gsol])/(τc+Evaluate[τg/.gsol]))-
Evaluate[Bg/.gsol]*((τc*Evaluate[τg2/.gsol])/(τc+Evaluate[τg2/.gsol]))-Evaluate[cg/.gsol]*τc)) +7.5*^-8
]]^2+(Abs[7.5*^-7-N[((ka1)*pgea*mw*csat)/(pge*na)*((-
Evaluate[Ag/.gsol]*((τc*Evaluate[τg/.gsol])/(τc+Evaluate[τg/.gsol]))*Exp[-
(τc+Evaluate[τg/.gsol])*1800/(τc*Evaluate[τg/.gsol])]-
Evaluate[Bg/.gsol]*((τc*Evaluate[τg2/.gsol])/(τc+Evaluate[τg2/.gsol]))*Exp[-
(τc+Evaluate[τg2/.gsol])*1800/(τc*Evaluate[τg2/.gsol])]-Evaluate[cg/.gsol]*τc*Exp[-1800/τc])- (-
Evaluate[Ag/.gsol]*((τc*Evaluate[τg/.gsol])/(τc+Evaluate[τg/.gsol]))-
Evaluate[Bg/.gsol]*((τc*Evaluate[τg2/.gsol])/(τc+Evaluate[τg2/.gsol]))-Evaluate[cg/.gsol]*τc)) +7.5*^-8
]]^2+(Abs[6.55*^-7-N[((ka1)*pgea*mw*csat)/(pge*na)*((-
Evaluate[Ag/.gsol]*((τc*Evaluate[τg/.gsol])/(τc+Evaluate[τg/.gsol]))*Exp[-
(τc+Evaluate[τg/.gsol])*3600/(τc*Evaluate[τg/.gsol])]-
Evaluate[Bg/.gsol]*((τc*Evaluate[τg2/.gsol])/(τc+Evaluate[τg2/.gsol]))*Exp[-
(τc+Evaluate[τg2/.gsol])*3600/(τc*Evaluate[τg2/.gsol])]-Evaluate[cg/.gsol]*τc*Exp[-3600/τc])- (-
Evaluate[Ag/.gsol]*((τc*Evaluate[τg/.gsol])/(τc+Evaluate[τg/.gsol]))-
Evaluate[Bg/.gsol]*((τc*Evaluate[τg2/.gsol])/(τc+Evaluate[τg2/.gsol]))-Evaluate[cg/.gsol]*τc)) +7.5*^-8
]]^2)

```

Out[101]:=0

In[103]:= NMinimize[{opt[ka1, ka2, kdes], 450 < ka1 < 700, 160 < ka2 < 400, 1 * ^ - 6 < kdes < 1 * ^ - 1}, {ka1, ka2, kdes}, Method -> DifferentialEvolution, EvaluationMonitor -> n + +]

Out[103]:= {2.09569 × 10⁻¹⁴, {ka1 -> 494.619, ka2 -> 175.299, kdes -> 0.0513582}}

In[104]:= Evaluate[n++]

Out[104]:= 2

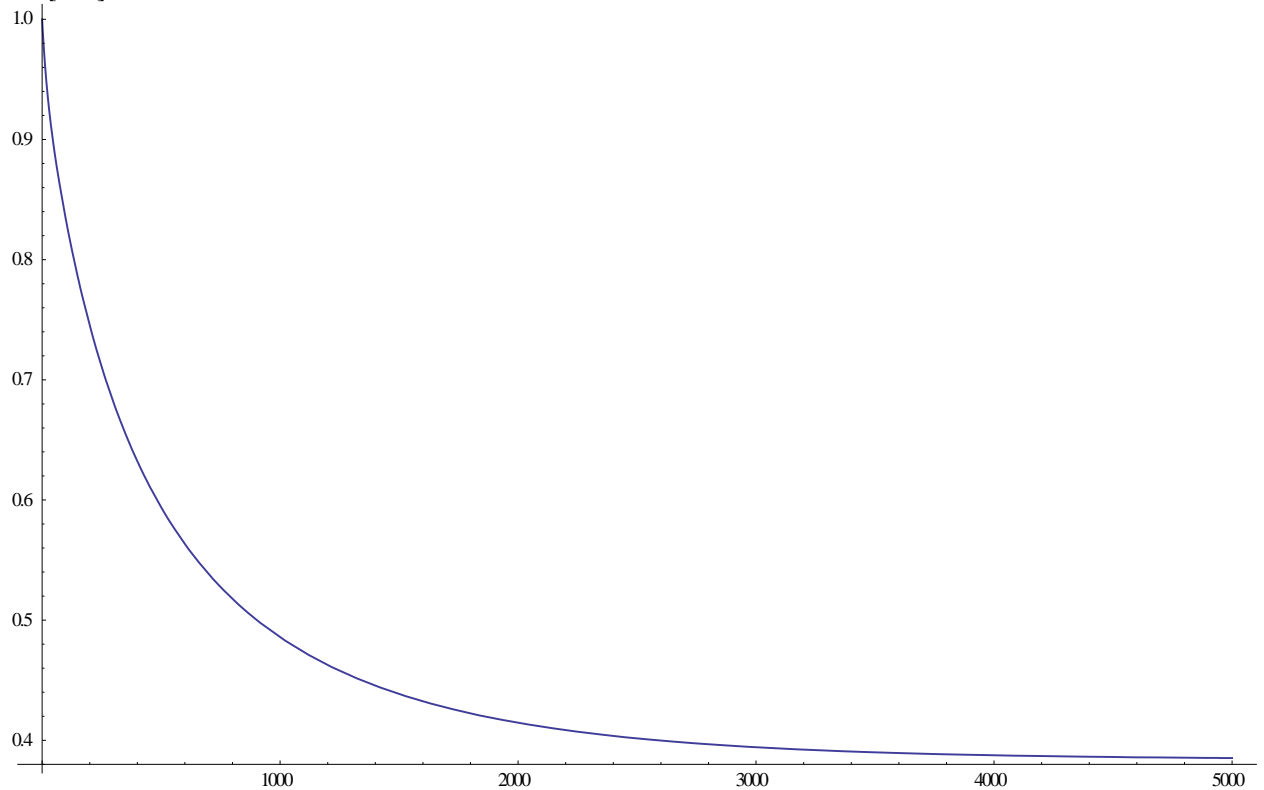
Output of “ThetaVtime” with optimized values from “Opt”

This script demonstrates the output of model *g* when the optimized values from “Opt” are inserted in the input [101] for *ka1*, *kdes* and *ka2*. This allows the general fit to the experimental data to be plotted real time when the optimization is complete with the “Opt” script.

Mathematica™ script “ThetaVtime” using double exponential to solve differential equation for $\theta_{Ge}(t)$.

```
-----  
In[100]:=Clear[ka1,csat,kdes,ka2,cl,a,n,pgea,pge,mw,na,τc,c]  
In[101]:=ka1=494.619  
          csat=1.59*^-4  
          kdes=.0513582  
          ka2=175.299  
          cl=4.7*^-4  
          n=1  
          pgea=6.61*^14  
          pge=5.323  
          mw=72.59  
          na=6.022*^23  
          τc=960  
          c=0  
          g=NDSolve[{y'[t]-(ka1*csat*E^(-t/τc)-kdes ka2*cl)*y[t]□kdes,y[0]□1},y,{t,0,5000}]  
Out[101]:= 494.619  
Out[102]:= 0.000159  
Out[103]:= .0513582  
Out[104]:= 175.299  
Out[105]:= 0.00047  
Out[106]:= 1  
Out[107]:= 6.61×1014  
Out[108]:= 5.323  
Out[109]:= 72.59  
Out[110]:= 6.022×1023  
Out[111]:= 1800  
Out[112]:= 0  
  
Out[113]:= {y→InterpolatingFunction[{{0.,5000.}},<>]}  
  
In[114]:= Plot[{Evaluate[{y[t]}/.g]},{t,0,5000},PlotRange→Full]
```

Out[114]:=



```
In[115]:= datag=Table[{t,N[y[t]/.g]},{t,0,4000,20}]
           datag2=Flatten[datag]
           datag3=Partition[datag2,2]
```

Out[114]:=

```
{{0,{1}}, {20,{0.943473}}, {40,{0.907285}}, {60,{0.879281}}, {80,{0.855148}}, {100,{0.83333}}, {120,{0.813217}}, {140,{0.794522}}, {160,{0.777071}}, {180,{0.760738}}, {200,{0.745417}}, {220,{0.731017}}, {240,{0.717461}}, {260,{0.704676}}, {280,{0.692602}}, {300,{0.681182}}, {320,{0.670366}}, {340,{0.660109}}, {360,{0.650371}}, {380,{0.641114}}, {400,{0.632307}}, {420,{0.623917}}, {440,{0.615918}}, {460,{0.608285}}, {480,{0.600993}}, {500,{0.594023}}, {520,{0.587355}}, {540,{0.58097}}, {560,{0.574853}}, {580,{0.568987}}, {600,{0.56336}}, {620,{0.557957}}, {640,{0.552767}}, {660,{0.547778}}, {680,{0.54298}}, {700,{0.538363}}, {720,{0.533918}}, {740,{0.529636}}, {760,{0.525509}}, {780,{0.521531}}, {800,{0.517693}}, {820,{0.513989}}, {840,{0.510414}}, {860,{0.506961}}, {880,{0.503624}}, {900,{0.5004}}, {920,{0.497282}}, {940,{0.494266}}, {960,{0.491349}}, {980,{0.488525}}, {1000,{0.485791}}, {1020,{0.483143}}, {1040,{0.480578}}, {1060,{0.478092}}, {1080,{0.475683}}, {1100,{0.473347}}, {1120,{0.471082}}, {1140,{0.468884}}, {1160,{0.466752}}, {1180,{0.464683}}, {1200,{0.462675}}, {1220,{0.460724}}, {1240,{0.45883}}, {1260,{0.456991}}, {1280,{0.455203}}, {1300,{0.453466}}, {1320,{0.451778}}, {1340,{0.450137}}, {1360,{0.448542}}, {1380,{0.44699}}, {1400,{0.445481}}, {1420,{0.444013}}, {1440,{0.442584}}, {1460,{0.441194}}, {1480,{0.439842}}, {1500,{0.438525}}, {1520,{0.437243}}, {1540,{0.435995}}, {1560,{0.434779}}, {1580,{0.433595}}, {1600,{0.432442}}, {1620,{0.431319}}, {1640,{0.430224}}, {1660,{0.429158}}, {1680,{0.428119}}, {1700,{0.427106}}, {1720,{0.426118}}, {1740,{0.425156}}, {1760,{0.424217}}, {1780,{0.423302}}, {1800,{0.42241}}, {1820,{0.421539}}, {1840,{0.42069}}, {1860,{0.419862}}, {1880,{0.419055}}, {1900,{0.418266}}, {1920,{0.417497}}, {1940,{0.416747}}, {1960,{0.416015}}, {1980,{0.4153}}, {2000,{0.414603}}, {2020,{0.413922}}, {2040,{0.413257}}, {2060,{0.412609}}, {2080,{0.411975}}, {2100,{0.411357}}, {2120,{0.410753}}, {2140,{0.410163}}, {2160,{0.409587}}, {2180,{0.409}}
```

```

025}}, {2200, {0.408475}}, {2220, {0.407939}}, {2240, {0.407414}}, {2260, {0.406902}}, {2280, {0.406402}}
}, {2300, {0.405914}}, {2320, {0.405436}}, {2340, {0.40497}}, {2360, {0.404514}}, {2380, {0.404068}}, {240
0, {0.403633}}, {2420, {0.403207}}, {2440, {0.402792}}, {2460, {0.402385}}, {2480, {0.401988}}, {2500, {0.
4016}}, {2520, {0.40122}}, {2540, {0.400849}}, {2560, {0.400487}}, {2580, {0.400132}}, {2600, {0.399785}}
}, {2620, {0.399447}}, {2640, {0.399115}}, {2660, {0.398791}}, {2680, {0.398475}}, {2700, {0.398165}}, {27
20, {0.397862}}, {2740, {0.397566}}, {2760, {0.397276}}, {2780, {0.396993}}, {2800, {0.396716}}, {2820, {0
.396445}}, {2840, {0.39618}}, {2860, {0.395921}}, {2880, {0.395667}}, {2900, {0.395419}}, {2920, {0.39517
6}}, {2940, {0.394939}}, {2960, {0.394707}}, {2980, {0.39448}}, {3000, {0.394258}}, {3020, {0.394041}}, {3
040, {0.393828}}, {3060, {0.39362}}, {3080, {0.393417}}, {3100, {0.393218}}, {3120, {0.393023}}, {3140, {0
.392832}}, {3160, {0.392646}}, {3180, {0.392463}}, {3200, {0.392285}}, {3220, {0.39211}}, {3240, {0.39193
9}}, {3260, {0.391772}}, {3280, {0.391608}}, {3300, {0.391448}}, {3320, {0.391292}}, {3340, {0.391138}}, {
3360, {0.390988}}, {3380, {0.390841}}, {3400, {0.390697}}, {3420, {0.390557}}, {3440, {0.390419}}, {3460,
{0.390284}}, {3480, {0.390153}}, {3500, {0.390023}}, {3520, {0.389897}}, {3540, {0.389774}}, {3560, {0.38
9652}}, {3580, {0.389534}}, {3600, {0.389418}}, {3620, {0.389305}}, {3640, {0.389194}}, {3660, {0.389085
}}, {3680, {0.388978}}, {3700, {0.388874}}, {3720, {0.388772}}, {3740, {0.388673}}, {3760, {0.388575}}, {3
780, {0.388479}}, {3800, {0.388386}}, {3820, {0.388294}}, {3840, {0.388204}}, {3860, {0.388116}}, {3880, {
0.38803}}, {3900, {0.387946}}, {3920, {0.387864}}, {3940, {0.387783}}, {3960, {0.387704}}, {3980, {0.3876
27}}, {4000, {0.387551}}

```

Out[115]:=

```

{0,1.,20,0.943473,40,0.907285,60,0.879281,80,0.855148,100,0.83333,120,0.813217,140,0.794522,160,0.7
77071,180,0.760738,200,0.745417,220,0.731017,240,0.717461,260,0.704676,280,0.692602,300,0.681182,
320,0.670366,340,0.660109,360,0.650371,380,0.641114,400,0.632307,420,0.623917,440,0.615918,460,0.
608285,480,0.600993,500,0.594023,520,0.587355,540,0.58097,560,0.574853,580,0.568987,600,0.56336,6
20,0.557957,640,0.552767,660,0.547778,680,0.54298,700,0.538363,720,0.533918,740,0.529636,760,0.52
5509,780,0.521531,800,0.517693,820,0.513989,840,0.510414,860,0.506961,880,0.503624,900,0.5004920
,0.497282,940,0.494266,960,0.491349,980,0.488525,1000,0.485791,1020,0.483143,1040,0.480578,1060,0
.478092,1080,0.475683,1100,0.473347,1120,0.471082,1140,0.468884,1160,0.466752,1180,0.464683,1200
,0.462675,1220,0.460724,1240,0.45883,1260,0.456991,1280,0.455203,1300,0.453466,1320,0.451778,134
0,0.450137,1360,0.448542,1380,0.44699,1400,0.445481,1420,0.444013,1440,0.442584,1460,0.441194,14
80,0.439842,1500,0.438525,1520,0.437243,1540,0.435995,1560,0.434779,1580,0.433595,1600,0.432442,
1620,0.431319,1640,0.430224,1660,0.429158,1680,0.428119,1700,0.427106,1720,0.426118,1740,0.42515
6,1760,0.424217,1780,0.423302,1800,0.42241,1820,0.421539,1840,0.42069,1860,0.419862,1880,0.41905
5,1900,0.418266,1920,0.417497,1940,0.416747,1960,0.416015,1980,0.4153,2000,0.414603,2020,0.41392
2,2040,0.413257,2060,0.412609,2080,0.411975,2100,0.411357,2120,0.410753,2140,0.410163,2160,0.409
587,2180,0.409025,2200,0.408475,2220,0.407939,2240,0.407414,2260,0.406902,2280,0.406402,2300,0.4
05914,2320,0.405436,2340,0.40497,2360,0.404514,2380,0.404068,2400,0.403633,2420,0.403207,2440,0.
402792,2460,0.402385,2480,0.401988,2500,0.4016,2520,0.40122,2540,0.400849,2560,0.400487,2580,0.4
00132,2600,0.399785,2620,0.399447,2640,0.399115,2660,0.398791,2680,0.398475,2700,0.398165,2720,0
.397862,2740,0.397566,2760,0.397276,2780,0.396993,2800,0.396716,2820,0.396445,2840,0.39618,2860,
0.395921,2880,0.395667,2900,0.395419,2920,0.395176,2940,0.394939,2960,0.394707,2980,0.39448,3000
,0.394258,3020,0.394041,3040,0.393828,3060,0.39362,3080,0.393417,3100,0.393218,3120,0.393023,314
0,0.392832,3160,0.392646,3180,0.392463,3200,0.392285,3220,0.39211,3240,0.391939,3260,0.391772,32
80,0.391608,3300,0.391448,3320,0.391292,3340,0.391138,3360,0.390988,3380,0.390841,3400,0.390697,
3420,0.390557,3440,0.390419,3460,0.390284,3480,0.390153,3500,0.390023,3520,0.389897,3540,0.38977
4,3560,0.389652,3580,0.389534,3600,0.389418,3620,0.389305,3640,0.389194,3660,0.389085,3680,0.388
978,3700,0.388874,3720,0.388772,3740,0.388673,3760,0.388575,3780,0.388479,3800,0.388386,3820,0.3
88294,3840,0.388204,3860,0.388116,3880,0.38803,3900,0.387946,3920,0.387864,3940,0.387783,3960,0.
387704,3980,0.387627,4000,0.387551}

```

Out[116]:=

```

{{0,1.}, {20,0.943473}, {40,0.907285}, {60,0.879281}, {80,0.855148}, {100,0.83333}, {120,0.813217}, {140,
0.794522}, {160,0.777071}, {180,0.760738}, {200,0.745417}, {220,0.731017}, {240,0.717461}, {260,0.7046
76}, {280,0.692602}, {300,0.681182}, {320,0.670366}, {340,0.660109}, {360,0.650371}, {380,0.641114}, {4
00,0.632307}, {420,0.623917}, {440,0.615918}, {460,0.608285}, {480,0.600993}, {500,0.594023}, {520,0.5
87355}, {540,0.58097}, {560,0.574853}, {580,0.568987}, {600,0.56336}, {620,0.557957}, {640,0.552767}, {

```

660,0.547778},{680,0.54298},{700,0.538363},{720,0.533918},{740,0.529636},{760,0.525509},{780,0.521531},{800,0.517693},{820,0.513989},{840,0.510414},{860,0.506961},{880,0.503624},{900,0.5004},{920,0.497282},{940,0.494266},{960,0.491349},{980,0.488525},{1000,0.485791},{1020,0.483143},{1040,0.480578},{1060,0.478092},{1080,0.475683},{1100,0.473347},{1120,0.471082},{1140,0.468884},{1160,0.466752},{1180,0.464683},{1200,0.462675},{1220,0.460724},{1240,0.45883},{1260,0.456991},{1280,0.455203},{1300,0.453466},{1320,0.451778},{1340,0.450137},{1360,0.448542},{1380,0.44699},{1400,0.445481},{1420,0.444013},{1440,0.442584},{1460,0.441194},{1480,0.439842},{1500,0.438525},{1520,0.437243},{1540,0.435995},{1560,0.434779},{1580,0.433595},{1600,0.432442},{1620,0.431319},{1640,0.430224},{1660,0.429158},{1680,0.428119},{1700,0.427106},{1720,0.426118},{1740,0.425156},{1760,0.424217},{1780,0.423302},{1800,0.42241},{1820,0.421539},{1840,0.42069},{1860,0.419862},{1880,0.419055},{1900,0.418266},{1920,0.417497},{1940,0.416747},{1960,0.416015},{1980,0.4153},{2000,0.414603},{2020,0.413922},{2040,0.413257},{2060,0.412609},{2080,0.411975},{2100,0.411357},{2120,0.410753},{2140,0.410163},{2160,0.409587},{2180,0.409025},{2200,0.408475},{2220,0.407939},{2240,0.407414},{2260,0.406902},{2280,0.406402},{2300,0.405914},{2320,0.405436},{2340,0.40497},{2360,0.404514},{2380,0.404068},{2400,0.403633},{2420,0.403207},{2440,0.402792},{2460,0.402385},{2480,0.401988},{2500,0.4016},{2520,0.40122},{2540,0.400849},{2560,0.400487},{2580,0.400132},{2600,0.399785},{2620,0.399447},{2640,0.399115},{2660,0.398791},{2680,0.398475},{2700,0.398165},{2720,0.397862},{2740,0.397566},{2760,0.397276},{2780,0.396993},{2800,0.396716},{2820,0.396445},{2840,0.39618},{2860,0.395921},{2880,0.395667},{2900,0.395419},{2920,0.395176},{2940,0.394939},{2960,0.394707},{2980,0.39448},{3000,0.394258},{3020,0.394041},{3040,0.393828},{3060,0.39362},{3080,0.393417},{3100,0.393218},{3120,0.393023},{3140,0.392832},{3160,0.392646},{3180,0.392463},{3200,0.392285},{3220,0.39211},{3240,0.391939},{3260,0.391772},{3280,0.391608},{3300,0.391448},{3320,0.391292},{3340,0.391138},{3360,0.390988},{3380,0.390841},{3400,0.390697},{3420,0.390557},{3440,0.390419},{3460,0.390284},{3480,0.390153},{3500,0.390023},{3520,0.389897},{3540,0.389774},{3560,0.389652},{3580,0.389534},{3600,0.389418},{3620,0.389305},{3640,0.389194},{3660,0.389085},{3680,0.388978},{3700,0.388874},{3720,0.388772},{3740,0.388673},{3760,0.388575},{3780,0.388479},{3800,0.388386},{3820,0.388294},{3840,0.388204},{3860,0.388116},{3880,0.38803},{3900,0.387946},{3920,0.387864},{3940,0.387783},{3960,0.387704},{3980,0.387627},{4000,0.387551}}

In[117]:= modelg=Ag*Exp[-t/τg]+Bg*Exp[-t/τg2]+cg
 gsol={FindFit[datag3,modelg,{Ag,.3},{τg,2000},{Bg,.3},{τg2,2000},{cg,.004}],t,EvaluationMonitorfc+
 +]}

Out[117]:=cg + Age $\frac{t}{\tau_g}$ + Bge $\frac{t}{\tau_{g^2}}$

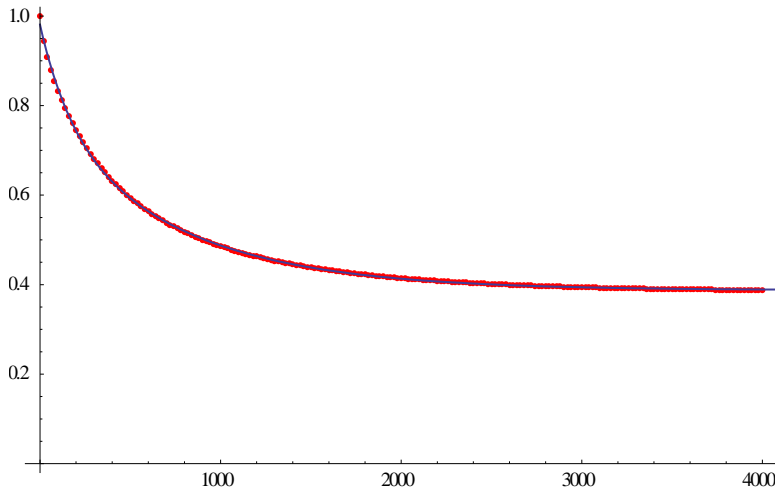
Out[118] := {{Ag → 0.381799, τg → 744.035, Bg → 0.211793, τg2 → 168.175, cg → 0.38736}}

In[119]:=Evaluate[c++]

Out[119]:=30

In[120]:=Show[ListPlot[datag3,PlotStyle → Red,PlotRange → Full],Plot[{Evaluate[modelg/
 .gsol]},{t,0,7000},PlotRange → Full]]

Out[120]:=

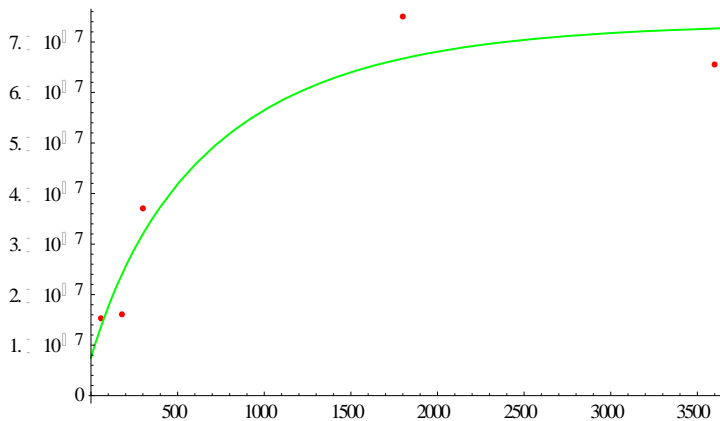


```
In[121]:=datar={{60,1.525*^-7},{180,1.6*^-7},{300,3.7*^-7},{1800,7.5*^-7},{3600,6.55*^-7}}
modelrg=(1*ka1*pgea*mw*csat)/(pge*na)*((-
Evaluate[Ag/.gsol]*((τc*Evaluate[τg/.gsol])/(τc+Evaluate[τg/.gsol]))*Exp[-
(τc+Evaluate[τg/.gsol])*t/(τc*Evaluate[τg/.gsol])]-
Evaluate[Bg/.gsol]*((τc*Evaluate[τg2/.gsol])/(τc+Evaluate[τg2/.gsol]))*Exp[-
(τc+Evaluate[τg2/.gsol])*t/(τc*Evaluate[τg2/.gsol])]-Evaluate[cg/.gsol]*τc*Exp[-t/τc])-
Evaluate[Ag/.gsol]*((τc*Evaluate[τg/.gsol])/(τc+Evaluate[τg/.gsol]))-
Evaluate[Bg/.gsol]*((τc*Evaluate[τg2/.gsol])/(τc+Evaluate[τg2/.gsol]))-Evaluate[cg/.gsol]*τc)) +7.5*^-8
```

```
Out[121]:={{60,1.525*10^-7},{180,1.6*10^-7},{300,3.7*10^-7},{1800,7.5*10^-7},{3600,6.55*10^-7}}
Out[122]:={7.5*10^-8 + 1.1772*10^-9(562.211 - 30.3086e^-0.00698786t - 160.037e^-0.00238569t -
371.866e^-t/960)}
```

```
In[123]:=Show[ListPlot[datar, PlotStyle -> Red, PlotRange ->
Full], Plot[{Evaluate[modelrg]}, {t, 0, 5000}, PlotStyle -> Green, PlotRange -> Full]]
```

```
Out[123]:=
```



Mathematica™ script “ThetaVtime” using Partial analytical method to solve differential equation for $\theta_{Ge}(t)$.

```
In[100]:=Clear[ka1, csat, kdes, ka2, cl, a, n, pgea, pge, mw, na, tc]
```

```
In[101]:= ka1=494.619
          csat=1.59*^-4
          kdes=.0513582
          ka2=175.299
          cl=4.7*^-4
          n=1
          pgea=6.61*^14
          pge=5.323
          mw=72.59
          na=6.022*^23
          tc=960
          g[t_]:=kdes*(NIntegrate[(Exp[(kdes*x+ka2*cl*x+ka1*csat*tc*Exp[-
x/τc])])/(Exp[(kdes*t+ka2*cl*t+ka1*csat*tc*Exp[-
t/τc])])],{x,0,mtime}])+Exp[(ka1*csat*tc)/Exp[(kdes*t+ka2*cl*t+ka1*csat*tc*Exp[-t/τc])])]
```

```
Out[101]:=494.619
```

```
Out[102]:=0.000159
```

```
Out[103]:=0.0513582
```

```
Out[104]:=175.299
```

```
Out[105]:=0.00047
```

```
Out[106]:=1
```

```
Out[107]:=6.61×1014
```

```
Out[108]:=5.323
```

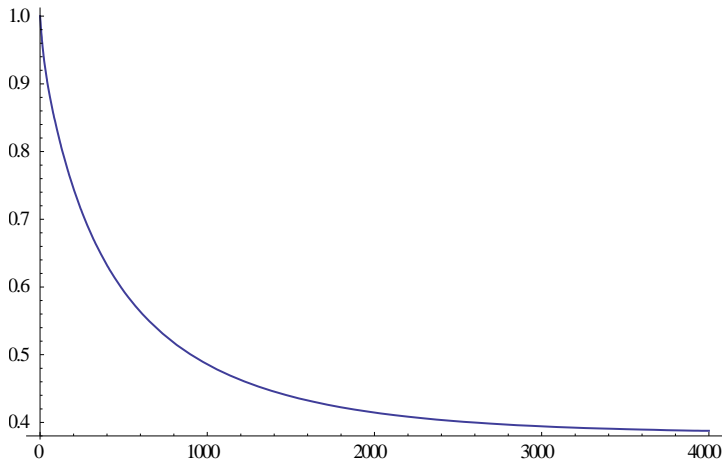
```
Out[109]:=72.59
```

```
Out[110]:=6.022×1023
```

```
Out[111]:=960
```

```
In[113]:=Plot[{N[g[mtime]]}, {mtime, 0,4000}, PlotRange → Full]
```

```
Out[113]:=
```



```
In[114]:= datag=Table[{mtime, N[g[mtime]]}, {mtime, 0, 4000, 20}]
          datag2=Flatten[datag]
```

```
          datag3=Partition[datag2, 2]
```

```
Out[114]:=
```

```
{ {0, 1.}, {20, 0.943473}, {40, 0.907285}, {60, 0.879281}, {80, 0.855148}, {100, 0.83333}, {120, 0.813217}, {140, 0.794522}, {160, 0.777071}, {180, 0.760738}, {200, 0.745417}, {220, 0.731017}, {240, 0.717461}, {260, 0.704676}, {280, 0.692602}, {300, 0.681182}, {320, 0.670366}, {340, 0.660109}, {360, 0.650371}, {380, 0.641114}, {400, 0.632307}, {420, 0.623917}, {440, 0.615918}, {460, 0.608285}, {480, 0.600993}, {500, 0.594023}, {520, 0.587355}, {540, 0.58097}, {560, 0.574853}, {580, 0.568987}, {600, 0.56336}, {620, 0.557957}, {640, 0.552767}, {660, 0.547778}, {680, 0.54298}, {700, 0.538363}, {720, 0.533918}, {740, 0.529636}, {760, 0.525509}, {780, 0.521531}, {800, 0.517693}, {820, 0.513989}, {840, 0.510414}, {860, 0.506961}, {880, 0.503624}, {900, 0.5004}, {920, 0.497282}, {940, 0.494266}, {960, 0.491349}, {980, 0.488525}, {1000, 0.485791}, {1020, 0.483143}, {1040, 0.480578}, {1060, 0.478092}, {1080, 0.475683}, {1100, 0.473347}, {1120, 0.471082}, {1140, 0.468884}, {1160, 0.466752}, {1180, 0.464683}, {1200, 0.462675}, {1220, 0.460724}, {1240, 0.45883}, {1260, 0.456991}, {1280, 0.455203}, {1300, 0.453466}, {1320, 0.451778}, {1340, 0.450137}, {1360, 0.448542}, {1380, 0.44699}, {1400, 0.445481}, {1420, 0.444013}, {1440, 0.442584}, {1460, 0.441194}, {1480, 0.439842}, {1500, 0.438525}, {1520, 0.437243}, {1540, 0.435995}, {1560, 0.434779}, {1580, 0.433595}, {1600, 0.432442}, {1620, 0.431319}, {1640, 0.430224}, {1660, 0.429158}, {1680, 0.428119}, {1700, 0.427106}, {1720, 0.426118}, {1740, 0.425156}, {1760, 0.424217}, {1780, 0.423302}, {1800, 0.42241}, {1820, 0.421539}, {1840, 0.42069}, {1860, 0.419862}, {1880, 0.419055}, {1900, 0.418266}, {1920, 0.417497}, {1940, 0.416747}, {1960, 0.416015}, {1980, 0.4153}, {2000, 0.414603}, {2020, 0.413922}, {2040, 0.413257}, {2060, 0.412609}, {2080, 0.411975}, {2100, 0.411357}, {2120, 0.410753}, {2140, 0.410163}, {2160, 0.409587}, {2180, 0.409025}, {2200, 0.408475}, {2220, 0.407939}, {2240, 0.407414}, {2260, 0.406902}, {2280, 0.406402}, {2300, 0.405914}, {2320, 0.405436}, {2340, 0.40497}, {2360, 0.404514}, {2380, 0.404068}, {2400, 0.403633}, {2420, 0.403207}, {2440, 0.402792}, {2460, 0.402385}, {2480, 0.401988}, {2500, 0.4016}, {2520, 0.40122}, {2540, 0.400849}, {2560, 0.400487}, {2580, 0.400132}, {2600, 0.399785}, {2620, 0.399447}, {2640, 0.399115}, {2660, 0.398791}, {2680, 0.398475}, {2700, 0.398165}, {2720, 0.397862}, {2740, 0.397566}, {2760, 0.397276}, {2780, 0.396993}, {2800, 0.396716}, {2820, 0.396445}, {2840, 0.39618}, {2860, 0.395921}, {2880, 0.395667}, {2900, 0.395419}, {2920, 0.395176}, {2940, 0.394939}, {2960, 0.394707}, {2980, 0.39448}, {3000, 0.394258}, {3020, 0.394041}, {3040, 0.393828}, {3060, 0.39362}, {3080, 0.393417}, {3100, 0.393218}, {3120, 0.393023}, {3140, 0.392832}, {3160, 0.392646}, {3180, 0.392463}, {3200, 0.392285}, {3220, 0.39211}, {3240, 0.391939}, {3260, 0.391772}, {3280, 0.391608}, {3300, 0.391448}, {3320, 0.391292}, {3340, 0.391138}, {3360, 0.390988}, {3380, 0.390841}, {3400, 0.390697}, {3420, 0.390557}, {3440, 0.390419}, {3460, 0.390284}, {3480, 0.390153}, {3500, 0.390023}, {3520, 0.389897}, {3540, 0.389774}, {3560, 0.389652}, {3580, 0.389534}, {3600, 0.389418}, {3620, 0.389305}, {3640, 0.389194}, {3660, 0.389085}, {3680, 0.388978}, {3700, 0.388874}, {3720, 0.388772}, {3740, 0.388673}, {3760, 0.388575}, {3780, 0.388479}, {3800, 0.388386}, {3820, 0.388294}, {3840, 0.388204}, {3860, 0.388116}, {3880, 0.38803}, {3900, 0.387946}, {3920, 0.387864}, {3940, 0.387783}, {3960, 0.387704}, {3980, 0.387627}, {4000, 0.387551} }
```

```
Out[115]:=
```

{0,1.,20,0.943473,40,0.907285,60,0.879281,80,0.855148,100,0.83333,120,0.813217,140,0.794522,160,0.77071,180,0.760738,200,0.745417,220,0.731017,240,0.717461,260,0.704676,280,0.692602,300,0.681182,320,0.670366,340,0.660109,360,0.650371,380,0.641114,400,0.632307,420,0.623917,440,0.615918,460,0.608285,480,0.600993,500,0.594023,520,0.587355,540,0.58097,560,0.574853,580,0.568987,600,0.56336,620,0.557957,640,0.552767,660,0.547778,680,0.54298,700,0.538363,720,0.533918,740,0.529636,760,0.525509,780,0.521531,800,0.517693,820,0.513989,840,0.510414,860,0.506961,880,0.503624,900,0.5004,920,0.497282,940,0.494266,960,0.491349,980,0.488525,1000,0.485791,1020,0.483143,1040,0.480578,1060,0.478092,1080,0.475683,1100,0.473347,1120,0.471082,1140,0.468884,1160,0.466752,1180,0.464683,1200,0.462675,1220,0.460724,1240,0.45883,1260,0.456991,1280,0.455203,1300,0.453466,1320,0.451778,1340,0.450137,1360,0.448542,1380,0.44699,1400,0.445481,1420,0.444013,1440,0.442584,1460,0.441194,1480,0.439842,1500,0.438525,1520,0.437243,1540,0.435995,1560,0.434779,1580,0.433595,1600,0.432442,1620,0.431319,1640,0.430224,1660,0.429158,1680,0.428119,1700,0.427106,1720,0.426118,1740,0.425156,1760,0.424217,1780,0.423302,1800,0.42241,1820,0.421539,1840,0.42069,1860,0.419862,1880,0.419055,1900,0.418266,1920,0.417497,1940,0.416747,1960,0.416015,1980,0.4153,2000,0.414603,2020,0.413922,2040,0.413257,2060,0.412609,2080,0.411975,2100,0.411357,2120,0.410753,2140,0.410163,2160,0.409587,2180,0.409025,2200,0.408475,2220,0.407939,2240,0.407414,2260,0.406902,2280,0.406402,2300,0.405914,2320,0.405436,2340,0.40497,2360,0.404514,2380,0.404068,2400,0.403633,2420,0.403207,2440,0.402792,2460,0.402385,2480,0.401988,2500,0.4016,2520,0.40122,2540,0.400849,2560,0.400487,2580,0.400132,2600,0.399785,2620,0.399447,2640,0.399115,2660,0.398791,2680,0.398475,2700,0.398165,2720,0.397862,2740,0.397566,2760,0.397276,2780,0.396993,2800,0.396716,2820,0.396445,2840,0.39618,2860,0.395921,2880,0.395667,2900,0.395419,2920,0.395176,2940,0.394939,2960,0.394707,2980,0.39448,3000,0.394258,3020,0.394041,3040,0.393828,3060,0.39362,3080,0.393417,3100,0.393218,3120,0.393023,3140,0.392832,3160,0.392646,3180,0.392463,3200,0.392285,3220,0.39211,3240,0.391939,3260,0.391772,3280,0.391608,3300,0.391448,3320,0.391292,3340,0.391138,3360,0.390988,3380,0.390841,3400,0.390697,3420,0.390557,3440,0.390419,3460,0.390284,3480,0.390153,3500,0.390023,3520,0.389897,3540,0.389774,3560,0.389652,3580,0.389534,3600,0.389418,3620,0.389305,3640,0.389194,3660,0.389085,3680,0.388978,3700,0.388874,3720,0.388772,3740,0.388673,3760,0.388575,3780,0.388479,3800,0.388386,3820,0.388294,3840,0.388204,3860,0.388116,3880,0.38803,3900,0.387946,3920,0.387864,3940,0.387783,3960,0.387704,3980,0.387627,4000,0.387551}

Out[116]:=

{0,1.}, {20,0.943473}, {40,0.907285}, {60,0.879281}, {80,0.855148}, {100,0.83333}, {120,0.813217}, {140,0.794522}, {160,0.77071}, {180,0.760738}, {200,0.745417}, {220,0.731017}, {240,0.717461}, {260,0.704676}, {280,0.692602}, {300,0.681182}, {320,0.670366}, {340,0.660109}, {360,0.650371}, {380,0.641114}, {400,0.632307}, {420,0.623917}, {440,0.615918}, {460,0.608285}, {480,0.600993}, {500,0.594023}, {520,0.587355}, {540,0.58097}, {560,0.574853}, {580,0.568987}, {600,0.56336}, {620,0.557957}, {640,0.552767}, {660,0.547778}, {680,0.54298}, {700,0.538363}, {720,0.533918}, {740,0.529636}, {760,0.525509}, {780,0.521531}, {800,0.517693}, {820,0.513989}, {840,0.510414}, {860,0.506961}, {880,0.503624}, {900,0.5004}, {920,0.497282}, {940,0.494266}, {960,0.491349}, {980,0.488525}, {1000,0.485791}, {1020,0.483143}, {1040,0.480578}, {1060,0.478092}, {1080,0.475683}, {1100,0.473347}, {1120,0.471082}, {1140,0.468884}, {1160,0.466752}, {1180,0.464683}, {1200,0.462675}, {1220,0.460724}, {1240,0.45883}, {1260,0.456991}, {1280,0.455203}, {1300,0.453466}, {1320,0.451778}, {1340,0.450137}, {1360,0.448542}, {1380,0.44699}, {1400,0.445481}, {1420,0.444013}, {1440,0.442584}, {1460,0.441194}, {1480,0.439842}, {1500,0.438525}, {1520,0.437243}, {1540,0.435995}, {1560,0.434779}, {1580,0.433595}, {1600,0.432442}, {1620,0.431319}, {1640,0.430224}, {1660,0.429158}, {1680,0.428119}, {1700,0.427106}, {1720,0.426118}, {1740,0.425156}, {1760,0.424217}, {1780,0.423302}, {1800,0.42241}, {1820,0.421539}, {1840,0.42069}, {1860,0.419862}, {1880,0.419055}, {1900,0.418266}, {1920,0.417497}, {1940,0.416747}, {1960,0.416015}, {1980,0.4153}, {2000,0.414603}, {2020,0.413922}, {2040,0.413257}, {2060,0.412609}, {2080,0.411975}, {2100,0.411357}, {2120,0.410753}, {2140,0.410163}, {2160,0.409587}, {2180,0.409025}, {2200,0.408475}, {2220,0.407939}, {2240,0.407414}, {2260,0.406902}, {2280,0.406402}, {2300,0.405914}, {2320,0.405436}, {2340,0.40497}, {2360,0.404514}, {2380,0.404068}, {2400,0.403633}, {2420,0.403207}, {2440,0.402792}, {2460,0.402385}, {2480,0.401988}, {2500,0.4016}, {2520,0.40122}, {2540,0.400849}, {2560,0.400487}, {2580,0.400132}, {2600,0.399785}, {2620,0.399447}, {2640,0.399115}, {2660,0.398791}, {2680,0.398475}, {2700,0.398165}, {2720,0.397862}, {2740,0.397566}, {2760,0.397276}, {2780,0.396993}, {2800,0.396716}, {2820,0.396445}, {2840,0.39618}, {2860,0.395921}, {2880,0.395667}, {2900,0.395419}, {2920,0.395176}, {2940,0.394939}, {2960,0.394707}, {2980,0.39448}, {3000,0.394258}, {3020,0.394041}, {3040,0.393828}, {3060,0.39362}, {3080,0.393417}, {3100,0.393218}, {3120,0.393023}, {3140,0.392832}, {3160,0.392646}, {3180,0.392463}, {3200,0.392285}, {3220,0.39211}, {3240,0.391939}, {3260,0.391772}, {3280,0.391608}, {3300,0.391448}, {3320,0.391292}, {3340,0.391138}, {3360,0.390988}, {3380,0.390841}, {3400,0.390697}, {3420,0.390557}, {3440,0.390419}, {3460,0.390284}, {3480,0.390153}, {3500,0.390023}, {3520,0.389897}, {3540,0.389774}, {3560,0.389652}, {3580,0.389534}, {3600,0.389418}, {3620,0.389305}, {3640,0.389194}, {3660,0.389085}, {3680,0.388978}, {3700,0.388874}, {3720,0.388772}, {3740,0.388673}, {3760,0.388575}, {3780,0.388479}, {3800,0.388386}, {3820,0.388294}, {3840,0.388204}, {3860,0.388116}, {3880,0.38803}, {3900,0.387946}, {3920,0.387864}, {3940,0.387783}, {3960,0.387704}, {3980,0.387627}, {4000,0.387551}

```

3080,0.393417},{3100,0.393218},{3120,0.393023},{3140,0.392832},{3160,0.392646},{3180,0.392463},
{3200,0.392285},{3220,0.39211},{3240,0.391939},{3260,0.391772},{3280,0.391608},{3300,0.391448},
{3320,0.391292},{3340,0.391138},{3360,0.390988},{3380,0.390841},{3400,0.390697},{3420,0.390557},
{3440,0.390419},{3460,0.390284},{3480,0.390153},{3500,0.390023},{3520,0.389897},{3540,0.389774},
{3560,0.389652},{3580,0.389534},{3600,0.389418},{3620,0.389305},{3640,0.389194},{3660,0.38908},
{3680,0.388978},{3700,0.388874},{3720,0.388772},{3740,0.388673},{3760,0.388575},{3780,0.3884},
{3800,0.388386},{3820,0.388294},{3840,0.388204},{3860,0.388116},{3880,0.38803},{3900,0.3879},
{3920,0.387864},{3940,0.387783},{3960,0.387704},{3980,0.387627},{4000,0.387551}}

```

```
In[117]:= {{modelg=Ag*Exp[-t/τg]+Bg*Exp[-t/τg2]+cg
```

```

gsoL=FindFit[datag3,modelg,{ {Ag,.3},{τg,2000},{Bg,.3},{τg2,2000},{cg,.004}},t]

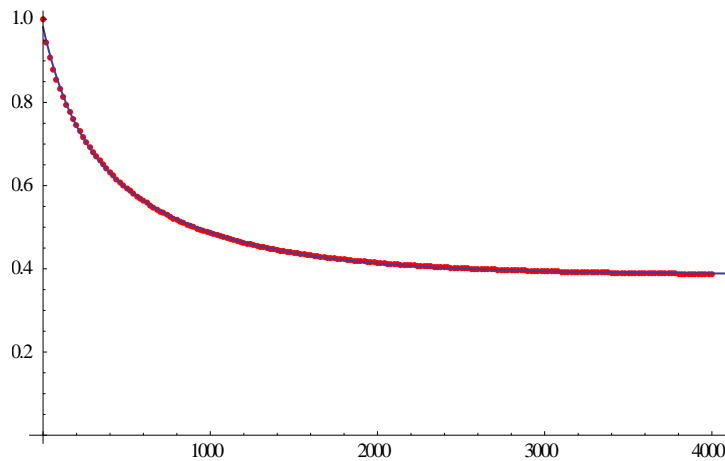
```

```
Out[117]:= {cg+Ag Exp[-t/τg]+Bg Exp[-t/τg2]
```

```
Out[118]:= {Ag → 0.381799, τg → 744.035, Bg → 0.211793, τg2 → 168.175, cg → 0.38736}
```

```
In[119]:= Show[ListPlot[datag3, PlotStyle→Red,PlotRange→Full], Plot[{Evaluate[modelg/.gsoL]}, {t, 0,
7000},PlotRange→Full]]
```

```
Out[119]:=
```



```
In[120]:= datar={{60,1.525*10^-7},{180,1.6*10^-7},{300,3.7*10^-7},{1800,7.5*10^-7},{3600,6.55*10^-7}}
```

```

modelrg=(1*ka1*pgea*mw*csat)/(pge*na)*((-
Evaluate[Ag/.gsoL]*((τc*Evaluate[τg/.gsoL])/(τc+Evaluate[τg/.gsoL]))*Exp[-
(τc+Evaluate[τg/.gsoL])*t/(τc*Evaluate[τg/.gsoL])]-
Evaluate[Bg/.gsoL]*((τc*Evaluate[τg2/.gsoL])/(τc+Evaluate[τg2/.gsoL]))*Exp[-
(τc+Evaluate[τg2/.gsoL])*t/(τc*Evaluate[τg2/.gsoL])]-Evaluate[cg/.gsoL]*τc*Exp[-t/τc])-
Evaluate[Ag/.gsoL]*((τc*Evaluate[τg/.gsoL])/(τc+Evaluate[τg/.gsoL]))-
Evaluate[Bg/.gsoL]*((τc*Evaluate[τg2/.gsoL])/(τc+Evaluate[τg2/.gsoL]))-Evaluate[cg/.gsoL]*τc))+7.5*10^-8

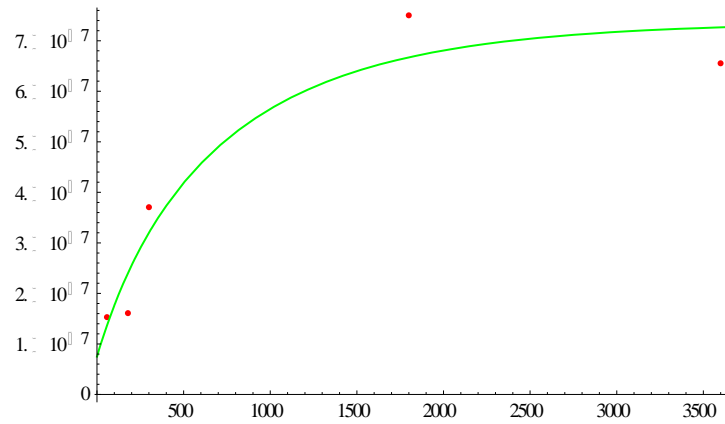
```

```
Out[121]:= {{60,1.525*10^-7},{180,1.6*10^-7},{300,3.7*10^-7},{1800,7.5*10^-7},{3600,6.55*10^-7}}
```

```
Out[122]:= {7.5 × 10-8 + 1.1772 × 10-9(562.211 - 30.3086e-0.00698786t - 160.037e-0.00238569t -  
371.866e-t/960)}
```

```
In[123]:= Show[ListPlot[datarg, PlotStyle → Red, PlotRange →  
Full], Plot[{Evaluate[modelrg]}, {t, 0, 5000}, PlotStyle → Green, PlotRange → Full]]
```

```
Out[123]:=
```



References

1. Pan, B.F., et al., *Study on growth kinetics of CdSe nanocrystals in oleic acid/dodecylamine*. JOURNAL OF CRYSTAL GROWTH, 2006. **286**(2): p. 318-323.
2. Peng, Z.A. and X.G. Peng, *Mechanisms of the shape evolution of CdSe nanocrystals*. JOURNAL OF THE AMERICAN CHEMICAL SOCIETY, 2001. **123**(7): p. 1389-1395.
3. Xie, C., et al., *Crystallization kinetics of CdSe nanocrystals synthesized via the TOP-TOPO-HDA route*. Journal of Crystal Growth. **310**: p. 3504-3507.
4. Murray, C.B., D.J. Norris, and M.G. Bawendi, *SYNTHESIS AND CHARACTERIZATION OF NEARLY MONODISPERSE CDE (E = S, SE, TE) SEMICONDUCTOR NANOCRYSTALLITES*. JOURNAL OF THE AMERICAN CHEMICAL SOCIETY, 1993. **115**(19): p. 8706-8715.
5. Peng, X., J. Wickham, and A.P. Alivisatos, *Kinetics of II-VI and III-V Colloidal Semiconductor Nanocrystal Growth: 'Focusing' of Size Distributions*. JOURNAL-AMERICAN CHEMICAL SOCIETY, 1998. **120**(21): p. 5343-5344.
6. LaMer, V.K. and R.H. Dinegar, *Theory, Production and Mechanism of Formation of Monodispersed Hydrosols*. Journal of the American Chemical Society, 1950. **72**(11): p. 4847-4854.
7. Bullen, C.R. and P. Mulvaney, *Nucleation and growth kinetics of CdSe nanocrystals in octadecene*. NANO LETTERS, 2004. **4**(12): p. 2303-2307.
8. Sugimoto, T., *Preparation of monodispersed colloidal particles*. Advances in Colloid and Interface Science. **28**: p. 65-108.
9. Talapin, D.V., et al., *Evolution of an ensemble of nanoparticles in a colloidal solution: Theoretical study*. JOURNAL OF PHYSICAL CHEMISTRY B, 2001. **105**(49): p. 12278-12285.
10. Gerung, H., et al., *Anhydrous solution synthesis of germanium nanocrystals from the germanium(II) precursor $Ge[N(SiMe_3)_2](2)$* . CHEMICAL COMMUNICATIONS, 2005(14): p. 1914-1916.
11. Boyle, T.J., et al., *Synthesis and Characterization of Germanium Coordination Compounds for Production of Germanium Nanomaterials*. EUROPEAN JOURNAL OF INORGANIC CHEMISTRY, 2009(36): p. 5550-5560.
12. Gerung, H., et al., *Solution synthesis of germanium nanowires using a Ge^{2+} alkoxide precursor*. JOURNAL OF THE AMERICAN CHEMICAL SOCIETY, 2006. **128**(15): p. 5244-5250.
13. L.J. Tribby, Shoop, N., and S.M. Han, *Modeling of Kinetically Limited Growth Rate for Solution-Synthesized Germanium Nanocrystals*, Unpublished results, 2013.
14. Jiang, Q., N. Aya, and F.G. Shi, *Nanotube size-dependent melting of single crystals in carbon nanotubes*. Applied Physics A, 1997. **64**(6): p. 627-629.
15. Paul, E.L., V.A. Atiemo-Obeng, and S.M. Kresta, *Handbook of industrial mixing [electronic resource] : science and practice / edited by Edward L. Paul, Victor A.*

- Atiemo-Obeng, Suzanne M. Kresta*. 2004: Hoboken, N.J. : Wiley-Interscience, c2004.
16. Mehrotra, A.K., *GENERALIZED ONE-PARAMETER VISCOSITY EQUATION FOR LIGHT AND MEDIUM LIQUID HYDROCARBONS*. INDUSTRIAL & ENGINEERING CHEMISTRY RESEARCH, 1991. **30**(6): p. 1367-1372.
 17. Yaws, C.L., *Thermophysical properties of chemicals and hydrocarbons [electronic resource] / Carl L. Yaws*. 2008: Norwich, NY : William Andrew, c2008.
 18. Bird, R.B., W.E. Stewart, and E.N. Lightfoot, *Transport Phenomena*. Wiley International edition. 2007: Wiley.
 19. Sitaraman, R., S.H. Ibrahim, and N.R. Kuloor, *A Generalized Equation for Diffusion in Liquids*. Journal of Chemical & Engineering Data, 1963. **8**(2): p. 198-201.
 20. Etherington, G., et al., *A neutron diffraction study of the structure of evaporated amorphous germanium*. Journal of Non-Crystalline Solids, 1982. **48**(2-3): p. 265-289.
 21. Kōga, J., et al., *Computer analysis on the structure of low-density and high-density amorphous germanium*. Journal of Non-Crystalline Solids, 2004. **345-346**(0): p. 742-745.
 22. Incropera, F.P. and D.P. DeWitt, *Fundamentals of heat transfer*. 1981: Wiley.
 23. Ranz, W.E., Marshall, W. R., *Evaporation from Drops, Part I*. Chemical Engineering Progress, 1952. **48**(3): p. 141-146.
 24. Kosuri, M.R., et al., *Adsorption kinetics of 1-alkanethiols on hydrogenated Ge(111)*. LANGMUIR, 2004. **20**(3): p. 835-840.
 25. Schlier, R.E. and H.E. Farnsworth, *Structure and Adsorption Characteristics of Clean Surfaces of Germanium and Silicon*. Journal of Chemical Physics, 1959. **30**(4): p. 917.
 26. Xiaohui, J., et al., *Ligand Bonding and Dynamics on Colloidal Nanocrystals at Room Temperature: The Case of Alkylamines on CdSe Nanocrystals*. Journal of the American Chemical Society, 2008. **130**(17): p. 5726-5735.
 27. Zhang, H., et al., *Enhanced Adsorption of Molecules on Surfaces of Nanocrystalline Particles*. The Journal of Physical Chemistry B, 1999. **103**(22): p. 4656-4662.
 28. Qing, A., *Differential evolution [electronic resource] : fundamentals and applications in electrical engineering / Anyong Qing*. 2009: Singapore ; Hoboken, NJ : J. Wiley & Sons Asia ; [Piscataway, NJ] : IEEE Press, c2009.
 29. Storn, R. and K. Price, *Differential Evolution - A simple and efficient adaptive scheme for global optimization over continuous spaces*. INTERNATIONAL COMPUTER SCIENCE INSTITUTE -PUBLICATIONS- TR, 1995(12): p. ALL.
 30. Lu, H.M., Z. Wen, and Q. Jiang, *Size dependent adsorption on nanocrystal surfaces*. Chemical Physics. **309**: p. 303-307.
 31. Fang, J.X. and W.H. Marlow, *Monte Carlo studies of effects of substrate size on water-substrate interaction energy and water*. Journal of Chemical Physics, 1997. **107**(13): p. 5212.
 32. Irzhak, V. and B. Rozenberg, *Role of adsorption in formation of inorganic nanoparticles: Kinetic model*. Colloid Journal, 2009. **71**(2): p. 177-184.

33. Wang, H. and F. Shadman, *Effect of Particle Size on the Adsorption and Desorption Properties of Oxide Nanoparticles*. AICHE JOURNAL, 2013. **59**(5): p. 1502-1510.
34. Chu, N. and W.H. Marlow, *Equilibrium adsorption on single and aggregated nanospheres*. Journal of Chemical Physics, 2006. **125**(17): p. 174702.
35. Jiang, F., et al., *Ligand-Tuned Shape Control, Oriented Assembly, and Electrochemical Characterization of Colloidal ZnTe Nanocrystals*. Chemistry of Materials, 2010. **22**(16): p. 4632-4641.
36. Jin, X., et al., *Shape control of CdTe nanocrystals synthesized in presence of in situ formed CdO particles*. Journal of Nanoparticle Research, 2011. **13**(12): p. 6963-6970.
37. Buhro, W.E. and V.L. Colvin, *Semiconductor nanocrystals - Shape matters*. NATURE MATERIALS, 2003. **2**(3): p. 138-139.